PATERNAL ALCOHOL EXPOSURES, THE MICROBIOME-METABOLOME AXIS, OXIDATIVE STRESS, AND THEIR IMPACTS ON IVF OUTCOMES

A Dissertation

by

ALEXIS NICOLE ROACH

Submitted to the Graduate and Professional School of
Texas A&M University
in partial fulfillment of the requirements for the degree of

DOCTOR OF PHILOSOPHY

Chair of Committee,	Michael Golding
Committee Members,	Tracy Clement
	Robert Burghardt
	Qinglei Li
Head of Department,	Larry Suva

August 2023

Major Subject: Biomedical Sciences

ABSTRACT

This dissertation utilizes a mouse model to investigate how paternal alcohol consumption affects in vitro fertilization (IVF) success, assisted reproductive technology (ART) fetoplacental development, the transcriptional profiles of sperm and epididymis, the male microbiome-metabolome, and the female response to seminal fluid. Previous alcohol research concentrates on the maternal influence during gestation. Males provide half of the genetic material and should be considered for their contributions to pregnancy and offspring development. Our earlier studies revealed that preconception paternal alcohol alters fetoplacental growth and F1 offspring metabolism. These experiments support our hypothesis that the epigenetic memory of alcohol is retained by sperm and is inherited by offspring via biological mechanisms, such as RNA and histones.

Expanding on this, we employed a clinically relevant mouse model of voluntary paternal alcohol consumption. We observe preconception paternal alcohol exposure decreases IVF embryo survival and pregnancy success rates in a dose-dependent manner. By analyzing embryonic RNA profiles, we find that preconception paternal alcohol exposure disrupts placental gene expression and modifies mitochondrial function and oxidative phosphorylation. Histologically, we identify lasting impacts on late-term placental organization. Using RNA analyses and mitochondrial DNA counts, we establish paternal cessation of ethanol exposure for one month provides limited epigenetic recovery. We then focus on bioinformatic analyses of alcohol, with or without saccharin, exposed male gastrointestinal microbiomes and blood metabolite concentrations where we show altered microbial populations and increased acetic acid levels in EtOH combined with saccharin. Lastly, using RNA sequencing, we characterize

changes in gene expression of the female tract after alcohol-exposed seminal plasma insemination. These studies highlight the necessity to change reproductive health messaging for family planning and stress the hazards of parental alcohol use.

Discoveries from our lab elucidate combined extrinsic factors that are inherited by offspring. These studies contribute to the developmental toxicology field by examining the influence of paternal alcohol consumption on multiple facets of reproduction. Future explorations concentrating on alcohol-exposed sperm mitochondrial function can use similar methods to assess contributions to the sperm epigenome. This effort will assist in discerning the mechanism(s) by which alcohol modifies spermatozoa and transmits adverse health conditions intergenerationally and, possibly, transgenerationally.

ACKNOWLEDGMENTS

First and foremost, I must thank myself. I'm proud of myself for pursuing my aspiration and accomplishing my degree. I stayed determined throughout this process, so this is a written pat on the back to me.

Next, I want to acknowledge and thank my family members for always being in my corner. Thank you, Travis Williams, for your encouragement, understanding, and love through every step of graduate school. I am also thankful for Lisa Mutchler, Alyssa Roach Sims, Arthur J. Roach III and Carol Roach and family, Monte Mutchler and Dr. Laura Coleman and family, Kevin and Jill Roach and family, Katherine and Antonio Mondragon and many more adopted family members for being constants in my life and believing in me since the beginning. Furthermore, I would not have found my passion for reproductive biology if it wasn't for my grandparents making sure I had the best opportunities and resources available. Thank you, Dr. Arthur J. Roach Jr., Mary Ann Roach (RIP), Melvin C. Mutchler (RIP), and Ada Lee Mutchler. I love you all!

I will never forget my academic family. I want to thank my mentor, Dr. Michael Golding, for his guidance, instruction, expertise, and support throughout this course of research! I also want to recognize my committee members, Dr. Tracy Clement, Dr. Qinglei Li, Dr. Robert Burghardt, and department head, Dr. Larry Suva and thank them for their time, assistance, and positivity throughout my degree program. I greatly appreciate my collaborator, Dr. Giri Athrey, for his insight, inclusion, hard work, and time! Also, I would like to thank my lab members: Dr. Richard Chang, Dr. Yudhishtar Bedi, Dr. Kara Thomas, Dr. Nicole Mehta, Katherine Zimmel,

Alison Basel, Sanat Bahdsavle, Samantha Higgins, and Destani Derrico for sharing this experience with me, and for being the best teammates I could have asked for! Go Dream Team!

To my fierce friends, you know who you are, I cannot express how much I appreciate you all for our deep discussions and your warrior energy and enthusiasm for me to keep chasing my dreams. I am beyond lucky to have you all in my life, and I will cherish our friendship forever.

Lastly, I want to thank my cat-dogs Tuxie and Luna for making sure I take a break every now and then, and that I always feel emotionally supported and slightly smothered during data analysis and writing sessions. You are always learning through osmosis and the best research assistants in the world.

I could not have fathomed that this is where I would be at 28, that I would have such zeal for the developmental toxicology field, or how I was going to achieve my goal without my own persistence and my amazing village's encouragement. This time has been one of tremendous learning and growth. I am forever grateful and will recall my graduate experiences and education throughout my future biomedical science career and adventures.

CONTRIBUTORS AND FUNDING SOURCES

Contributors

This work was supervised by a dissertation committee consisting of Dr. Michael Golding (Chair), Dr. Tracy Clement, and Dr. Larry Suva (Department Head) of the Department of Veterinary Physiology and Pharmacology and Dr. Robert Burghardt, Dr. Qinglei Li of the Department of Veterinary Integrative Biosciences.

In Chapter 2, the sperm small noncoding RNA analyses depicted were conducted in part by Sanat Bhadsavle, the tissue mitochondrial DNA counts were performed by Samantha Higgins, and the qRT PCR was completed by Destani Derrico of the Golding Lab in the Department of Veterinary Physiology and Pharmacology and will be published in 2023. The advanced analysis of microbiota data described in Chapter 4 was provided by Dr. Giri Athrey from the Department of Poultry Science and will be published in 2023.

All other work conducted for this dissertation was completed independently by Alexis Roach.

Funding Sources

This work was supported and made possible in part by a Medical Research Grant from the W.M. Keck Foundation (M.C.G.) and NIH grant R01AA028219 from the NIAAA (M.C.G.).

NOMENCLATURE

ART	Assisted Reproductive Technology
AUD	Alcohol Use Disorder
DID	Drinking in the Dark
DNA	Deoxyribonucleic acid
diH_2O	Distilled water
EtOH	Ethanol
FASD	Fetal Alcohol Spectrum Disorder
GCMS	Gas Chromatography Mass Spectrometry
GD	Gestational Day
GIT	Gastrointestinal Tract
H_2SO_4	Sulfuric Acid
IPA	Ingenuity Pathway Analysis
IVF	In Vitro Fertilization
miRNA	microRNA
mtDNcn	Mitochondrial DNA Copy Number
NAS	Nonnutritive Artificial Sweeteners
NGS	Next Generation Sequencing
OTUs	Operational Taxonomic Units
PCA	Principal Component Analysis
PBS	phosphate buffered saline

piRNA	piwi interacting RNA
qRT-PCR	Real-Time Quantitative Reverse Transcription Polymerase chain reaction
RNA	Ribonucleic Acid
SCFA	short-chain fatty acid(s)
SNL	Sweet'N Low®
TAMU IMAC	Texas A&M University Integrated Metabolomics Analysis Core
TCA	Trichloroacetic Acid
TIGM	Texas Institute for Genomic Medicine
tRF	tRNA fragments
tRNA	transfer RNA

TABLE OF CONTENTS

Page

LIST OF FIGURES

Page

LIST OF TABLES

Page

1. INTRODUCTION

Alcohol is an infamous toxicant and teratogen that is socially accepted and consumed daily over a significant portion of the world (Mahnke et al., 2019). With extensive research, maternal consumption of alcohol and its negative effects on the fetus during development is well-documented. The health issues that can arise from gestational EtOH consumption are known as fetal alcohol spectrum disorders (FASDs), which are a group of conditions that occur in mammals that are exposed to alcohol before birth. Under the umbrella of FASDs, there are wide array of abnormalities from intellectual to physical complications, and it is difficult for physicians to identify because an FASD diagnosis necessitates multiple assessments and evaluations performed by an interdisciplinary team (Cook et al., 2016). Despite women's role in contributing to FASDs, research continues to verify that men consume more alcohol and engage in binge drinking more frequently than women (Wilsnack et al., 2018). Furthermore, fathers are often ignored for their influence on offspring because they do not physically participate in the act of gestation.

More recently, there is growing evidence revealing that male preconception alcohol exposure is linked to alterations to spermatozoa, which can induce a range of complications for their offspring. These investigations challenge the common belief that the solitary role of spermatozoa is to transfer genetic information to the conceptus (Soubry, 2018b; Hart and Tadros, 2019). Various internal and external factors can modify a father's fecundity, as well as the health and development of his progeny (Homan et al., 2007; Kusuyama et al., 2020). The main external elements that affect fertility are lifestyle choices, occupational pollutants, and environmental contaminants (Hart and Tadros, 2019; Kumar, 2009; Nicolau et al., 2014, Mews et al., 2019;

Billah et al., 2022). Being that spermatogenesis is a cycle of continuous gamete turnover, sperm cells are highly susceptible to external factors, and these influences have the capacity to cause short and long-term development and health issues for future young (Sánchez et al., 2018; Guo et al., 2021; Yin et al., 2021). Intrinsically, spermatic mutations can occur during one or both meiotic cell divisions; conversely, epigenetic modifications from extrinsic factors present an added opportunity for transmutation (Sánchez et al., 2018; Guo et al., 2021; Yin et al., 2021). Still, the role of paternal epigenetic programming in the development of offspring disease is not well established, and it is difficult to determine the basic mechanism(s) that induce undesirable health outcomes in offspring.

The term epigenetics describes a relatively new area of study and is defined as the inheritance of gene expression based on components other than DNA (Deichmann, 2016; Lempiäinen and Garcia, 2023). Specifically, epigenetic marks involve various mechanisms such as small alterations to noncoding RNAs, DNA methylation, and chromatin reorganization of DNA binding proteins, such as histones, that have the capability to revise gene expression without changing the DNA sequence (Chastain and Sarkar, 2017). These epigenetic adaptations control gene expression and how cells interpret signals from the outside environment and within the body, affecting processes such as differentiation and cell growth (Lempiäinen and Garcia, 2023). Alterations in gametes due to epigenetic modifications are the primary external factors that can be passed on to descendants and program intergenerational and/or transgenerational effects (Grover and Jenkins, 2020). Thus, Paternal Origins of Health and Disease (POHaD) was established (Soubry, 2018a). Nonetheless, the mechanisms by which epigenetic memories of parental (or paternal) environmental exposures transmit to future generations remain poorly defined.

Over the last four decades, epidemiological research has shown that preconception male EtOH exposure can harm sperm and induce to the development of FASDs in progeny. Exposure to alcohol alters the epigenetics of male gametes and can have acute or prolonged negative effects on the health of their future heirs (Chastain and Sarkar, 2017). Human research studies have revealed that men with alcohol use disorder (AUD), or alcoholism, fathered children that experienced reduced growth, impaired neuronal system function, hormonal imbalances, and behavioral problems (Cicero, 1994; Luan et al., 2022). Furthermore, clinical reports have linked paternal alcohol intake, before conception, to congenital heart diseases in both developing and mature progeny (Zhang et al., 2020). These human accounts have bolstered the role of alcohol in influencing the Paternal Origins of Health and Disease (POHaD), but there are several factors that limit the effectiveness of these investigations. For instance, the amount of alcohol consumed by alcoholic men on a daily basis varied, the sample sizes were small, and the symptoms and physical characteristics of children born to fathers with AUD were diverse. Therefore, future alcohol POHaD research requires better controlled models.

The use of animal model research has also confirmed that alcohol-exposed sires can cause deleterious consequences for the next generation, including restricted fetal and postnatal growth, disruptions in placental histoarchitecture, craniofacial defects, increased psychosocial abnormalities, and metabolic programming alterations (Bedi et al., 2019; Chang et al., 2017; Thomas et al., 2021; Kim et al., 2014; Finegersh et al., 2014; Finegersh et al., 2015; Chang et al., 2019a; Chang et al., 2019b; Thomas et al., 2022; Thomas et al., 2023).

These reports challenge established paradigm that maternal drinking during pregnancy is the singular origin of alcohol-induced etiologies. Therefore, it is crucial for successive research to uncover and understand how alcohol and other toxic substances prompt gametic epigenetic

changes that are inherited by subsequent generations. To provide society with accurate information, alcohol warning messaging should emphasize the consequences of EtOH intake for both parents, rather than solely concentrating on maternal consumption. This means that each parent should be extremely careful with their alcohol use before conception to minimize the risk of birth defects. Such knowledge will empower both men and women of reproductive age to make informed decisions when considering having children and creating a prepregnancy plan.

In this dissertation, I focus on determining the impact of chronic preconception paternal alcohol exposures on ART fetoplacental development, alcohol cessation effects on male reproductive physiology, alcohol use on male gut health, and reproductive signaling mechanisms in both sexes. Through these studies, we intend to help uncover the mechanisms by which alcohol modifies spermatozoa and can lead to negative health consequences for future generations. To accomplish this, we examine fundamental epigenetic mechanisms that are related to modified transcriptomic profiles in IVF generated embryos sired by alcohol-exposed males, alcohol-treated male reproductive tract tissue and spermatozoa, and conduct some preliminary studies in the female reproductive tract post-coitus examining differences between copulation with control and alcohol-exposed males.

Within Chapter 2, I evaluate the impact of preconception paternal alcohol exposure on IVF generated embryo total RNA profiles and fetoplacental measurements. Our laboratory's earlier studies have consistently found that a physiologically relevant, C57BL/6J strain, mouse model of paternal alcohol consumption programmed an increase in placental weights and decrease placental efficiency in male offspring at gestational day 16.5 (GD 16.5) (Chang et al., 2019a; Bedi et al., 2019; Thomas et al., 2021; Thomas et al., 2022). Moreover, there are sex specific modifications in the histoarchitecture of the placenta when the sire chronically

consumed alcohol and placental disparities at gestational day 16.5 (GD 16.5) (Thomas et al., 2022). Using IVF techniques to generate progeny, we observed no decrease in alcohol-sired male offspring placental weights, but placental efficiency remained significantly lower (Roach et al., 2023). Recipient dams were terminated at GD 16.5, and placental histology also revealed extensive alterations in placental layer organization and ratios and were more severe for male offspring.

Further, research described in Chapter 2 demonstrates that preconception paternal alcohol exposure affects IVF embryo development rates and pregnancy outcomes. Using a natural mating paradigm, our previous works found no effect of alcohol on litter sizes (Chang et al., 2017; Bedi et al., 2019; Thomas et al., 2022). However, we observe substantially smaller IVF litter sizes from alcohol-treated sperm in a dose-dependent manner. Other mouse models report a cumulative effect of ARTs on fetoplacental growth and other epigenetic concerns (de Waal et al., 2015). At this juncture, we explore the factor of male alcohol consumption since previous studies over the effects of alcohol on IVF have only concentrated on female alcohol consumption (Homan et al., 2007; Rossi et al., 2011; Nicolau et al., 2014; Wdowiak et al., 2014; Hornstein, 2016). This is the first study that targets and categorizes these perturbations in the milieu of paternal alcohol exposure and will provide future preclinical and clinical studies a foundation to continue evaluating the role of paternal lifestyle choices in the programming of alcohol related deficits in progeny. Moreover, these investigations will aid in prompting change in reproductive health messaging to include men and warn them of the potential risks of alcohol consumption on their children.

In Chapter 3, I apply our previous knowledge of alcohol-induced shifts to sperm chromatin and noncoding RNA profiles (Bedi et al., 2019; Bedi et al., 2022). Here, we begin to

uncover how alcohol cessation affects the mitochondrial DNA copy number (mtDNcn) and transcriptional profiles of the caput portion of the epididymis in relationship to mature sperm-borne small noncoding RNAs. We show alterations to noncoding RNAs remain dysregulated after 28 days of alcohol cessation, which is one week less than a full round of spermatogenesis in mice (Griswold, 2016) but almost three times the amount of time required for mouse sperm to transit the epididymis. To achieve this, we use next generation sequencing (NGS) on epididymal tissues. This investigation confirms that paternal environmental exposures have lasting impacts on the male reproductive tract and sperm epigenome before total reproductive restoration is accomplished.

Evidence has shown that RNA transfer to maturing sperm occurs through the transmission from soma-to-germline communication in the epididymal tract (Sharma et al., 2018; Sharma, 2019; Paul et al., 2021; Conine et al., 2018; Conine and Rando, 2022). As sperm undergo post-testicular maturation, specialized epithelial cells in the epididymis transmit significant amounts of small noncoding RNA (sncRNA) to the sperm through extracelluar vesicles called epididymosomes (Sullivan, 2015; Sharma et al., 2018; Kuo et al., 2016; Ren, X et al., 2017; James et al., 2020). This cellular communication from each section of the epididymis to developing sperm cells is crucial for successful fertilization, implantation, embryo, and fetal development (Sharma et al., 2018; Conine et al., 2018; Conine and Rando 2022). However, many of the functions of these sncRNAs remain unclear. Several studies have indicated that modifications to sncRNAs drive the epigenetic inheritance of undesirable health outcomes, such as oxidative stress on sperm transfer RNA (tRNA) and ribosomal RNA (rRNA) induce anxiety and depression in F1 offspring (Ren, L et al., 2022). In our study, we extract RNA from the sperm of sires that were exposed to alcohol and then experienced alcohol cessation for four

weeks, then subject sncRNAs to deep-sequencing. Next, we compare the resulting mapped reads to established records of tRFs, tRNAs, piRNAs, and microRNAs to evaluate the sncRNA makeup in reaction to alcohol cessation. We demonstrate that alcohol cessation for 28 days did not induce a full recovery of altered sncRNA populations relating to alcohol exposure. Also, we determine that mitochondrial DNA copy number (mtDNcn) is substantively elevated in the cauda and corpus epididymal regions, trended upward in the liver, but no alterations of mtDNAcn were found in the testes after discontinued EtOH consumption.

In Chapter 4, I observe the alcohol-exposed male gastrointestinal environment in the context of microbiome modifications and downstream affects to the metabolome. Previous studies have determined that alcohol or nonnutritive artificial sweeteners (NAS) can wreak havoc on the gut causing dysbiosis, oxidative injury, and metabolic derangements (Engen et al., 2015; Suez et al., 2014; Perez et al., 2020). Change to the microbiome directly impacts levels of circulating metabolites that could alter sperm during spermatogenesis. Here, we present that EtOH and NAS, together and separately, alter intestinal microbial communities and the concentrations of short-chain fatty acids (SCFAs). We use fecal DNA whole-genome shotgun sequencing and informatic analysis to identify any altered microbiota taxonomic ranks, and we employ gas chromatography and mass spectrometry (GCMS) to detect blood serum metabolite levels. Based on our findings, this work calls for deeper investigation into the role of the microbiome-metabolome axis on the male reproductive tract. Our effort alludes to how the beginning of the complex shaping of alcohol-exposed sperm could be obtained. Future investigations will concentrate on whether the altered levels of metabolites are crossing the blood-testis barrier and programming the epigenetic memory of developing spermatozoa.

Lastly, in the final chapter, I describe a preliminary study examining the response of the female reproductive tract to alcohol-treated seminal fluid. Using vasectomized alcohol-treated males, we mate them to naïve females and use next generation sequencing (NGS) on post-coitus oviducts where we identify differential gene expression. We then use ingenuity pathway analysis (IPA) and detect disturbed gene regulatory networks in neuron, estrogen, and immune signaling pathways. This study is a continuation of the influences that alcohol has downstream, before fertilization, that may also control the transmission of adverse phenotypes in offspring.

2. PRECONCEPTION PATERNAL ALCOHOL EXPOSURE DECREASES IVF EMBRYO SURVIVAL AND PREGNANCY SUCCESS RATES IN A MOUSE MODEL[1]

2.1 **Introduction**

IVF is a medical technique where spermatozoa fertilize oocytes outside the body, generating embryos that are subsequently transferred into the female reproductive tract and carried to term (Serafini, 2001). Couples experiencing infertility who desire a biological family turn toward IVF when they have failed to conceive naturally (Bavister, 2002; Johnson, 2019). After almost half a century of research and advancement, over 9 million infants have been conceived via IVF, and today, ARTs account for 2% of all infants born in the USA (Carson and Kallen, 2021).

To date, most investigations into pregnancy loss and poor IVF success rates have focused on the influence of maternal stressors and periconceptional health (Homan et al., 2007; Rossi et al., 2011; Nicolau et al., 2014; Wdowiak et al., 2014; Hornstein, 2016). However, a recent wave of research demonstrates that a wide range of stressors and toxicants alters the sperm-inherited developmental program, negatively affecting offspring fetoplacental growth and long-term health (Fleming et al., 2018). Unfortunately, despite the demonstrated importance of the sperm epigenome to offspring development, studies examining IVF outcomes seldom consider paternal exposures or explore dimensions of male fertility beyond sperm morphology and motility.

---

[1] Reprinted with permission from "Preconception paternal alcohol exposure decreases IVF embryo survival and pregnancy success rates in a mouse model." by Roach AN, Zimmel KN, Thomas KN, Basel A, Bhadsavle SS, Golding MC, 2023. *Molecular Human Reproduction*, 29 (2), https://doi.org/10.1093/molehr/gaad002, Copyright [2023] by Alexis Roach via Open Access CC BY-NC Oxford University Press.

In the USA, alcohol use is widespread (Esser et al., 2014; Mahnke et al., 2019), with annual sales reaching 252 billion US dollars in 2019 alone (Castaldelli-Maia et al., 2021). It is well established that men drink more than women, and significantly, 72% of men consume alcohol on a weekly basis (Naimi et al., 2003; White et al., 2006; Kanny et al., 2018). However, despite the emerging importance of paternal alcohol use to child health and development, very few studies consider the impact of male alcohol use on reproductive function, while the small number of studies that do are confounded and often contradictory. For example, some studies using animal models suggest chronic moderate-level (Anderson et al., 1980; Salonen et al., 1992) and supraphysiological alcohol exposures induce lower fecundity, decrease in gonad function and alter semen parameters (Akingbemi et al., 1997; Emanuele et al., 2001; Lee et al., 2010; Sánchez et al., 2018). In contrast, studies examining limited binge-like exposures suggest no impacts (Bedi et al., 2019). Clinical studies also provide conflicting data on the impacts of alcohol intake on hormone production, sperm count and morphology, and overall fertility (Gümüş et al., 1998; Muthusami and Chinnaswamy, 2005; Jensen et al., 2014; Condorelli et al., 2015; Van Heertum and Rossi, 2017). Therefore, the effects of alcohol use on male reproductive physiology remain unclear. Nevertheless, alcohol is associated with intranuclear changes in mature spermatozoa, resulting in irregular chromatin condensation (Sánchez et al., 2018) as well as modifications to the sperm epigenome (Rompala et al., 2018; Bedi et al., 2019, 2022).

Unfortunately, most human studies examining interactions between alcohol use and IVF either neglect the male's drinking habits and exclusively focus on female drinking (Rossi et al., 2013; Wdowiak et al., 2014; Dodge et al., 2017; Lyngsø et al., 2019) or are significantly confounded by multiple lifestyle factors (Nicolau et al., 2014; Hornstein, 2016). Only two studies have examined the effects of both maternal and paternal alcohol use on IVF outcomes. A

5-year IVF and gamete intrafallopian transfer (GIFT) study in California found decreased chances of achieving a live birth and increased risks of miscarriage when the father consumed alcohol. Notably, alcohol intake did not significantly affect sperm concentration, motility or morphology (Klonoff-Cohen et al., 2003). In contrast, a 10-year IVF analysis in Boston revealed no statistically significant association between live births and male drinking (Rossi et al., 2011). Unlike the California report, the Boston study identified significantly lower sperm counts and irregular morphologies in semen samples from men who drank but only those who drank wine (Rossi et al., 2011). However, these limited studies were too underpowered to reliably detect an impact of paternal alcohol use and are significantly confounded by differing genetics, environmental exposures and often unknown causes of infertility. Therefore, the influence of paternal alcohol use on IVF outcomes remains poorly described (Nicolau et al., 2014; Hornstein, 2016).

In clinical studies, IVF babies are predisposed to preterm birth, lower birth weights and increased rates of congenital disabilities (Chang et al., 2020). In support of these clinical observations, several preclinical studies have revealed that ovarian stimulation, IVF and embryo culture lead to placental defects, including placentomegaly, reduced placental efficiency, modified histoarchitecture and altered metabolic function (Collier et al., 2009; Delle Piane et al., 2010; Bloise et al., 2012; de Waal et al., 2015; Tan et al., 2016; Dong et al., 2021; Bai et al., 2022). Notably, the IVF-associated changes in placental growth correlate with disruptions in imprinted gene expression, suggesting that epigenetic mechanisms potentially contribute to these pathological outcomes (Mann et al., 2004; de Waal et al., 2015).

Our previous studies using a C57BL/6J mouse model reveal that preconception paternal alcohol exposures transmit an intergenerational stressor that also negatively affects placental

growth, efficiency, histology, and metabolism (Bedi et al., 2019; Chang et al., 2019a and 2019b; Thomas et al., 2021, 2022). Specifically, paternal alcohol use correlates with sex-specific, dose-dependent changes in placental histoarchitecture and alterations in the control of imprinted gene expression (Thomas et al., 2021, 2022). Based on these shared phenotypic outcomes, we hypothesized that alcohol-induced changes in the paternal epigenetic program would exacerbate the placental growth phenotypes induced by IVF, resulting in increased rates of congenital disabilities and pregnancy loss. Using a physiologically relevant mouse model of chronic alcohol exposure, we found that male alcohol use negatively impacts IVF embryo development and pregnancy success rates. Critically, our data reveal that evaluating male exposure history and lifestyle choices is essential to optimizing the chances of achieving a healthy pregnancy and that male alcohol use may be a crucial, unrecognized factor affecting IVF outcomes.

2.2 Materials and Methods

2.2.1 Ethics Statement

We conducted all experiments under AUP 2017-0308, approved by the Texas A&M University IACUC. All experiments were performed following IACUC guidelines and regulations. Here, we report our data per ARRIVE guidelines.

2.2.2 Animal Husbandry and Preconception Paternal Alcohol Exposures

In our studies, we used C57BL/6J strain (RRID:IMSR_JAX:000664) mice, which we obtained and housed in the Texas A&M Institute for Genomic Medicine, fed a standard diet (catalog # 2019, Teklad Diets, Madison, WI, USA), and maintained on a reverse 12-h light/dark cycle. To reduce stress, a known confounder modulating paternal epigenetic inheritance (Chan et

al., 2018), we subjected males to minimal handling and provided them with additional cage enrichments, including shelter tubes (catalog # K3322, Bio-Serv, Flemington, NJ, USA).

Before initiating the Ethanol (EtOH) and Control preconception treatments, we acclimated male mice to individual housing conditions for 1 week. We then randomly assigned sexually mature, postnatal day 90 male mice to one of three treatment groups (n = 8). Using a prolonged version of the Drinking in the Dark model of voluntary alcohol consumption (Rhodes et al., 2005), we exposed males to the Control or EtOH treatments for 4 h per day, beginning 3 h after the initiation of the dark cycle. Using methods described previously (Thomas et al., 2022), we replaced the home cage water bottle with a bottle containing either: 0% (Control), 6% (6% EtOH) or 10% (10% EtOH) w/v ethanol (catalog # E7023; Millipore-Sigma, St. Louis, MO, USA). We simultaneously exchanged the water bottles of Control and EtOH-exposed males to ensure identical handling and stressors. We recorded the weekly weight of each male (g) and the amount of fluid consumed (g) and then calculated weekly fluid consumption and average daily EtOH dose as described previously (Thomas et al., 2022).

During the mating phase, we bred exposed males to naive postnatal day 90 C57BL/6J females. We synchronized the female reproductive cycles using the Whitten method (Whitten et al., 1968), then placed the female in the male's home cage immediately after the male's daily exposure window. After 18 h, we recorded the presence of a vaginal plug and returned females to their original cages.

2.2.3 **IVF and Embryo Culture**

The process used for IVF and embryo culture is described in Figure 2.1 A. After 10 weeks of exposure, we sacrificed exposed males using CO_2 asphyxiation followed by cervical

dislocation, then extracted mature caudal sperm, which we cryopreserved using CARD MEDIUM (catalog # KYD-003-EX, Cosmo Bio USA, Carlsbad, CA, USA) and methods described by Nakagata (2011). We visually confirmed sperm motility, then transferred frozen sperm to liquid nitrogen for long-term storage. We then superovulated 3- to 5-week-old C57BL/6J female mice using timed intraperitoneal injections of 6.25 IU PMSG (catalog # HOR-272, Prospec Bio, East Brunswick, NJ, USA), followed 48 h later by 6.25 IU HCG (catalog # C1063, Millipore-Sigma, St. Louis, MO, USA). We then sacrificed the superovulated females and isolated cumulus–oocyte complexes, which we placed in prewarmed CARD MEDIUM. Next, we thawed sperm straws in a 37°C water bath, then added 10 µl of sperm to 90 µl of FERTIUP preincubation medium (catalog # KYD-002-05-EX, Cosmo Bio USA, Carlsbad, CA, USA) in a 37 °C incubator (5% CO_2 in air). We placed cumulus–oocyte complexes in 90 µl of CARD MEDIUM. After 35 min of capacitation in FERTIUP, we added 10 µl of sperm for a total culture volume of 100 µl, then incubated sperm and cumulus–oocyte complexes for 4 h.

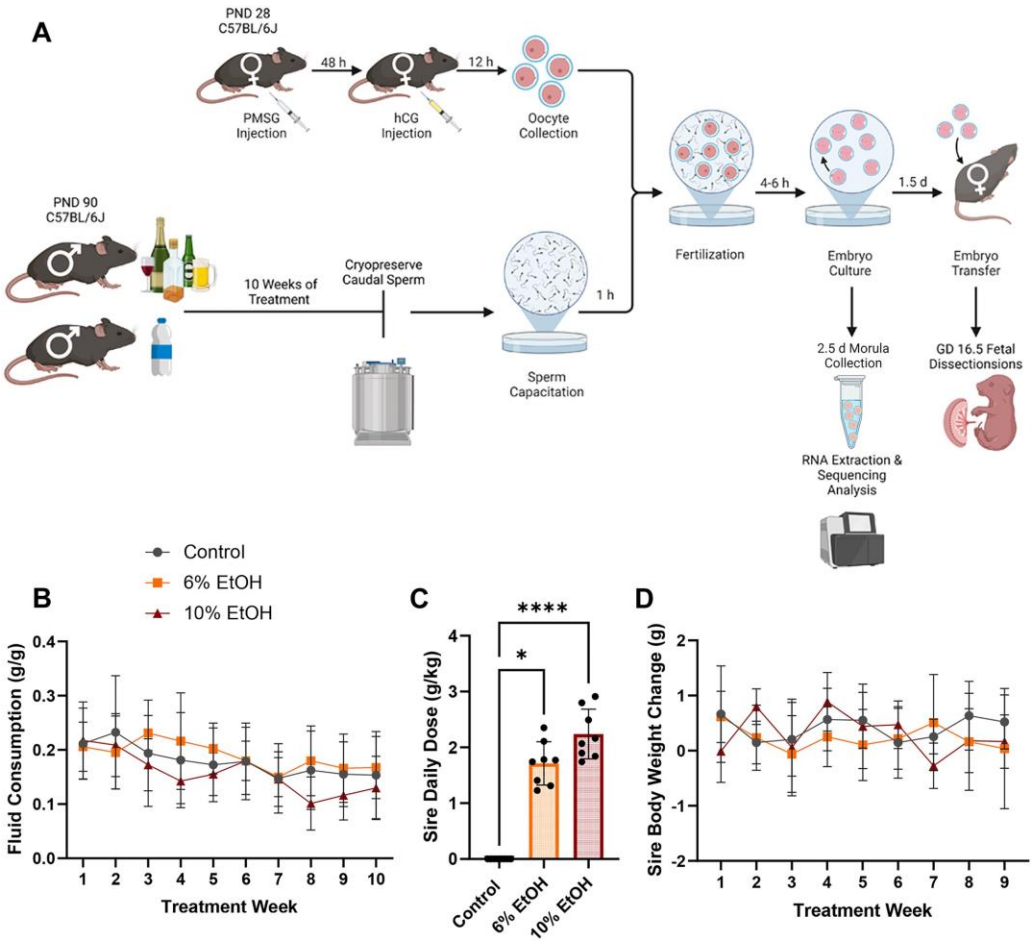

Figure 2.1. A mouse model to determine the impact of chronic paternal alcohol use on IVF-embryo development and pregnancy success rates. (A) Experimental paradigm used to investigate the impact of chronic paternal EtOH exposure on IVF offspring growth and survival. Comparison of sire (B) average weekly fluid consumption and (C) average daily dose of ethanol between treatment groups (n = 8). (D) Comparison of average weekly weight gain between treatment groups (n = 8). We compared treatments using either a one-way or two-way ANOVA. Error bars represent the standard error of the mean, *P < 0.05, ****P < 0.0001.

We counted one-cell stage embryos after 3–5 h of culture, then collected two-cell embryos after 1.5 days of culture, which we transferred (maximum of 8–14 two-cell embryos per dam) into 10- to 12-week-old pseudopregnant recipient C57BL/6J females (see below). Finally, we cultured the remaining embryos for a total of 60 h, collected morula-stage embryos, then snap-froze pools of 10–15 morulae in 350 µl of RLT lysis buffer (catalog # 74136, Qiagen, Germantown, MD, USA) containing 1% 2-mercaptoethanol (catalog # M6250, Millipore-Sigma,

St. Louis, MO, USA). We then sent samples to Quick Biology (Pasadena, CA, USA) for mRNA isolation and deep sequencing.

We bred 10- to 12-week-old recipient C57BL/6J females to vasectomized C57BL/6J males and selected pseudopregnant dams based on the presence of a copulation plug. After anesthetizing the recipient dams, we opened the abdominal cavity under a dissection stereomicroscope, created an incision in the oviduct, then inserted a glass capillary containing the two-cell embryos and expelled the embryos toward the ampulla. Finally, we pushed the ovary, oviduct and uterine horn back into the abdomen, closed the wound using wound clips, then kept the mice warm on a 37°C warming pad until the animal recovered from the effects of anesthesia.

2.2.4 **Fetal Dissection and Tissue Collection**

We co-housed recipient dams and provided them with additional nesting materials and cage enrichment, including igloo huts (catalog # K3570, Bio-Serv). The two-cell embryos were transferred after 1.5 days of culture. We then sacrificed recipient dams 15 days later, corresponding to embryonic day 16.5, using CO_2 asphyxiation followed by cervical dislocation. Subsequently, we dissected the female reproductive tract and recorded fetoplacental measures. We either fixed tissue samples in 10% neutral buffered formalin (catalog # 16004-128, VWR, Radnor, PA, USA) or snap-froze the tissues on dry ice and stored them at −80°C.

2.2.5 **Fetal Sex Determination**

We isolated genomic DNA from the fetal tail using the HotSHOT method (Truett et al., 2000) and then determined fetal sex using a PCR-based assay described previously (Thomas et al., 2021).

2.2.6 **Placental RNA Isolation and RT-qPCR Gene Expression**

We isolated RNA from gestational day 16.5 placentae using the Qiagen RNeasy Plus Mini Kit (catalog # 74136, Qiagen). We then seeded ~1 µg of RNA into a reverse transcription reaction using the High-Capacity cDNA Reverse Transcription Kit (catalog # 4368814, Thermo-Fisher, Waltham, MA, USA). Using published methods and primer sequences (Thomas et al., 2021, 2022), we determined the relative levels of candidate gene transcripts using the AzuraView GreenFast qPCR Blue Mix LR kit (Cat No. AZ-2320: Azura Genomics, Raynham, MA, USA). We describe the data normalization and handling procedures below.

2.2.7 **Analysis of Placental Histology**

To increase tissue contrast, we treated tissue samples with phosphotungstic acid (Lesciotto et al., 2020) and then processed samples for imaging using MicroComputed tomography (microCT), using methods described previously (Thomas et al., 2021, 2022). Briefly, we incubated half placentae in 5% (w/v) phosphotungstic acid dissolved in 90% methanol for 4 h and then held samples in 90% methanol overnight. We then incubated samples in progressive reductions of methanol (80%, 70%, 50%) each for 1 day, then moved placentae into PBS with 0.01% sodium azide for long-term storage. Finally, we embedded placentae in a 50/50 mixture of polyester and paraffin wax to prevent tissue desiccation, then imaged samples on a SCANCO vivaCT 40 (SCANCO Medical AG Brüttisellen, Switzerland) using a 55 kVp voltage X-ray tube and 29 µA exposure. The resulting microCT image voxel size was 0.0105 mm^3, with a resolution of 95.2381 pixels/mm. After scanning, we used the open-source medical image analysis software Horos (Version 3.3.6; Nibble Co LLC, Annapolis, MD, USA; https://horosproject.org/) to measure placental features.

To contrast placental glycogen levels between treatments, we processed and sectioned paraffin-embedded placental samples as described previously (Thomas et al., 2022), then stained the slides using a Periodic Acid Schiff (PAS) Stain Kit (Mucin Stain) (catalog # ab150680, Abcam, Boston, MA, USA) following the manufacturer's provided protocol. We imaged samples using the VS120 Virtual Slide Microscope (Olympus, Waltham, MA, USA) and analyzed the images with the included desktop software, OlyVIA (Version 2.8, Olympus Soft Imaging Solutions GmbH, Muenster, Germany). Using Photoshop (Version 21.0.1, Adobe, San Jose, CA, USA) and ImageJ (Version 1.53f51, Wayne Rasband and contributors, National Institutes of Health, USA), we calculated the PAS-stained area of the decidua and junctional zones, then normalized this value to the area of the decidua and junctional zone.

2.2.8 **Informatic Analysis**

We used the open-source, web-based Galaxy server (Afgan et al., 2018) (https://usegalaxy.org/) to process and analyze our data files. First, we used MultiQC (Ewels et al., 2016) to perform quality control on the raw paired-end, total RNA sequence files and then trimmed the sequences of Illumina adapters using Trimmomatic (Bolger et al., 2014). Next, we used RNA STAR (Dobin et al., 2013) to map the reads to the *Mus musculus* reference genome (UCSC version GRCm39/mm39). We then used featureCounts (Liao et al., 2014) with a minimum mapping quality per read of 10 to determine read abundance for all genes, followed by annotation versus M27 GTF (GENCODE, 2020). Finally, we analyzed the generated featureCounts files using the DESeq2 (Love et al., 2014) function with default parameters to generate the PCA plots and the Volcano Plot function to produce graphical representations of the (log2FC, *q*-value <0.05) gene expression levels for the top 25 significant genes. Next, we

exported the differentially expressed genes (DEGs) (log2FC, unadjusted *P*-value < 0.05) into the Ingenuity Pathway Analysis software package and conducted gene enrichment analysis (Jiménez-Marín et al., 2009; Krämer et al., 2014).

We generated heatmaps for DEGs using the 'pheatmap' (Kolde, 2012) package on R version 4.2.1 (R Core Team, 2022) We transformed the raw counts using variance stabilized transformation (VST) in DESeq2 (Love et al., 2014) and used the VST counts to plot the heatmap. We calculated *z*-scores using the scale = 'row' function. We used Venny 2.1 (Oliveros, 2007–2015) to generate Venn diagrams comparing DEGs between treatments.

2.2.9 **Data Management**

The data generated in this study were managed using a detailed data management plan that prioritizes safe and efficient data handling. For long-term storage, retrieval and preservation, we have stored all data on Google Drive. The sequence files generated from this project can be obtained in the GEO database under accession number GSE214726.

2.2.10 **Statistical Analysis**

We initially collected physiological measures for each exposed male, embryo or fetus by hand and then transcribed these data into Google Sheets or Microsoft Excel, where we collated the data. We then transferred the physiological and molecular data into the statistical analysis program GraphPad Prism 9 (RRID: SCR_002798; GraphPad Software, Inc., La Jolla, CA, USA), set the statistical significance at alpha = 0.05, used the ROUT test ($Q = 1\%$) to identify outliers, and then verified the normality of the datasets using the Shapiro–Wilk test. If data passed normality (alpha = 0.05), we employed either a One-way or Two-way ANOVA or an unpaired, parametric (two-tailed) *t*-test. If the data failed the test for normality or we observed unequal

variance (Brown Forsythe test), we ran a Kruskal–Wallis test followed by Dunn's multiple comparisons test or a non-parametric Mann–Whitney test.

For measures of fetoplacental growth, we determined the male and female average for each litter and used this value as the individual statistical unit. As we observed differences in litter size (Fig. 2.2B), which can exert stage-specific impacts on fetal weight (Ishikawa et al., 2006), we also compared the collective measures of individual fetuses and reported the analysis of both datasets. To calculate placental efficiency (Hayward et al., 2016), we divided fetal weight by placental weight. For offspring organ weights and the analysis of placental histology, we randomly selected male and female offspring from each litter and used measures of these samples as the statistical unit. For RT-qPCR analysis of gene expression, we imported the replicate cycle threshold (Ct) values for each transcript into Excel, then normalized expression to the geometric mean of two validated reference genes, including transcripts encoding Phosphoglycerate kinase 1 (*Pgk1*) and 3-monooxygenase/tryptophan 5-monooxygenase activation protein zeta (*Ywhaz*). We then used the $-\Delta\Delta$CT method (Schmittgen and Livak, 2008) to calculate the relative fold change for each biological replicate. Data presented are mean ± standard error of the mean. For each figure presented, we provide detailed descriptions of each statistical test in Supplemental Table 1 in Appendix A.

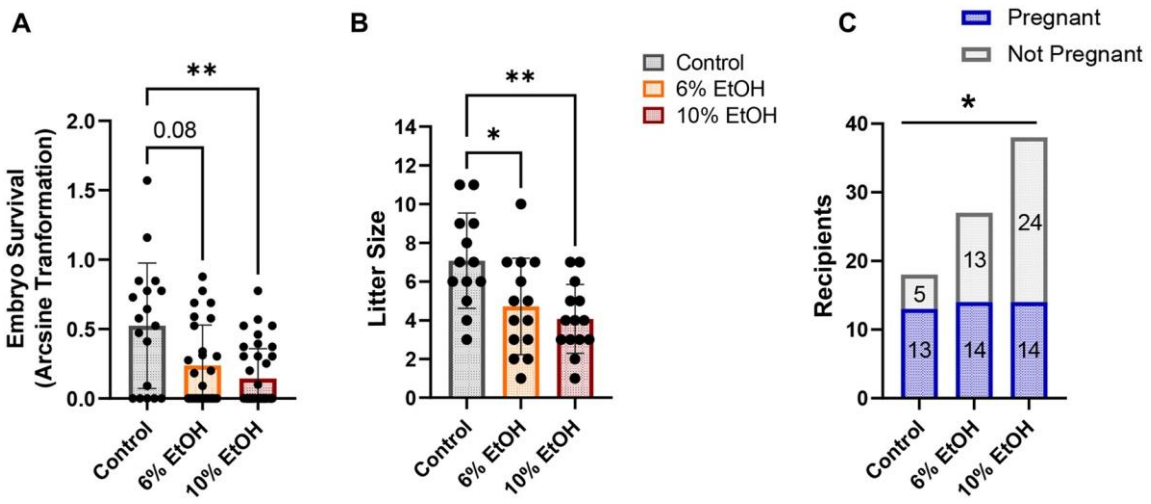

Figure 2.2. Chronic paternal alcohol exposure impedes IVF embryo survival and decreases pregnancy success rates. Chronic male alcohol exposure reduces (A) the percentage of two-cell stage embryos per transfer surviving to gestational day 16.5 and (B) the number of live offspring or litter size at gestational day 16.5. We arcsine transformed the percentage of surviving two-cell embryos and used a one-way ANOVA to compare treatments on each litter. (C) Paternal alcohol use reduces IVF pregnancy success rates. We used a chi-squared test to identify differences in pregnancy success rates between treatments ($P = 0.0448$, $n = 18$ Control, $n = 27$ 6% EtOH, $n = 38$ 10% EtOH litters). Error bars represent the standard error of the mean, $^{*}P < 0.05$, $^{**}P < 0.01$.

2.3 Results

2.3.1 A Physiologically Relevant Mouse Model to Examine the Impacts of Chronic Preconception Paternal Alcohol Use on IVF Outcomes

To understand the impact of preconception paternal alcohol use on IVF outcomes, we employed an established mouse model of voluntary alcohol exposure that mimics chronic binge drinking (Boehm et al., 2008), isolated sperm from exposed males, then used these samples in an established IVF protocol (Nakagata, 2011) (Fig. 2.1A). Using a physiologically relevant, prolonged version of the limited access Drinking in the Dark model, we exposed postnatal day 90, C57BL/6J male mice to 6% and 10% (w/v) ethanol (EtOH) treatments. We have previously found that these treatments exert dose-dependent effects on offspring placental growth and histology, with the 6% treatment increasing litter average placental weights while the 10%

treatment (2.1–4.86 g/kg) was associated with placental growth restriction (Thomas et al., 2022). We exposed Control males to water alone and ensured identical handling by concurrently switching between two identical water bottles. We maintained treatments for 6 weeks, then bred exposed males to naïve C57BL/6J dams during a 3-week mating phase while maintaining the preconception treatments. We did not observe any differences in fluid consumption between the Control and EtOH treatment groups (Fig. 2.1B). During the 3-week breeding phase, a subset of the exposed males produced litters (Supplemental Table 2 in Appendix A). After resting for 1 week, we sacrificed exposed males at 10 weeks of total exposure, then collected and cryopreserved the sperm (Nakagata, 2011). Males in the 6% EtOH treatment group received an average daily dose of 1.7 g/kg, while males in the 10% EtOH treatment group received an average daily dose of 2.2 g/kg (Fig. 2.1C). Consistent with our previous studies using this model, plasma alcohol concentrations averaged ∼100 and ∼115 mg/dl for the 6% EtOH and 10% EtOH treatment groups, respectively (data not shown). We did not observe any difference in weekly weight gain between treatment groups (Fig. 2.1D).

2.3.2 **Preconception Paternal Alcohol Use Reduces IVF Embryo Survival and Pregnancy Success Rates**

Using sperm isolated from treated males, we employed an established IVF protocol (Nakagata, 2011) to generate preimplantation embryos. Despite the potential for stressors associated with superovulation and *in vitro* embryo culture to obscure paternal epigenetic effects on offspring development, we found that, compared with Control IVF offspring, embryos generated using alcohol-exposed sperm exhibited decreased development rates and survival. For example, compared to sperm isolated from Control males, we observed a dose-dependent

($P > 0.0134$) decrease in fertilization rates, as measured by the generation of one-cell zygotes after 36 h of culture (Table 1). However, we did not observe any significant differences in the number of one-cell transitioning to two-cell stage embryos (Table 2). We transferred two-cell stage embryos into naïve recipient dams and examined pregnancy rates at gestational day 16.5, a developmental phase where we have previously characterized alcohol-induced alterations to fetoplacental growth and patterning (Bedi et al., 2019; Thomas et al., 2021, 2022). Preconception paternal EtOH exposure significantly decreased both the number of surviving offspring from each embryo transfer (Fig. 2.2A) and the total number of two-cell embryos surviving to gestational day (GD)16.5 (Table 3), with the 6% EtOH treatment group exhibiting a 24% decline and the 10% EtOH treatment group displaying a 32% reduction in total embryo survival, compared to sperm derived from males in the Control treatment. In contrast to our previous studies, which did not identify any impacts on litter size (Chang et al., 2017, 2019b; Bedi et al., 2019; Thomas et al., 2021, 2022), both the 6% EtOH and 10% EtOH IVF treatment groups exhibited reductions in the number of live offspring (Fig. 2.2B). Finally, we observed a significant (Chi-square analysis, $P = 0.0448$) reduction in our pregnancy success rates, with the 6% EtOH treatment displaying a 20% decline, while pregnancy rates from the 10% EtOH treatment were half those of the Control treatment (Fig. 2.2C). For the full dataset, please see Supplemental Table 3 in Appendix A. These results demonstrate that chronic preconception male alcohol use significantly decreases IVF embryo survival and pregnancy success rates.

Table 1

Fertilization success rates.

Sire treatment	# oocytes	# oocytes to one-cells	% success
Control	967	515	53.25%
6% EtOH	1296	589	45.44%*
10% EtOH	1837	707	38.48%****,#

Number of one-cell embryos after 4 h culture. Comparisons to Control. * $P < 0.05$, **** $P < 0.0001$; comparing 6% EtOH to 10% EtOH. # $P < 0.05$.

Table 2

Developmental progression of one-cell embryos to the two-cell stage.

Sire treatment	# one-cells	# one-cells to two-cells	% success
Control	515	441	85.63%
6% EtOH	589	506	85.90%
10% EtOH	707	625	88.40%

Table 3

Embryo success rate.

Sire treatment	# two-cells transferred	# GD 16.5 live offspring	% success
Control	197	90	45.69%
6% EtOH	301	66	21.93%****
10% EtOH	414	57	13.77%****,#

Total number of two-cell embryos transferred compared to the number of live offspring at gestational day 16.5. Comparisons to Control.**** $P < 0.0001$; comparing 6% EtOH to 10% EtOH. # $P < 0.05$.

2.3.3 **Paternal Alcohol Exposures Disrupt Embryonic Gene Expression Patterns**

To better understand the molecular basis of the reduced IVF success rates, we used deep sequencing to contrast the embryonic transcriptome between the three treatment groups. Previous studies demonstrate that IVF procedures alter the allocation of cells between the embryonic and extraembryonic lineages, disrupting the earliest phases of placental development initiated at the blastocyst stage (Bai et al., 2022). We suspected that alcohol might exacerbate these molecular changes and wanted to determine their developmental origins. Therefore, we focused our analyses on the morula stage, which precedes differentiation into the founding lineages. To this end, we pooled 10–15 morulae per male, isolated RNA, sequenced the generated cDNA libraries (n = 3 per treatment), and compared gene expression patterns using DESeq2. After adjusting for false discovery (log2-fold change, *q*-value < 0.05), our analysis identified a small number of DEGs between treatment groups (16 Control vs 6% EtOH, 35 Control vs 10% EtOH, and 30 6% EtOH vs 10% EtOH). Of note, when comparing the 10% EtOH treatment to Controls, we identified increased enrichment of transcripts encoding genes functioning as critical regulators of trophectoderm stem cell growth and placental patterning, including Fibroblast growth factor 4 (*Fgf4*), epidermal growth factor receptor (*Egfr*) and Marvel domain containing 1 (*Marveld1*) (Tanaka et al., 1998; Chen et al., 2016, 2018) (Supplemental Table 4 in Appendix A). These observations suggest that preconception paternal alcohol exposures may disrupt critical pathways regulating placental development.

To further understand the impacts of paternal drinking on embryonic development, we relaxed the stringency of our informatic analysis to include genes with an unadjusted *P*-value of <0.05 and used this list to conduct Ingenuity Pathway Analysis (Jiménez-Marín et al., 2009). Using these criteria, we found a wide variation in embryonic gene expression patterns, with

largely distinct sets of genes and genetic pathways emerging across comparisons between the Control—6% EtOH, Control—10% EtOH, and 6% EtOH—10% EtOH treatments (Fig. 2.3A-H). Importantly, in our comparisons of morulae derived from the 6% EtOH and 10% EtOH treatment groups, we identified alterations in genetic pathways associated with mitochondrial dysfunction, oxidative phosphorylation and Sirtuin signaling (Fig. 2.3I). We have previously identified disruptions in these same pathways in the gestational day 16.5 placentae of naturally conceived offspring sired by alcohol-exposed males (Thomas et al., 2021, 2022).

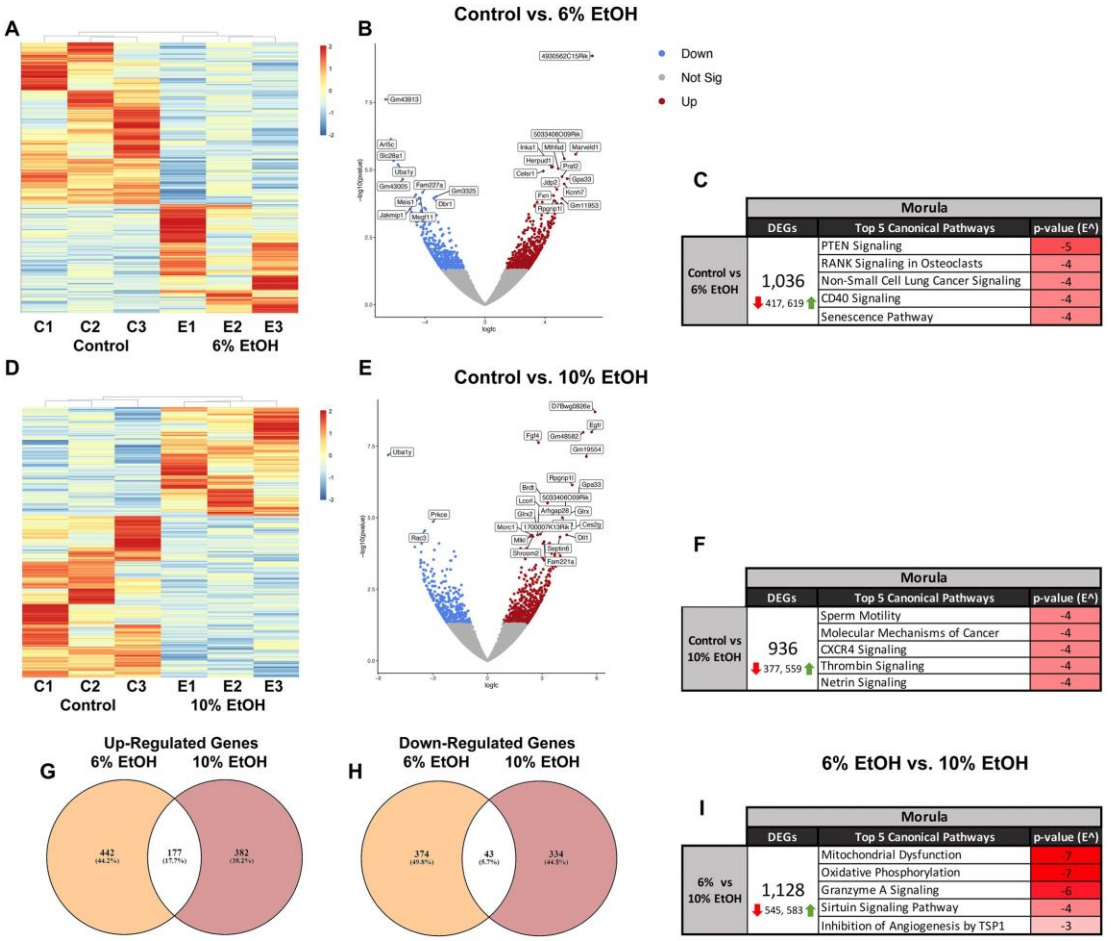

Figure 2.3. Chronic paternal alcohol exposures induce changes in morula-stage embryonic gene expression patterns. Analysis of differential patterns of embryonic gene expression between Control and 6% EtOH morulae: (A) heatmap comparing gene expression patterns, (B) volcano plot contrasting down- and upregulated differentially expressed genes and (C) ingenuity pathway analysis of differentially expressed genes. Comparison of embryonic gene expression patterns between Control and 10% EtOH morulae: (D) Heatmap comparing gene expression patterns, (E) volcano plot contrasting down- and upregulated differentially expressed genes and (F) ingenuity pathway analysis of differentially expressed genes. Venn diagrams comparing the number of overlapping (G) upregulated and (H) downregulated differentially expressed genes between treatment groups. Baseline comparisons were made to the Control treatment. (I) Ingenuity pathway analysis comparing differentially expressed genes identified between the 6% EtOH and 10% EtOH treatment groups. C1, C2, and C3 reference Control samples 1 through 3, while E1, E2, and E3 reference EtOH samples 1 through 3. (For the analysis presented above, we selected differentially expressed genes exhibiting a log2-fold change and unadjusted P-value of <0.05, n = 3 pools of 10–15 morulae per treatment.)

2.3.4 **Preconception Paternal Alcohol Exposure Alters the Growth and Development of IVF Offspring**

We next examined the impact of paternal alcohol exposure on IVF fetal offspring growth and development at gestational day 16.5. Despite observing smaller litter sizes (6% EtOH *P*-value = 0.0265, 10% EtOH *P*-value = 0.0039), we did not observe any significant impacts of paternal EtOH exposure on gestational sac weights or fetal weights (Fig. 2.4A and B). However, we did observe reductions in fetal crown-rump lengths for the male offspring of alcohol-exposed sires (Fig. 2.4C). However, we only observed these differences when comparing individual offspring, not litter averages. Next, we compared offspring normalized organ weights to determine whether paternal EtOH could induce programmed changes in organogenesis. We did not observe any differences in normalized brain weights (Fig. 2.4D). However, male IVF offspring from the 10% EtOH group displayed reduced heart weights (Fig. 2.4E). Interestingly, male and female offspring generated using sperm from alcohol-exposed sires displayed reduced thymic weights (Fig. 2.4F). The 6% EtOH and 10% EtOH treatment groups both displayed reduced thymic weights in males, while in the female offspring, only the 10% EtOH treatment group was significantly different. These observations indicate that paternal alcohol use programs dose and sex-specific changes in IVF offspring growth and organogenesis.

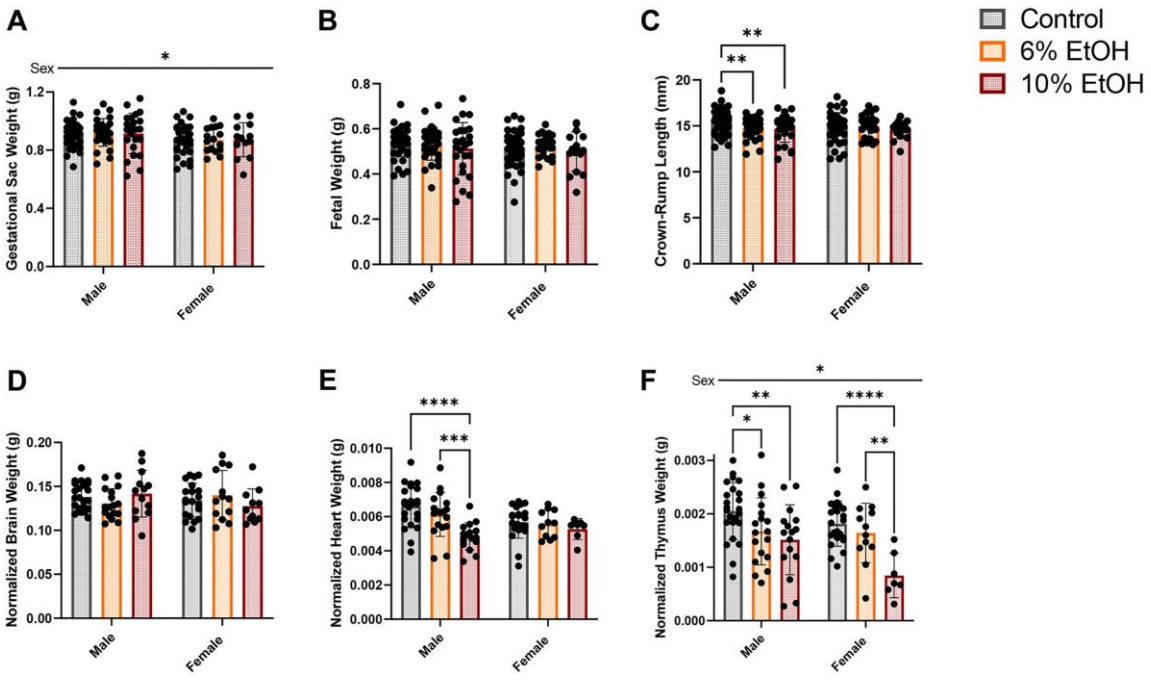

Figure 2.4. Chronic paternal ethanol exposure alters IVF-embryo growth and organ development. Comparison of gestational day 16.5 (A) gestational sac weights, (B) fetal weights, and (C) crown-rump lengths between treatment groups (n = 45 Control, 31 6% EtOH, 26 10% EtOH male offspring; n = 44 Control, 23 6% EtOH, 16 10% EtOH female offspring). Comparison of body weight-normalized (D) brain weights, (E) heart weights and (F) thymus weights between IVF offspring generated using sperm derived from Control and EtOH-exposed males. We randomly selected approximately two male and two female offspring from each litter to examine organ weights (n = 23 Control, 17 6% EtOH, 13 10% EtOH male offspring; 20 Control, 13 6% EtOH, 7–11 10% EtOH female offspring). We used a two-way ANOVA to contrast differences between sex and treatment or Kruskal–Wallis test, depending on the normality of the data. Sex differences are indicated above the figures, while treatment effects are demarcated directly above the bar graphs. Error bars represent the standard error of the mean, *P < 0.05, **P < 0.01, ***P < 0.001, ****P < 0.0001.

2.3.5 **Paternal Ethanol Exposure Modifies the Histological Organization of IVF-Offspring Placentae**

Given the identified up-regulation of genes controlling trophoblast differentiation and placental patterning, we next examined the gestational day 16.5 placenta. In contrast to our previous studies examining naturally conceived offspring (Bedi et al., 2019; Thomas et al., 2021, 2022), we did not observe any influence of paternal alcohol exposure on placental weights and only modest effects on placental diameter and placental efficiency (Fig. 2.5A−C). Notably,

we did not observe any differences when comparing litter averages, only when comparing individual offspring. Previous studies demonstrate that IVF procedures induce changes in placental histoarchitecture (Collier et al., 2009; Delle Piane et al., 2010; Bloise et al., 2012; de Waal et al., 2015; Tan et al., 2016; Dong et al., 2021; Bai et al., 2022). Similarly, we have found that chronic paternal EtOH exposures program male-specific changes in the histological organization of the placenta (Thomas et al., 2021, 2022). Therefore, we stained male and female placentae from each treatment group with phosphotungstic acid to enhance tissue contrast and then used microCT imaging to quantify the volumes of the different placental layers (Lesciotto et al., 2020).

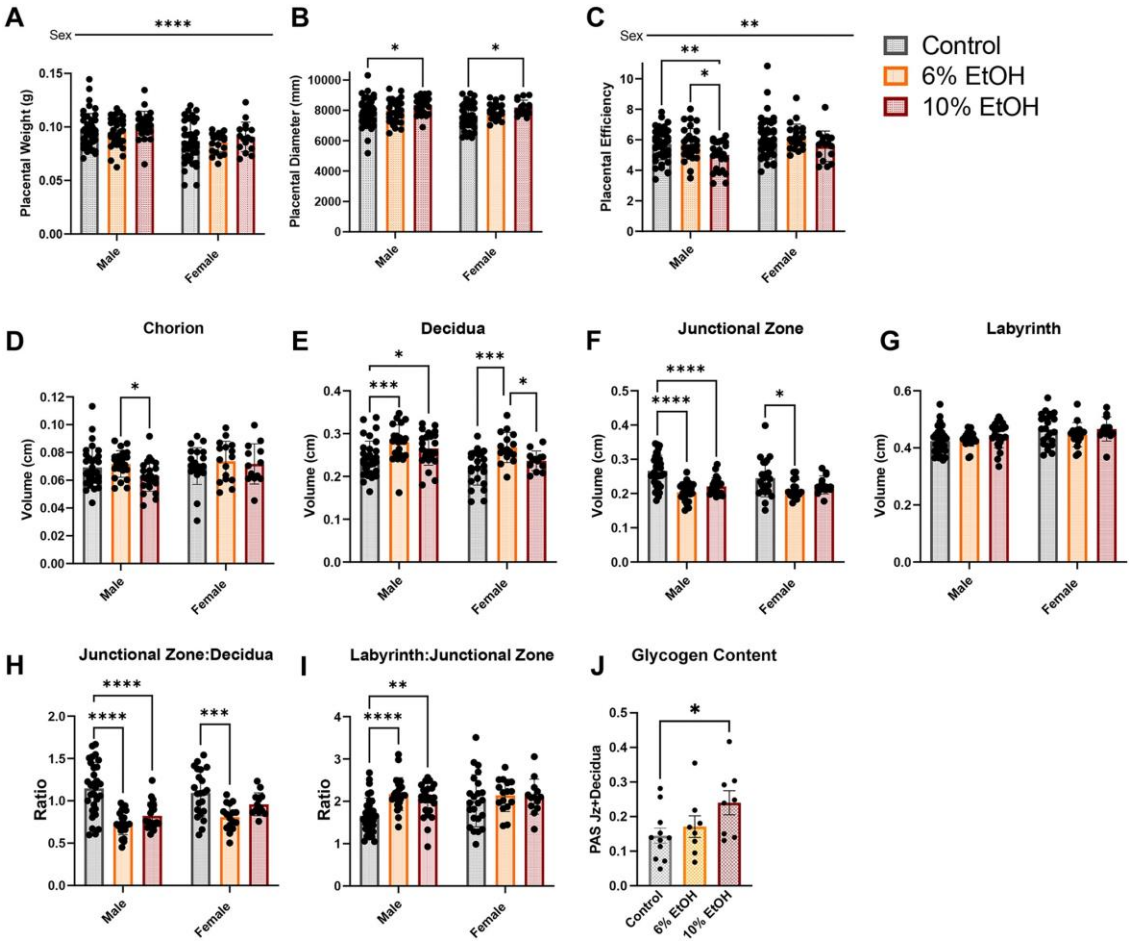

Figure 2.5. Preconception paternal alcohol exposure alters IVF-embryo placental development. Comparison of (A) placental weight, (B) placental diameter and (C) placental efficiency between IVF offspring generated using sperm derived from Control and EtOH-exposed males (n = 45 Control, 31 6% EtOH, 26 10% EtOH male offspring; n = 44 Control 23, 6% EtOH 16, 10% EtOH female offspring). Using microCT, we measured the proportional volume of each placental layer and used a two-way ANOVA to compare measures between male and female offspring across treatment groups. Volumes for the (D) chorion, (E) decidua, (F) junctional zone and (G) labyrinth are expressed as a ratio of the total placental volume. We randomly selected placentae from each litter to examine histological changes (n = 32 Control, 23 6% EtOH, 23 10% EtOH males; 23 Control, 16 6% EtOH, 13 10% EtOH females). Ratios comparing the proportional volumes of the (H) junctional zone to decidua and (I) labyrinth to junctional zone between male and female offspring across treatment groups. (J) Quantification of placental glycogen content in male offspring. PAS-stained area normalized to the decidua and junctional zone area, compared between treatment groups (n = 11 Control, 8 6% EtOH and 8 10% EtOH). Sex differences are indicated above the figures, while treatment effects are demarcated directly above the bar graphs. Error bars represent the standard error of the mean, *P < 0.05, **P < 0.01, ***P < 0.001, ****P < 0.0001.

In contrast to our previous studies examining placentae derived from EtOH-exposed sires, we did not observe any differences in the proportional volumes of the chorion or the labyrinth layers (Fig. 2.5D and G). We did, however, observe increases in the maternal decidua and decreases in the fetal junctional zone (Fig. 2.5E and F). Unexpectedly, compared to our previous studies, which identified male-specific changes in placental histology, we observed histological changes in the decidua and junctional zone, as well as proportional changes in the labyrinth junctional zone, in both sexes (Fig. 2.5H and I). Finally, reductions in the junctional zone may be due to decreased phosphotungstic acid staining arising from increased glycogen content. Further, IVF procedures are known to increase the glycogen content of the placenta (Dong et al., 2021). Therefore, we utilized PAS-stained tissue sections to quantify placental glycogen levels in male placentae. These analyses identified a significant increase ($P < 0.05$) in glycogen levels in placentae isolated from male offspring in the 10% EtOH treatment group but not in the 6% EtOH treatment (Fig. 2.5J). We did not observe any differences in the number of glycogen islands in the labyrinth layer between treatment groups (data not shown). Our morphometric and histological data reveal that the IVF offspring of EtOH-exposed sires display histological changes in placental patterning and increases in placental glycogen beyond those induced by IVF procedures (Dong et al., 2021) and that, unlike natural matings, female IVF offspring also display EtOH-induced changes.

2.3.6 **Chronic Male Alcohol Exposure Disrupts IVF-Embryo Placental Gene Expression**

Our comparisons of embryonic gene expression patterns between morulae derived from the 6% EtOH and 10% EtOH treatment groups identified alterations in genetic pathways associated with mitochondrial dysfunction, oxidative phosphorylation and sirtuin signaling.

Given our previous identification of these gene sets and altered imprinted gene expression in placentae derived from alcohol-exposed males using natural matings (Thomas et al., 2021, 2022), we assayed Control and 10% EtOH placentae to determine if this same transcriptional signature presents in IVF embryos. RT-qPCR analysis confirmed the disruption of multiple imprinted genes and genes involved in the identified pathways in placentae derived from IVF offspring (Fig. 2.6). These data reveal the persistence of an alcohol-induced transcriptional signature in placentae derived from IVF offspring generated using alcohol-exposed sperm.

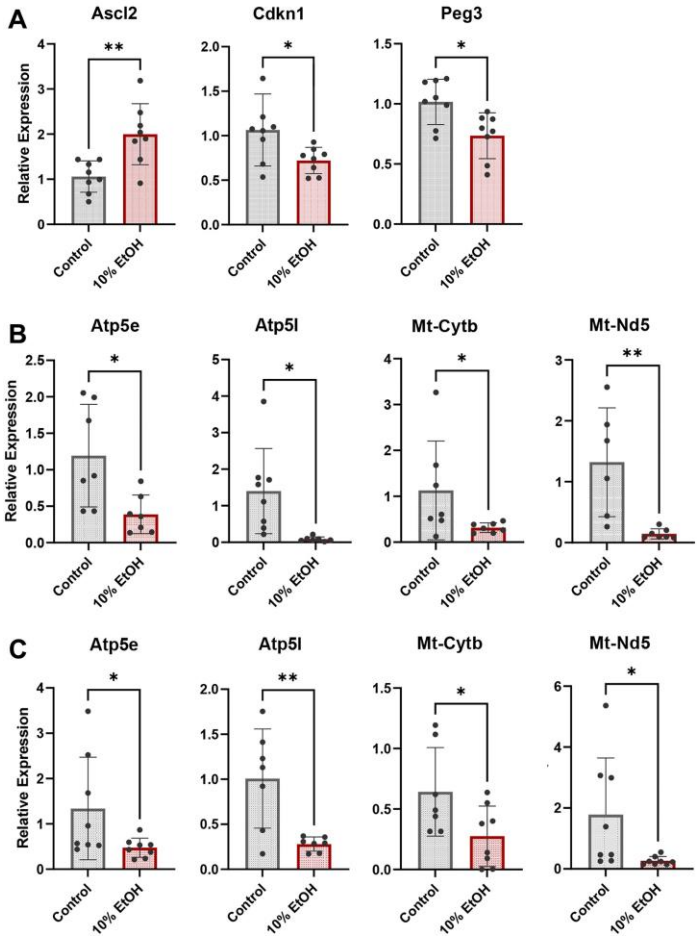

Figure 2.6. IVF placentae derived from alcohol-exposed males exhibit transcriptional changes in select imprinted and mitochondrial genes. (A) Analysis of imprinted gene expression in the placentae of the male offspring of Control and 10% EtOH-exposed sires. Comparison of mitochondrial-encoded transcripts in placentae of (B) male and (C) female IVF offspring derived from Control and 10% EtOH treated males. We analyzed gene expression using RT-qPCR. Gene expression was normalized to transcripts encoding Pgk1 and Ywhaz; (n = 8). For analysis, we used an unpaired, parametric (two-tailed) t-test or a Mann–Whitney test (unpaired, non-parametric t-test) if the data failed the test for normality. Error bars represent the standard error of the mean, *P < 0.05, **P < 0.01.

2.4 **Discussion**

Emerging biomedical and clinical evidence convincingly demonstrates that epigenetic factors carried in sperm significantly influence the health of future generations (Lane et al., 2014; Fleming et al., 2018). However, across the spectrum of male reproductive biology, there is a foundational lack of knowledge concerning the impacts of epigenetic processes on sperm

production and their heritable influences on embryonic development. This knowledge gap impedes our ability to recognize the importance of paternal health in the development of birth defects and disease, as well as larger aspects of male infertility. Consequently, through their maternal-centric focus, the medical community perpetuates the stigma that birth defects are exclusively the woman's fault and create an imbalance in clinical practice that forces females to bear the burden of male infertility (Barratt et al., 2018). This inequity is especially evident in fertility clinics where the perception that IVF success rates are the exclusive consequence of maternal health and lifestyle while, in contrast, men are given a 'free pass', and paternal periconceptional health and lifestyle choices are neither scrutinized nor recorded.

Using a physiologically relevant mouse model of chronic ethanol exposure, our study demonstrates that paternal alcohol use significantly reduces IVF embryo survival and pregnancy success rates. Furthermore, these adverse outcomes are associated with alterations in embryonic gene expression and downstream placental dysfunction, suggesting an epigenetic memory of preconception alcohol use transmits through sperm, disrupting the formation and function of the placenta. Given the higher prevalence of preterm birth, lower birth weights and congenital disabilities in IVF children (Chang et al., 2020) and that chronic male alcohol use is widespread (Naimi et al., 2003), we must investigate the impacts alcohol-induced alterations in sperm epigenetic programming have on IVF embryo growth and development. Further, given the established influences of poor placentation on infant health and adult onset of disease (Burton et al., 2016), a better understanding of the impacts paternal alcohol use has on placental biology may help explain why the life expectancy of people with fetal alcohol syndrome is 34 years, less than half of the broader population (Thanh and Jonsson, 2016).

Our studies utilized C57Bl6/J mice, which, although an established model for studying the teratogenic effects of alcohol (Petrelli et al., 2018), are an inbred strain exhibiting comparatively poor fecundity (Rennie et al., 2012). Using this genetic background, preconception paternal alcohol exposures reduced embryo development rates to the point that obtaining the requisite number of litters required for our analysis necessitated conducting 1.5× to 2× the number of embryo transfers (Fig. 2.2C). Although mouse models do not strictly translate to humans (mice metabolize alcohol 5.5 times faster than men and, therefore, require higher doses to feel the effects (Jeanblanc et al., 2019)), the average daily dose observed in the 6% treatment group (1.7 g EtOH/kg of body weight) is roughly equivalent to a 75 kg man drinking two and a quarter beers per hour for 4 h (total of 9), while the 10% treatment (2.2 EtOH/kg body weight) is equivalent to a 75 kg man consuming 12 beers in 4 h, both of which are exposure levels commonly observed among US males (Naimi et al., 2003; White et al.,, 2006; Kanny et al., 2018). Therefore, if these data translate to humans, our research suggests that preconception paternal alcohol use may be an unappreciated yet easily modified factor that significantly impedes IVF success rates, increasing patient financial burden and emotional stress.

The junctional zone, located between the maternal decidua and the fetal labyrinth layer, functions as the endocrine component of the murine placenta, releasing a diverse suite of hormones, cytokines and growth factors, but also serves as the primary energy reserve via the storage of glycogen (Woods et al., 2018). Previous studies have confirmed that the proportional size of the junctional zone significantly affects fetal growth. For example, gene loss-of-function and overexpression mouse models reveal that reductions, expansion or mislocalization of junctional zone glycogen cells correlate with fetal growth restriction (Li and Behringer, 1998; Rampon et al., 2008; Esquiliano et al., 2009; Tunster et al., 2016a,b). Additionally,

experiments comparing offspring derived using *in vitro* embryo culture to naturally conceived offspring or maternal hypoxia reveal a late-term enlargement of the junctional zone and reductions in fetal weights (de Waal et al., 2015; Higgins et al., 2016; Vrooman et al., 2020, 2022). In contrast, reductions in the junctional zone arise in mouse models of maternal nutrient restriction (Coan et al., 2010; Sferruzzi-Perri et al., 2011).

Here, we provide new data describing the impact of preconception paternal EtOH exposures on IVF placental morphology and fetal growth. IVF offspring of alcohol-exposed sires exhibited a decrease in the junctional zone and the proportional relationship to the decidua (Fig. 2.5F and H). Therefore, the histological changes we observe in the offspring of alcohol-exposed sires contrast with the changes normally induced by IVF and more closely resemble the relative changes induced by starvation or hypoxia. However, we did not observe any changes in fetal weights between treatments, possibly due to the reductions in litter size. These results suggest that the volume of the junctional zone and glycogen cell quantities are modified when the sire regularly consumes alcohol before an IVF procedure. However, whether this altered phenotype results from placental dysfunction or as a compensatory modification is unknown and remains to be elucidated.

Although compelling, there are several limitations to our study. First, we and others have observed alcohol-induced alterations in sperm non-coding RNAs and post-translational histone modifications but not DNA methylation (Chang et al., 2017; Rompala et al., 2018; Bedi et al., 2019, 2022). However, the current study does not reveal which epigenetic factors carried in sperm are responsible for transmitting the observed phenotypes. Further, we do not know whether factors transported in the seminal plasma of alcohol-exposed males may also influence pregnancy outcomes (Bromfield et al., 2014). Consequently, we do not know which phases of

sperm production or maturation are impacted by alcohol and, therefore, cannot make informed recommendations as to the duration of time that may be required for the epigenetic impacts of alcohol to dissipate. Second, the processes of superovulation and *in vitro* embryo culture are known to disrupt maternal epigenetic factors regulating development and alter placental histoarchitecture (Collier et al., 2009; Delle Piane et al., 2010; Bloise et al., 2012; de Waal et al., 2015; Tan et al., 2016; Dong et al., 2021; Bai et al., 2022). Therefore, we do not know how much of the phenotypic changes or alterations in embryonic gene expression are directly attributable to paternal alcohol exposures versus a combinatorial interaction with ARTs. Third, because our IVF protocol prioritized the transfer of two-cell embryos, we only examined embryonic development to this stage and harvested the remaining morulae for transcriptomic analysis. Therefore, our embryological analysis does not address the observed pregnancy loss after the two-cell stage, nor do our experiments faithfully mimic human IVF studies, which focus on blastocyst stage outcomes. We require additional studies to determine how paternal alcohol use impacts blastocyst cell lineage specification, development rates and quality, and to determine how this may impact post-implantation survival. Fourth, we selected the 6% EtOH and 10% EtOH treatments as the average daily dose for these treatments (1.7 g/kg for 6% EtOH and 2.2 g/kg for 10% EtOH) spanned the previously described moderate and heavy drinker threshold; moderate daily doses (1.14–2.0 g/kg/day) were associated with increases in litter average placental weights while heavy drinking (2.1–4.86 g/kg/day) associated with placental growth restriction (Thomas et al., 2022). In our experiments, both treatments inhibited IVF success rates and altered placental histology, while neither treatment impacted litter average placental weights. Further, although we observed some overlap in altered embryonic gene expression between the 6% EtOH and 10% EtOH treatments (Fig. 2.3G and H), it was minimal, suggesting different doses exert

distinct impacts on the embryonic transcriptional program. A further limitation of this study was that we pooled morulae and could not separate male and female embryos. Thus, the transcriptional differences we describe may be confounded by an unequal representation of male and female embryos across treatments, although we did not observe any changes at GD16.5. Future studies will examine the time required for alcohol-induced changes in the sperm-inherited developmental program to dissipate and which epigenetic signals may drive the inheritance of these phenotypes and will employ single-cell sequencing approaches to more rigorously examine embryonic gene expression patterns.

The planning status of a pregnancy has a substantial impact on maternal behavior, which in turn, has a positive influence on infant health at birth (Institute of Medicine (US) Committee on Unintended Pregnancy, 1995; Kost et al., 1998; Mohllajee et al., 2007). Accordingly, maternal education on topics like the benefits of folic acid intake has helped significantly increase children's health (Prevention and Health, 2000). However, in the USA, 70% of men drink, and 40% engage in repetitive patterns of binge drinking (Naimi et al., 2003; White et al., 2006; Kanny et al., 2018). Although half of pregnancies are unplanned (Henshaw, 1998), many male partners are heavily engaged in family planning, particularly with couples struggling with infertility (Kost et al., 1998; Mohllajee et al., 2007). Our work, combined with other published studies (Klonoff-Cohen et al., 2003; Rompala and Homanics, 2019), indicates that we need to expand health messaging around prepregnancy planning to include the father and change IVF clinical practice to emphasize the dangers of periconceptional alcohol use by both parents.

3. ALTERATIONS IN SPERM RNAS PERSIST AFTER ALCOHOL CESSATION AND CORRELATE WITH EPIDIDYMAL MITOCHONDRIAL DYSFUNCTION

3.1 **Introduction**

Preconception exposures are an emerging area of interest in our efforts to understand the developmental origins of birth defects, disease, and neurological dysfunction (Fleming et al., 2018; Rompala and Homanics, 2019). Although researchers have long recognized the importance of preconception maternal health in pregnancy and child developmental outcomes, paternal exposures have only recently emerged as significant modifiers of placental function and offspring development (Bhadsavle and Golding, 2022; Lismer and Kimmins, 2023). Indeed, researchers now recognize that sperm contain a vast suite of epigenetic information (Le Blévec et al., 2020; Lee and Conine, 2022) and that a wide range of different stressors, including nutritional deficiencies or excess, inflammation, drugs of abuse, environmental toxicants, and psychological trauma, each modifies the sperm-inherited epigenome, with adverse impacts on offspring health (Braun et al., 2017; Donkin and Barrès, 2018; Soubry, 2018; Rompala and Homanics, 2019; Senaldi and Smith-Raska, 2020; Jawaid et al., 2021; Yin et al., 2022). Nevertheless, although we now recognize these influences, the biochemical mechanisms by which the epigenetic memories of paternal experiences and stressors influence fertility and transmit to offspring remain almost completely undefined.

One of the key outstanding questions in the field of paternal epigenetic inheritance concerns the resilience of the male reproductive tract and the germline's capacity to recover and correct sperm-inherited epigenetic errors after stressor withdrawal. Previous studies demonstrate that while some stressors exert transient impacts on overall male fertility, others permanently

affect sperm production and fecundity. For example, male exposures to anabolic steroids, heat stress, and COVID-19 infection each induce transient reductions in fertility that reverse after approximately one spermatogenic cycle (El Osta et al., 2016; Hamilton et al., 2016; Alves et al., 2021; Shcherbitskaia et al., 2022). Similarly, cessation from smoking and chronic alcohol use also associate with improvements in fertility, although the duration of recovery may extend across multiple spermatogenic cycles, depending on the severity of drug use (Vicari et al., 2002; Sermondade et al., 2010; Sansone et al., 2018; Tang et al., 2019; Kulaksiz et al., 2022). In contrast, infertility induced by male chemotherapy and radiotherapy treatments may persist for several years or be permanent (Meistrich, 2013; Okada and Fujisawa, 2019). However, although stressor or toxicant withdrawal generally associates with improvements in macro measures of male fertility, whether these exposures induce lasting changes to the sperm-inherited developmental program or if exposure-induced epigenetic errors self-correct after cessation remains unknown.

In the United States, 70% of men drink, and 40% engage in repetitive binge drinking (Naimi et al., 2003; White et al., 2006; Kanny et al., 2018). Moreover, men are likelier than women to engage in risky alcohol use patterns and less likely to modify their preconception behaviors when considering fatherhood (Esser et al., 2014). Clinical studies provide conflicting data on the impacts of alcohol intake on male fertility, with some studies suggesting modest declines while others report no observable effects (Pajarinen et al.,1996; Gümüş et al.,1998; Muthusami and Chinnaswamy, 2005; Jensen et al., 2014; Condorelli et al., 2015; Van Heertum and Rossi, 2017). Nonetheless, clinical studies examining high-level, chronic exposures demonstrate adverse impacts on overall health, increases in systemic oxidative stress, and decreases in fertility (Finelli et al., 2021). Notably, a small number of studies suggest that the

varied effects of alcohol on fertility across human populations may link to genetic differences in the capacity to mitigate oxidative stress, specifically polymorphisms in Glutathione S-transferase (Pajarinen et al., 1996; Finelli et al., 2021). However, even in cases of heavy chronic alcohol use disorder, patients demonstrate improvements in overall fertility after withdrawal (Vicari et al., 2002; Sermondade et al., 2010).

Using a mouse model, our group has demonstrated that chronic preconception paternal alcohol exposures induce dose-dependent changes in placental patterning, defects in craniofacial development, and long-term effects on glucose homeostasis (Chang et al., 2017; Chang et al., 2019a; Bedi et al., 2019; Chang et al., 2019b; Thomas et al., 2021; Bedi et al., 2022; Thomas et al., 2022; Roach et al., 2023; Thomas et al., 2023). In these previous studies, we did not observe any differences in sperm count, morphology, or offspring litter size (Chang et al., 2017; Chang et al., 2019a; Bedi et al., 2019; Thomas et al., 2021; Thomas et al., 2022; Thomas et al., 2023). However, using an *in vitro* fertilization system to model the impacts of paternal alcohol use on early embryonic development, we observed that chronic ethanol exposures reduce embryo development and pregnancy success rates in a dose-dependent manner (Roach et al., 2023). These intergenerational effects on fertility and offspring development correlate with alcohol-induced alterations in sperm-inherited noncoding RNAs and histone structure but do not associate with any significant changes in DNA methylation (Chang et al., 2017; Bedi et al., 2019; Bedi et al., 2022). Significantly, the Homanics group has also identified alcohol-induced changes in sperm noncoding RNAs using a vapor chamber exposure model, reinforcing the assertion that paternal ethanol exposures affect sperm small noncoding RNA abundance (Rompala et al., 2018). These reports join a growing body of clinical and preclinical studies indicating paternal alcohol use induces heritable epigenetic changes in offspring phenotypes that

correlate with fetal alcohol spectrum disorder (FASD) behavioral, neurological, and structural defects (Rompala and Homanics, 2019; Little and Sing,1987; Zuccolo et al., 2016; Xia et al. 2018; Peng et al., 2019; Zhang et al., 2020; Zhou et al., 2021; Montagnoli et al., 2021). However, whether, like clinical studies examining measures of overall fertility, alcohol withdrawal ameliorates the observed epigenetic changes in sperm is not known.

Two previous reports, including work from our group, identified alcohol-induced changes in sperm noncoding RNAs (Bedi et al., 2019; Rompala et al., 2018). Herein, we examined the impacts of cessation from chronic alcohol exposure on sperm small noncoding RNA abundance. The trafficking of sperm noncoding RNAs primarily occurs during epididymal transit (Montagnoli et al., 2021); in mice, this transit occurs across a ten-day period(Adler, 1996). However, previous studies examining mouse models of binge drinking demonstrate that the negative impacts of alcohol withdrawal, including anxiety- and depressive-like disturbances and molecular alterations in neurological activity, last for at least three weeks (Lee et al., 2015; Tonetto et al., 2023). Therefore, we hypothesized that alcohol cessation for one month would allow for the normalization of EtOH-induced changes in the sperm noncoding RNA profile. Instead, our analyses reveal that chronic alcohol exposures induce a molecular signature of mitochondrial dysfunction. Notably, even after one month of abstinence, elements of this signature remain in the corpus segment of the epididymis, and significant differences in the sperm noncoding RNA profile remain. These data suggest that, like neurological models examining alcohol withdrawal, the male reproductive tract and sperm-inherited epigenetic program continue to exhibit evidence of alcohol-induced disturbance after toxicant removal.

3.2 Materials and Methods

3.2.1 Animal Studies and Ethanol Exposures

We designed our study following ARRIVE guidelines and conducted all experiments following IACUC regulations, with prior approval by the Texas A&M University IACUC, under protocol number 2020-0211. We utilized male C57BL/6J strain mice (RRID:IMSR_JAX:000664), which we derived from a breeder nucleus and housed in the Texas A&M Institute for Genomic Medicine. We maintained males on a standard chow diet (catalog # 2019; Teklad Diets, Madison, WI, USA) with free water access and a reverse 12-hour light/dark cycle (lights off at 8:30 AM). As in our previous studies, we added shelter tubes (catalog # K3322; Bio-Serv, Flemington, NJ, United States) and additional nestlets to minimize animal stress and enhance cage enrichment.

Beginning on postnatal day 90, we individually caged males and initiated the control and ethanol (**EtOH**) treatments using a prolonged version of the Drinking in the Dark model (Boehm et al., 2008). Using published methods (Thomas et al., 2022; Roach et al., 2023), we exposed males to control (water alone), 6% or 10% (w/v) EtOH (catalog # E7023; Millipore-Sigma, St. Louis, MO, USA) treatments, with exposures beginning one hour after the beginning of the active (dark) cycle and lasting for four hours. To ensure identical handling, we simultaneously exchanged water bottles across the control and EtOH treatments. Each week, during the regular cage change, we recorded the weight of each mouse (kg) and the total weekly fluid consumption (g), then calculated their weekly fluid consumption as g of fluid consumed/kg body weight. To analyze tissues and sperm derived from active drinkers, we sacrificed cohort one (n=8 per treatment) after ten weeks of constant EtOH exposure using CO2 asphyxiation followed by cervical dislocation. For cohort two, we ceased the control and EtOH treatments and left the

mice undisturbed for an additional four weeks before sacrifice using CO2 asphyxiation and cervical dislocation, followed by tissue collection of the epididymal caput, corpus, and cauda with 1cm of vas deferens and sperm isolation. We refer to this latter group as the EtOH-Cessation treatment.

3.2.2 **Isolation of Mouse Sperm**

After sacrifice, we surgically isolated the male reproductive tract and separately placed the left and right cauda, with approximately 1 cm of the vas deferens, into one well of a 12-well plate containing 1 mL of warmed (37°C) phosphate-buffered saline (PBS). We extruded sperm from the vas deferens using dissection forceps and made four to five small incisions into the caudal epididymis to allow sperm to swim out. We incubated plates at 37°C for 30 minutes, then pelleted the sperm using centrifugation (3000 g for 5 min). Next, we washed sperm samples in PBS, pelleted the samples again, incubated sperm in somatic cell lysis buffer (SCLB: 0.1% SDS, 0.5% Triton X-100) on ice for 30 minutes, pelleted samples by centrifugation (3000 g for 5 min at 4°C) and conducted a second wash in SCLB. Next, we diluted a 10 µL aliquot 1:50 in distilled water (diH_2O) confirmed sample purity by microscopy, and determined sperm concentration using a Neubauer chamber slide. Lastly, we centrifuged isolated sperm at 3000 G-force at 4°C for 5 min, washed samples in PBS, snap-froze the sperm pellets, and stored them at -80°C.

3.2.3 **Nucleic Acid Isolation - Tissues**

We isolated DNA from tissue samples using the DNeasy Blood and Tissue kit (catalog # 69506; Qiagen, Germantown, MD, USA) and RNA using the RNeasy Plus mini kit (catalog # 74136; Qiagen, Germantown, MD, USA), following the manufacturer-recommended protocol.

3.2.4 **RNA Isolation - Sperm Small RNAs**

We isolated sperm RNAs following the Mansuy lab protocol (Roszkowski and Mansuy, 2021) with modest modifications. After thawing the sperm pellet on ice for 15 min, we resuspended the pellet in 100 µl of Buffer RLT (catalog # 74136; Qiagen, Germantown, MD, USA) fortified with 100 mM of 2-mercaptoethanol (catalog # M3148; Millipore-Sigma, St. Louis, MO, USA). After verifying the complete resuspension of the sperm cells, we added 900 µl of Trizol (catalog # 15596018; Thermo-Fisher, Waltham, MA, USA) fortified with 100mM Tris (2-carboxyethyl) phosphine hydrochloride (TCEP) (catalog # C4706; Millipore-Sigma, St. Louis, MO, USA) and vigorously vortexed samples until we could no longer visualize cellular clumps. We then added 200 µl of chloroform-isoamyl alcohol (catalog # 25666; Millipore-Sigma, St. Louis, MO, USA) to the samples, repeatedly mixed by inversion for 30 sec, followed by a rest at room temperature for three minutes. We then centrifuged the samples at 12000 G-force for 15 min at 4°C, then carefully removed the aqueous phase to a fresh RNase-free tube. Next, we added 10 µl of glycogen (catalog # R0551; Thermo-Fisher, Waltham, MA, USA) to the isolated aqueous phase and mixed the samples using inversion. We added one volume of 2-propanol (catalog # I9616; Millipore-Sigma, St. Louis, MO, USA), incubated the tubes for ten minutes at room temperature, then centrifuged the samples at 12000 G-force for 15 min at 4°C to precipitate the RNA and then discarded the supernatant. We washed precipitated RNA pellets with 75% ethanol twice, centrifuging after each wash at 12000 G-force for five minutes at 4°C. After the final wash, we air-dried the pellet and resuspended samples in 50 µl of RNase-free water. To improve the purity of isolated RNA and perform DNAse digestion, we used the Zymo

RNA Clean and Concentrator Kit (catalog # R1013; Zymo Research, Irvine, CA, USA), following the manufacturer-recommended protocol.

3.2.5 **Informatic Analysis Epididymal Tissues**

We isolated total RNA from the caput portion of the epididymis and sent samples to Quick Biology (Pasadena, California, USA) for deep sequencing. We used the open-source, web-based Galaxy server (Afgan et al., 2018) (usegalaxy.org) to process and analyze our data files. We used MultiQC (Ewels et al., 2016) to perform the initial quality control analysis of the raw paired-end, total RNA sequence files and then used Trimmomatic (Bolger et al., 2014) to remove the Illumina sequencing adapters. We used RNA STAR (Dobin et al., 2013) to map the reads to the *Mus musculus* reference genome (UCSC version GRCm39/mm39) and featureCounts (Liao et al., 2014) to determine the read abundance for all genes, followed by annotation versus M27 GTF (GENCODE, 2020). Next, we analyzed the generated featureCounts files and used DESeq2 (Love et al., 2014) to generate the PCA plots and the Volcano Plot function to produce graphical representations of the (log2FC, q-value <0.05) gene expression levels. Finally, we exported differentially expressed genes (log2FC, unadjusted p-value <0.05) into the Ingenuity Pathway Analysis software package and conducted pathway enrichment analysis (Jiménez-Marín et al., 2009; Krämer et al., 2014).

3.2.6 **Informatic Analysis Sperm RNAs**

We sent sperm small RNA samples to Quick Biology (Pasadena, California, USA) for deep sequencing analysis. Small RNA libraries were constructed using the Qiaseq miRNA library kit (catalog # 331502; Qiagen, Germantown, MD, USA) and sequenced to a depth of

approximately 15 million raw reads per sample. We trimmed the raw fastq files using Trimmomatic (Bolger et al., 2014) to remove the Qiagen small RNA adapters and the TESmall package (O'Neill et al., 2018) to map and count small RNA reads. We exported files generated by TESmall into R (version 4.2.1) and performed differential gene expression analysis using the DESeq2 (Love et al., 2014) package. Finally, we used GraphPad Prism 9 to generate the volcano plots.

3.2.7 **Sperm Histone Acid Extraction**

We acid-extracted histones following a previously described protocol (Luense et al., 2016). Briefly, we thawed sperm for 1 hour on ice, then resuspended the sperm pellets in 100 µl of Nuclei Isolation Buffer-250 (NIB-250) with 0.3% NP-40 (10% NP-40, catalog # 85124; Thermo-Fisher, Waltham, MA, USA). We mixed samples by gentle pipetting and incubated them on ice for 5 minutes, then centrifuged samples at 600 G-force at 4°C for five minutes. We repeated this process three times, then resuspended the pellet in 50 µl of 0.4 M sulfuric acid (H_2SO_4) and let the samples incubate on ice for 3 hours. After cold incubation, we centrifuged the samples at 14000 rpm for 5 minutes at 4°C, then precipitated the samples with 25% trichloroacetic acid (TCA). We let the mixture precipitate in a 4°C fridge for 36-48 hours without disturbing the samples. Following the precipitation step, we centrifuged the samples for 5 minutes at 4°C at 14000 rpm, discarded the supernatant, then resuspended the pellet in 50 µl of 100% ice-cold acetone. We centrifuged the samples at 14000 rpm at 4°C and repeated the acetone wash three more times. After the final wash, we allowed the pellets to air dry overnight and resuspended the pellets in 20 µl of diH2O.

3.2.8 **Western Blotting**

We isolated and homogenized tissue protein extracts in a Tris lysis buffer including 50 mM Tris, 1 mM EGTA, 150 mM NaCl, 1% Triton X-100, 1% β-mercaptoethanol, 50 mM NaF, 1 mM Na3VO4; at pH 7.5. We diluted samples in 2x Laemmli buffer and loaded ~20 µg of protein on 15% sodium dodecyl sulfate–polyacrylamide gels, then transferred the separated proteins onto PVDF membranes using a wet transfer system. We separated acid-extracted histones on 15% sodium dodecyl sulfate–polyacrylamide gels and transferred proteins to PVDF membranes. The primary antibodies used in this study were as follows: anti-H3K4me3 (catalog # ab8580; RRID: AB_306649; Abcam, Cambridge, MA, USA) and antiH3 (catalog # ab1791; RRID: AB_302613; Abcam). Finally, we visualized blots using secondary antibodies conjugated to horseradish peroxidase (catalog # sc-2004; RRID: AB_631746; Santa Cruz Biotechnology, Santa Cruz, CA, USA) and an enhanced chemiluminescence detection system (LI-COR, Lincoln, Nebraska USA).

3.2.9 **Quantitative PCR Analysis**

We seeded ~1 µg of RNA into a reverse transcription reaction using the High-Capacity cDNA Reverse Transcription Kit (catalog # 4368814; Thermo-Fisher, Waltham, MA, USA) and determined the relative levels of candidate gene transcripts using the AzuraView GreenFast qPCR Blue Mix LR kit (catalog # AZ-2320; Azura Genomics, Raynham, MA, USA). We measured mitochondrial DNA copy number using primer sequences described previously (West et al., 2015) and the AzuraView GreenFast qPCR Blue Mix LR kit. We measured the mitochondrial D-loop region [D-Loop2 Fwd CCCTTCCCCATTTGGTCT D-Loop2 Rev TGGTTTCACGGAGGATGG; D-Loop3 Fwd TCCTCCGTGAAACCAACAA; D-Loop3 Rev

AGCGAGAAGAGGGGCATT] and normalized measures of mtDNA to genomic DNA by measuring the abundance of the nuclear Tert gene, encoding the catalytic subunit of the telomerase complex [Tert Fwd CTAGCTCATGTGTCAAGACCCTCTT; Tert Rev GCCAGCACGTTTCTCTCGTT]. We describe the data normalization and handling procedures below.

3.2.10 **Data Management**

We managed the data generated in this study using a detailed data management plan that prioritizes safe and efficient data handling. We have stored all data on Google Drive for long-term storage, retrieval, and preservation. We have archived the sequencing files generated from this project in the GEO database under accession number GSE234535 and GSE234834.

3.2.11 **Statistical Analysis**

We initially collected alcohol consumption data and physiological measures for each exposed male by hand and then transcribed these data into Google Sheets or Microsoft Excel, where we collated the data. For qPCR analysis of mitochondrial copy number, we imported the replicate cycle threshold (Ct) values for the DLoop region into Excel, then normalized measures to the nuclear *Tert* gene. We then transferred the physiological and molecular data into the statistical analysis program GraphPad Prism 9 (RRID: SCR_002798; GraphPad Software, Inc., La Jolla, CA, USA), set the statistical significance at alpha = 0.05, used the ROUT test (Q = 1%) to identify outliers, and then verified the normality of the datasets using the Shapiro–Wilk test. If data passed normality (alpha = 0.05), we employed either a One-way or Two-way ANOVA or an unpaired, parametric (two-tailed) t-test. If the data failed the test for normality or we observed

unequal variance (Brown Forsythe test), we ran a Kruskal–Wallis test followed by Dunn's multiple comparisons test or a non-parametric Mann–Whitney test.

3.3 **Results**

3.3.1 **A Clinically Relevant Mouse Model to Determine the Capacity of the Sperm Epigenome to Recover One Month After the Cessation of Alcohol Exposures**

Here, we set out to determine if measures of the sperm-inherited epigenetic program revert to match the control treatment after withdrawing the ethanol-exposed animals from their daily alcohol treatments. To this end, we utilized our limited access model to expose adult C57BL/6J males to alcohol for ten consecutive weeks, encompassing approximately two murine spermatogenic cycles (Alder, 1996). We exposed males to three treatments, consisting of 6% and 10% ethanol (vol/vol EtOH) exposure groups, while we exposed the control group to water alone. After ten weeks, we sacrificed a cohort of exposed males (n=8), which we labeled active drinkers, and collected tissues and sperm. We then stopped the EtOH and Control treatments and left the second cohort of males undisturbed for four weeks, then sacrificed the males and collected tissues and sperm. We refer to this second cohort as EtOH-Cessation males (Fig. 3.1A). We did not observe any differences in the body weights of exposed males across the treatment course (Fig. 3.1B). Although we observed instances of treatment-specific differences in sire weekly fluid consumption across the ten-week treatment (Fig. 3.1C), we did not observe any differences in the average daily EtOH dose between the 6% and 10% EtOH treatments (Fig. 3.1D).

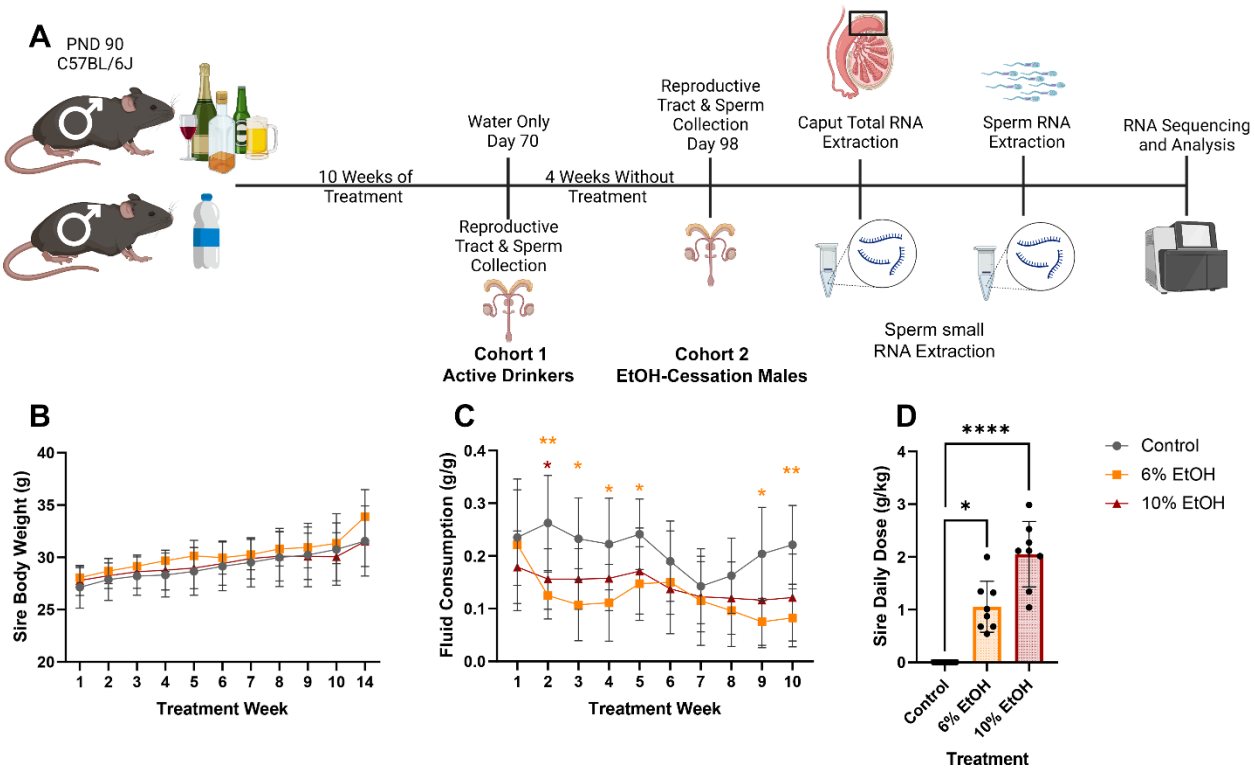

Figure 3.1. A mouse model to determine the capacity of the sperm epigenome to recover one month after the cessation of alcohol exposures. A) Experimental design: We exposed C57BL6/J males to 6% and 10% alcohol for ten weeks, then collected tissues from a cohort of active drinkers (Cohort 1). We then ceased the alcohol exposures, allowed males to recover for four weeks, collected tissues and sperm (Cohort 2), then used RNA-sequencing to compare RNA profiles between treatments. Comparison of male B) average weekly weight gain between treatment groups, C) average weekly fluid consumption, and D) average daily dose of ethanol between treatment groups (n = 8). We compared treatments using either a one-way or two-way ANOVA. Error bars represent the standard error of the mean, *P < 0.05, **P < 0.01, ****P < 0.0001.

3.3.2 **Chronic Alcohol Exposure Induces Altered Gene Expression Patterns in the Caput Section of the Epididymis**

Our group and others have reported differences in the small RNA content of sperm induced by chronic alcohol exposure (Rompala et al., 2018; Bedi et al., 2019). To further understand the physiological basis of these changes, we isolated RNA from the caput epididymis of active drinkers and EtOH-Cessation males across the three treatment groups and conducted deep sequencing analysis of the transcriptome (n=3). Principal component analysis revealed a

clear clustering of each treatment group within the cohort of active drinkers (Fig. 3.2A). In contrast, samples derived from EtOH-Cessation males displayed a wide dispersion with no overt clustering of treatment groups (Fig. 3.2A). Using DESeq2 (Love et al., 2014), we identified the differentially expressed genes (log2FC, q-value <0.05) between treatment groups within each cohort. We observed a dose-dependent increase in the number of differentially expressed genes in active drinkers, with 329 differentially expressed genes in comparisons of Controls to the 6% treatment group and 1423 in comparisons of Control males to the 10% treatment (Fig. 3.2B-C). Pathway analysis of differentially expressed genes (log2FC, p-value <0.05) in the 10% treatment identified alterations in processes linked to mitochondrial dysfunction, oxidative phosphorylation, the generalized stress response (EIF2 signaling), DNA methylation, protein ubiquitination, and Sirtuin signaling (Fig. 3.2D). Finally, we did not observe any significant (log2FC, q-value <0.05) differentially expressed genes in comparisons between the 6% and 10% treatment groups (data not shown).

In contrast to our analyses of active drinkers, our comparisons of EtOH-Cessation males identified minimal to no differentially expressed genes. For example, in comparisons between the Control and 6% treatments, we only identified three differentially expressed genes (*WAP Four-Disulfide Core Domain 13* (*Wfdc13*) and *Defensin Beta 123* and *128* (*Defb23*, *Defb28*)), while we did not identify any significant differentially expressed genes between the Control and 10% treatments (data not shown). These observations suggest that epididymides of active drinkers exhibit alterations in processes related to mitochondrial dysfunction, oxidative phosphorylation, and the generalized stress response and that these differences revert after the cessation of alcohol use. Notably, we previously identified differential expression of genetic pathways regulating oxidative phosphorylation, mitochondrial function, and Sirtuin signaling in

the early embryo and placentae of offspring derived from alcohol-exposed males (Thomas et al., 2021; Roach et al., 2023), suggesting this transcriptional signature may transmit to the early offspring through sperm.

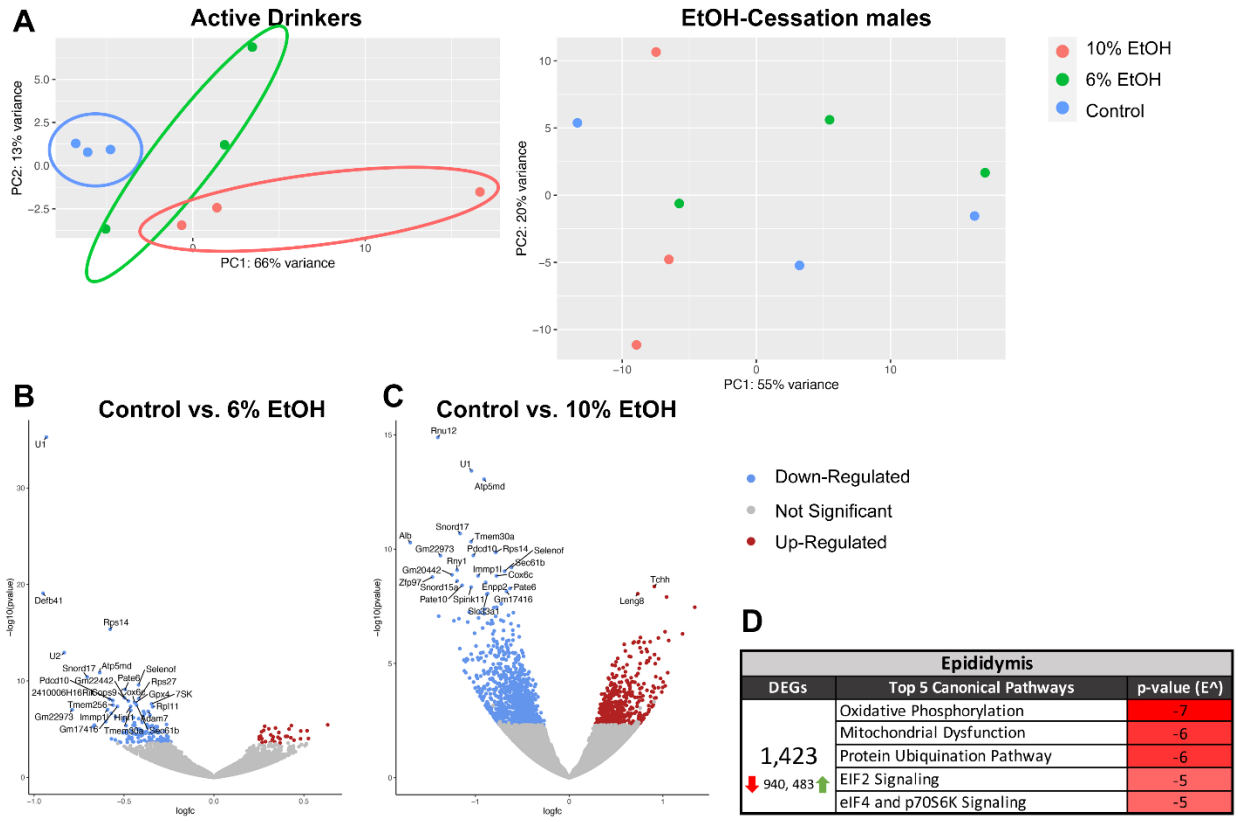

Figure 3.2. Chronic alcohol exposure induces altered gene expression patterns in the caput section of the epididymis. A) Principal Component Analysis of gene expression between the caput epididymis isolated from Control, 6% EtOH, and 10% EtOH-treated males (Left Cohort 1 Active Drinkers, Right Cohort 2 EtOH-Cessation Males). Volcano plot contrasting down- and upregulated differentially expressed genes between B) Control vs. 6%EtOH-treated males and C) Control vs. 10%EtOH-treated males (log2FC, q-value <0.05). D) Ingenuity Pathway Analysis of differentially expressed genes identified in the 10% EtOH treatment group (log2FC, p-value <0.05). n = 3 males per treatment for each cohort.

3.3.3 **Chronic Alcohol Exposure Induces Lasting Changes in Mitochondrial DNA Copy Number Within the Epididymis**

Alterations in the architecture, function, and number of mitochondria are one of the main hallmarks of alcohol-related liver disease (Nassir and Ibdah, 2014). Recent studies demonstrate that in the liver, alcohol exposure modulates mitochondrial DNA copy number (mtDNcn) and transcription, potentially driving the sequela of this disorder (Zhou et al., 2019). However, no studies have determined whether alcohol adversely impacts mitochondrial function in other organ systems, including the male reproductive tract. The extrachromosomal mitochondrial genome encodes 37 critical bioenergetic genes, is present in hundreds of copies per cell, and changes in mitochondrial DNA abundance serve as a proxy measure for disease-associated mitochondrial dysfunction (Wallace, 2018). Therefore, using previously described methods (Bedi et al., 2019), we assayed mtDNAcn in the male reproductive tracts of Active Drinkers and Cessation males.

Previous studies demonstrate differential expression of several mitochondrial genes across the three macro sections of the epididymis, with the corpus segment exhibiting the highest mitochondrial content (Shi et al., 2021). Consistent with these studies, we identified a significant increase in mtDNAcn across the corpus and cauda sections compared to the caput (Fig. 3.3A). We next compared the liver, testes, and the three sections of the epididymis isolated from Control and active drinkers for alterations in mtDNAcn. As the 10% treatment exhibited the greatest number of differentially expressed genes, we focused our analyses on these tissues. Consistent with studies examining alcohol-related liver disease (Zhou et al., 2019), our analyses identified alterations in hepatic mtDNAcn (Fig. 3.3B). In contrast, we did not observe any changes in mtDNAcn in the testes (Fig. 3.3C). Comparisons of mtDNAcn across the epididymis

identified segment-specific changes, with the caput and cauda each exhibiting alcohol-induced increases in mtDNAcn while the corpus segment exhibited a significant decline (Fig. 3.3D-F). Notably, when we examined epididymal segments isolated from EtOH-Cessation males, we did not identify any differences in mtDNAcn in the liver (data not shown). However, we identified persistent mtDNAcn changes in the corpus segment across both the 6% and 10% EtOH treatments, while in contrast, we did not identify any significant differences in the caput or cauda segments (Fig. 3.3G-I). These observations reveal that chronic alcohol exposure induces alterations in mtDNAcn in the liver and epididymis, but not the testis, and that aspects of this signature persist one month after alcohol cessation.

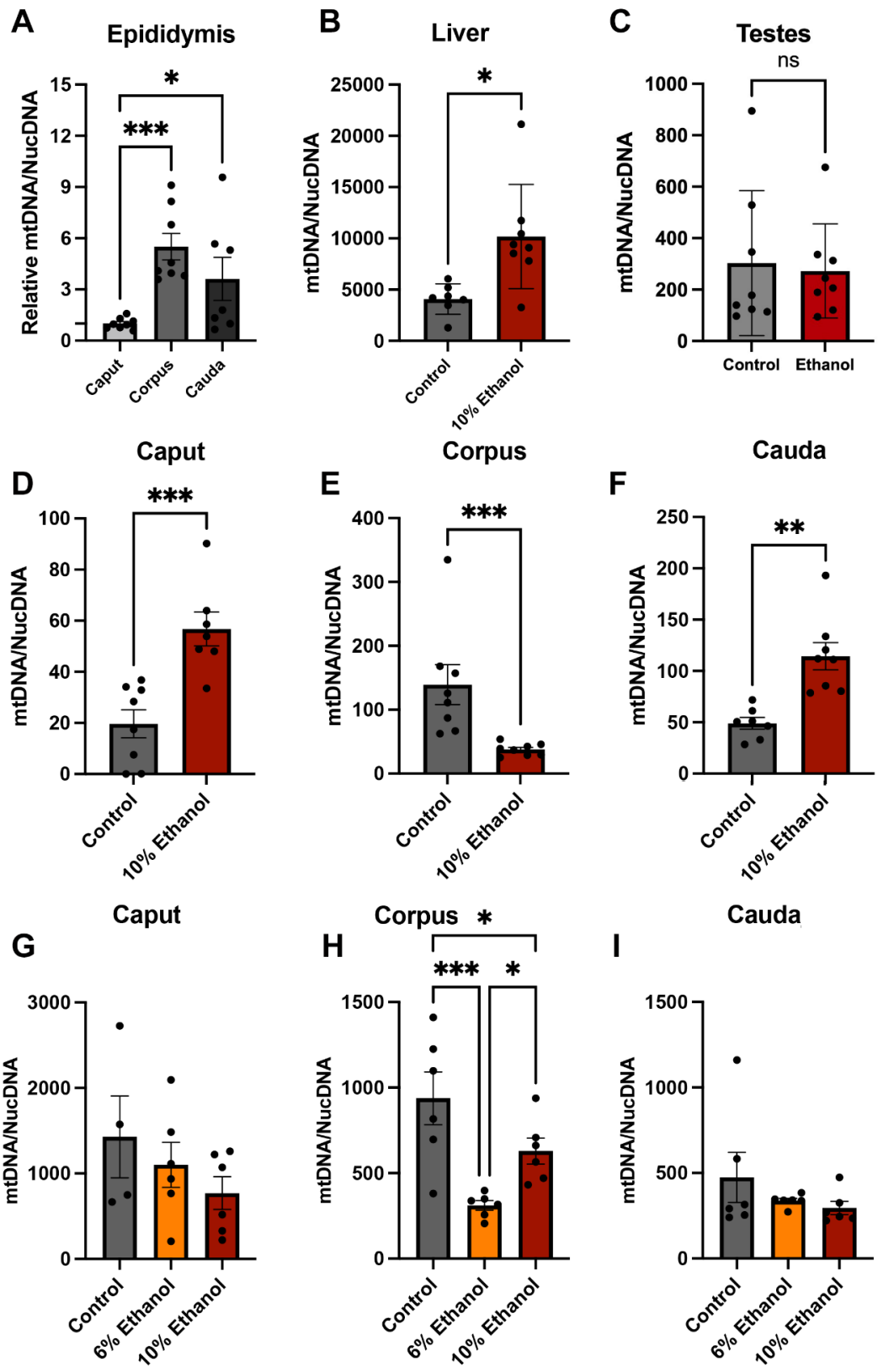
A
Epididymis
Relative mtDNA/NucDNA
15
12
9
6
3
0
*
***
Caput
Corpus
Cauda
B
Liver
mtDNA/NucDNA
25000
20000
15000
10000
5000
0
*
Control
10% Ethanol
C
Testes
ns
mtDNA/NucDNA
1000
800
600
400
200
0
Control
Ethanol
D
Caput
***
mtDNA/NucDNA
100
80
60
40
20
0
Control
10% Ethanol
E
Corpus
***
mtDNA/NucDNA
400
300
200
100
0
Control
10% Ethanol
F
Cauda
**
mtDNA/NucDNA
250
200
150
100
50
0
Control
10% Ethanol
G
Caput
mtDNA/NucDNA
3000
2000
1000
0
Control
6% Ethanol
10% Ethanol
H
Corpus
*
***
*
mtDNA/NucDNA
1500
1000
500
0
Control
6% Ethanol
10% Ethanol
I
Cauda
mtDNA/NucDNA
1500
1000
500
0
Control
6% Ethanol
10% Ethanol

Figure 3.3. Chronic alcohol exposure induces lasting changes in mitochondrial DNA copy number within the epididymis. A) Quantitative PCR analysis of mitochondrial DNA copy number (mtDNAcn) across the caput, corpus, and cauda sections of the epididymis isolated from Control males (n=8). For ease of comparison, we normalized qPCR ratios to the caput section. Comparison of mtDNAcn in the B) liver and C) testis isolated from Control and 10% EtOH males in the cohort of active drinkers (Cohort 1; n=8). Alcohol-induced alterations in mtDNAcn across the D) caput, E) corpus, and F) cauda sections of the epididymis isolated from actively drinking Control and 10% EtOH males (Cohort 1; n=8). Segment-specific differences in mtDNAcn across the G) caput, H) corpus, and I) cauda sections of the epididymis four weeks after the cessation of alcohol (Cohort 2; n=8). We compared the impacts of alcohol treatments on mtDNAcn using Kruskall-Wallis analysis followed by an Uncorrected Dunn's test, a student's t-test, or a Mann-Whitney test, depending on the normality of the dataset. Error bars represent the standard error of the mean, *P < 0.05, **P < 0.01, ***P < 0.001.

3.3.4 **Analysis of Mitochondrial Copy Number in Alcohol-Exposed Sperm**

In clinical studies examining IVF success rates, increases in sperm mtDNAcn correlate with lower odds of oocyte fertilization and reduced rates of high-quality Day 3 and transfer quality Day 5 embryos (Wu et al., 2019). Previously, we observed dose-dependent reductions in IVF embryo survival and pregnancy success rates, with the pregnancy success rate of the 10% EtOH treatment falling to half those of Controls (Roach et al., 2023). Therefore, we isolated mitochondrial DNA from a selection of the cryopreserved sperm samples we used in these previous experiments and compared mtDNAcn between the Control and 6% treatments. Consistent with clinical observations, we also identified a significant increase in mtDNAcn in cryopreserved samples derived from the 6% treatment group compared to the Controls (Fig. 3.4A). As the 10% treatment group required twice the number of IVF transfers, we did not have enough remaining cryopreserved samples to reliably assay mtDNAcn using this treatment cohort. However, when we compared mtDNAcn between the Control and 10% treatment using fresh sperm samples, we observed a significant increase in mtDNAcn in alcohol-exposed sperm (Fig. 3.4B). These observations indicate that similar to clinical studies examining IVF patients, the

alcohol-induced reductions in IVF outcomes we previously reported correlate with increased sperm mtDNAcn.

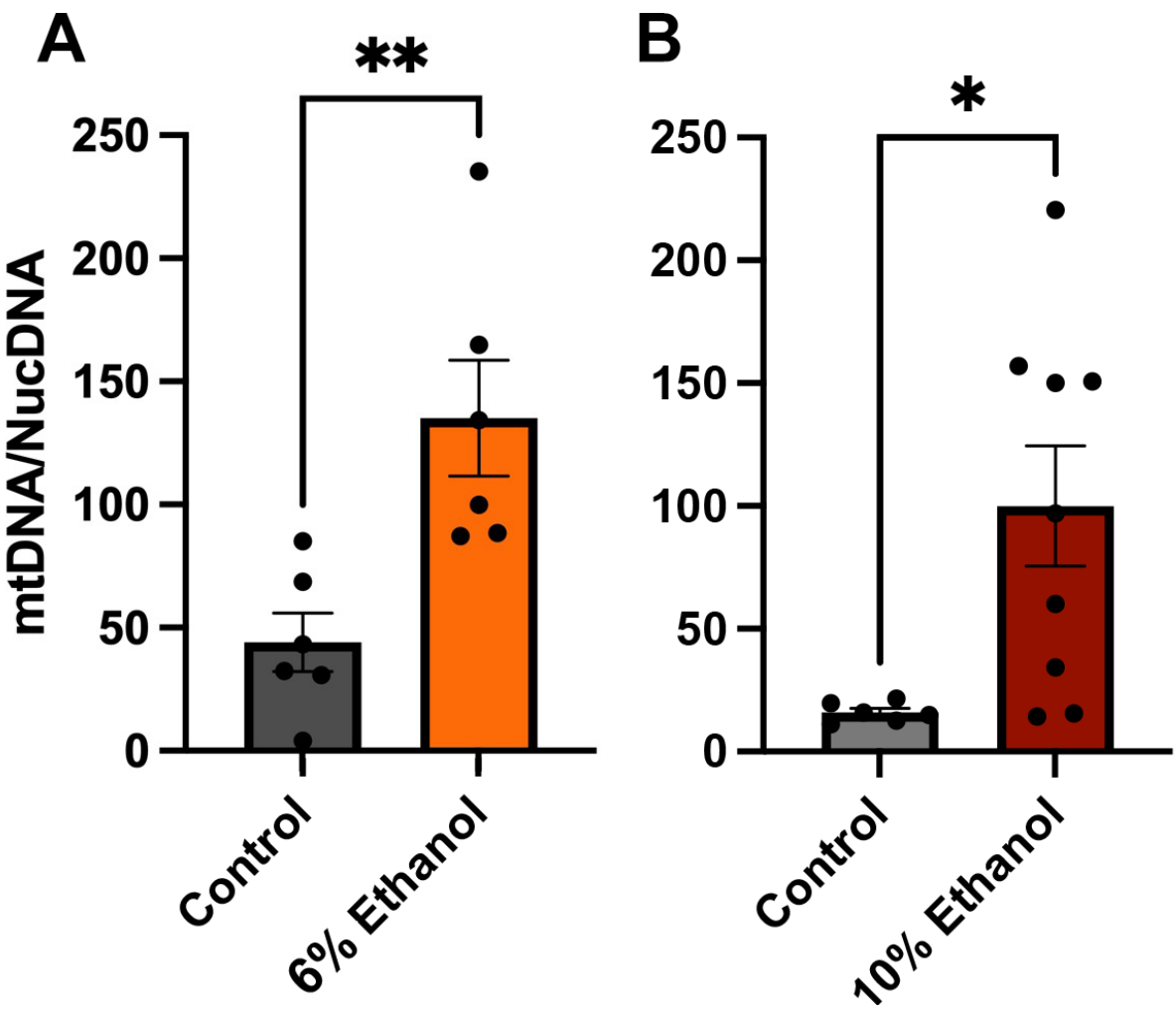

Figure 3.4. Analysis of mitochondrial copy number in alcohol-exposed sperm. A) Quantitative PCR analysis of mitochondrial DNA copy number (mtDNAcn) in cryopreserved sperm used in our previously published IVF experiments (Roach et al., 2023) (n=6). Analysis of mtDNAcn in fresh sperm isolated from Control and 10% EtOH-treated actively drinking males (Cohort 1; n=8). We used a student's t-test to compare treatments. Error bars represent the standard error of the mean, *P < 0.05, **P < 0.1

3.3.5 **Sperm Isolated from Alcohol-Exposed EtOH-Cessation Males Retain a Distinct Small RNA Signature**

We next determined if the cessation of alcohol exposure would rescue ethanol-induced changes in the small RNA content of sperm (Rompala et al., 2018; Bedi et al., 2019). Previously, we found that preconception paternal alcohol exposures induce dose-dependent changes in offspring fetoplacental growth (Thomas et al., 2022). To avoid the confounding influences of varying exposure levels, we selected Cessation males experiencing a similar average daily EtOH dose. The median daily EtOH dose for Cessation alcohol-exposed males across both the 6% and 10% treatment groups was 1.34 g/kg. Therefore, we isolated sperm small RNAs from alcohol-exposed males with an average daily dose around this population median (n=4; 1.04, 1.32, 1.34, and 1.35g/kg) and conducted deep-sequencing analysis. We sequenced sperm small RNAs to a depth of approximately 15 million raw reads per sample and obtained read lengths ranging from 16 to 40 nucleotides in length. Like previous examinations of the small RNA profiles of mouse sperm, we found that most small RNA reads mapped to transfer RNA-derived sequences (~40% tRNA or structural RNAs) and Piwi-interacting RNAs (~20% piRNAs) (Fig. 3.5A). Notably, we identified significant differences in the percentages of small RNAs mapping to microRNAs (miRNAs) and exonic regions, with Cessation-EtOH males exhibiting proportionally fewer miRNAs than Cessation-Controls and a greater percentage of exonic-derived fragments (Fig. 3.5B-D).

Principal component analysis of miRNA, piRNA, and tRNA-derived sequences did not identify clustering between Cessation Control and EtOH-exposed males (miRNA data shown in Fig. 3.5E). However, we did observe modest clustering of exonic- and transposable element (TE)-derived sequences (Fig. 3.5F-G). Analysis of small RNA reads using DESeq2 (log2FC, q-

value <0.05) identified multiple differentially enriched miRNA, tRNA-derived and exonic sequences (Fig. 3.5H-J). Finally, we identified one differentially enriched transposable element (LINE:L1:L1ME3A_sense_TE). Significantly, many differentially enriched miRNAs and tRNA-derived sequences associate with oxidative and cellular stress responses (Go et al., 2016; Liu et al., 2022; Watanabe et al., 2013; Schwenzer et al., 2019; Giorgi et al., 2011), similar to the genetic pathways identified in our transcriptomic analysis of the epididymis above (Fig. 3. 2D). These data reveal that sperm from EtOH-Cessation males retain a distinct small RNA signature compared to unexposed Cessation-Controls.

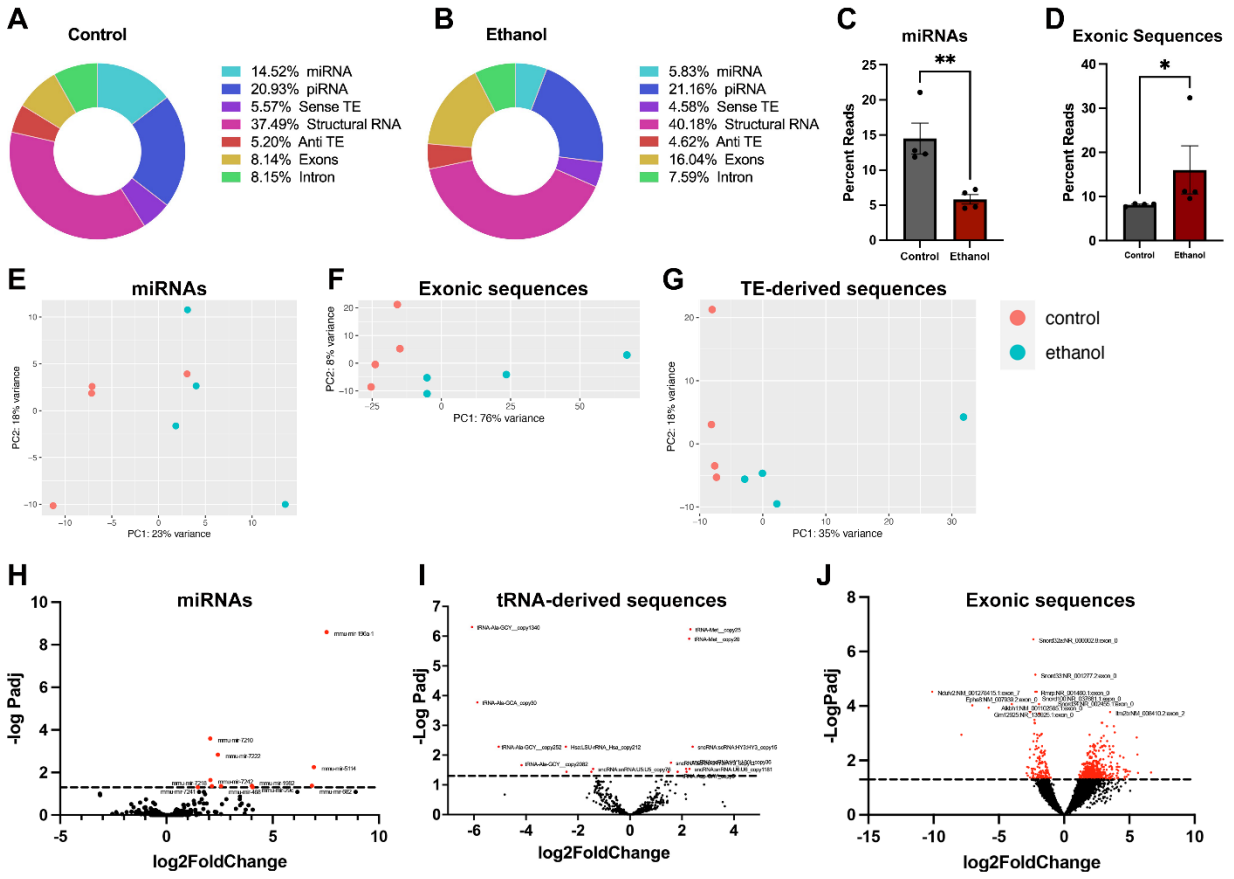

Figure 3.5. Sperm isolated from alcohol-exposed EtOH-Cessation males retain a distinct small RNA signature. Comparison of total small RNA species in sperm isolated from A) Control and B) EtOH-exposed males in the EtOH-Cessation cohort after four-weeks abstinence from alcohol (n=4). Differential enrichment of sequenced C) microRNAs (miRNAs) and D) exonic sequences between EtOH-Cessation Control and alcohol-exposed males (n=4). Principal Component Analysis comparing enrichment of sperm E) miRNA, F) exonic, and G) transposable element (TE)-derived sequences between EtOH-Cessation Control and alcohol-exposed males (n=4). Volcano plot comparing differentially enriched H) miRNA, I) tRNA-derived sequences and J) exonic sequences between Control and EtOH-exposed males after four weeks of abstinence from alcohol (log2FC, q-value <0.05; n=4). We used a student's t-test to compare the percentages of miRNA and exonic-derived sequences between treatments. Error bars represent the standard error of the mean, *P < 0.05, **P < 0.01.

3.4 **Discussion**

Chronic preconception male alcohol exposures alter the sperm-inherited developmental program and transmit an epigenetic memory to offspring, negatively impacting fetoplacental growth and inducing FASD-like phenotypes (Rompala and Homanics, 2019). Previous studies by our group and the Homanics lab have identified alcohol-induced changes in sperm noncoding RNAs (Bedi et al., 2019, Rompala et al. 2018), which we can correlate with transcriptional alterations in the genetic pathways regulating oxidative phosphorylation, mitochondrial function, and Sirtuin signaling in the early embryo and placentae (Thomas et al., 2021; Roach et al., 2023). As the trafficking of sperm noncoding RNAs primarily occur during epididymal transit (Sharma et al., 2018), which lasts approximately 7 to 10 days (Alder, 1996) in mice, we hypothesized that alcohol cessation for one month would allow for the normalization of this EtOH-induced epigenetic change. However, after one month of abstinence, we still identified alcohol-induced changes in sperm small RNAs and evidence of altered mitochondrial biology in the corpus segment of the epididymis. These observations suggest that some aspects of alcohol-induced mitochondrial dysfunction remain and that significant differences in the noncoding RNA signature of sperm persist during alcohol withdrawal.

Previous studies examining alcoholic liver disease induced by chronic EtOH exposures identified mitochondrial fragmentation, defective mitophagy, decreased abundance of cellular antioxidants, and a significant increase in mitochondrial reactive oxygen species (ROS) (Zhou et al., 2019). Consistent with these observations, in active drinkers, we identified a transcriptional signature of mitochondrial dysfunction in the caput segment of the epididymis and evidence of altered mtDNAcn across all segments of the epididymis but, notably, not in the testis. Previous studies describe segment-specific differences in epididymal mitochondrial content, with the

corpus displaying significantly higher levels than the caput and cauda portions (Shi et al. 2021). Our qPCR-based measures of mtDNAcn agree with these previous observations and confirm that the corpus and cauda sections contain a greater mtDNA enrichment than the caput. Further, our data demonstrate that chronic alcohol exposure induces segment-specific changes across the epididymis, some of which persist even one month after removing the toxicant. We speculate that mitochondrial differences across the epididymal epithelium enable this organ to sense the surrounding environment, including cellular metabolic and redox states, then communicate this information to spermatozoa in the form of noncoding RNAs.

In support of this assertion, our previous studies examining the miRNA content of sperm isolated from active drinkers identified an increased abundance of microRNA miR-30a and decreased miR142. miR-30a enhances activation of the master transcriptional regulator controlling the cellular antioxidant response, Nuclear Factor Erythroid 2-Related Factor 2 (Nrf2), by inhibiting its negative regulator Keap1 (Lv et al., 2021). In contrast, miR-142 is a direct suppressor of NRF2 (Wang et al., 2017). Therefore, the balance we previously identified in active drinkers favors miRNA-mediated activation of NRF2-driven genetic pathways responding to oxidative stress. Here, we identified differentially enriched miRNAs and tRNA-derived sequences in EtOH-Cessation males that also link with oxidative and cellular stress responses (Go et al., 2016; Liu et al., 2022; Watanabe et al., 2013; Schwenzer et al., 2019; Giorgi et al., 2011). Most notably, we identified a ~100-fold increase in mir-196a, an NRF2-controlled miRNA (Liu et al., 2022) that enhances the expression of antioxidant proteins, like heme oxygenase 1, by inhibiting their negative regulators (Go et al., 2016). Significantly, although not a top candidate, Rompala et al. also identified increased enrichment of this miRNA in sperm using a vapor chamber exposure model (supplemental information of reference (Rompala et al.,

2018)). Finally, presumed tRNA fragments, including tRNAMet identified here and tRNAGlu detected by the Homanics group (Rompala et al., 2018), selectively accumulate in the nucleus as part of the generalized stress response induced by mitochondrial dysfunction (Schwenzer et al., 2019). From these data, we postulate that alcohol-induced changes in epidydimal ROS lead to NRF2 activation and the packaging of miRNAs in sperm that reinforce the cellular antioxidant response. However, further experimentation is required to validate this assertion and to determine how this epigenetic memory impacts mitochondrial function in the developing offspring.

Although compelling, there are several limitations to this study. First, we did not generate offspring using the cessation males. Therefore, we do not know if the sperm noncoding RNA signature we identified correlates with changes in offspring fetoplacental growth or if the resulting offspring would develop normally. However, as significant differences in the ncRNA signature of EtOH-Cessation sperm and epididymal mtDNAcn remained, we speculate that abstinence for one month is insufficient for the epigenetic memory of paternal alcohol exposure to abate, likely due to the ongoing stress associated with alcohol withdrawal (Lee et al., 2015; Tonetto et al., 2023). Furthermore, we acknowledge that our analysis does not distinguish between changes in sperm ncRNAs that are causal drivers of altered epigenetic programming in the next generation versus abnormalities that are merely additional symptoms of alcohol-induced stress. However, while the individual miRNAs vary between studies, the potential interactions with NRF2 remained consistent. We also acknowledge that our analyses do not identify specific epididymal cell types impacted by alcohol or discern differences in the caput, corpus, or cauda sub-segments. Finally, we note that mtDNAcn is a widely used but crude proxy for mitochondrial function. However, the alignment of our data with clinical studies examining the

correlations between reduced fertility and alterations mtDNAcn is compelling. Future studies will explore mitochondrial dynamics in the male reproductive tract and sperm of alcohol-exposed males and their offspring.

Obstetricians do not routinely consider paternal influences on child health, and all alcohol messaging targets women. Therefore, there is a critical need to expand alcohol messaging to include men and educate both prospective parents on the reproductive dangers of alcohol use. Central to this effort, researchers must identify the length of time required for the paternal epigenome to recover from toxicant exposures so that patients may know how long in advance of trying to conceive they need to begin abstaining from alcohol. Our data suggest that the epididymis retains an alcohol-induced signature of mitochondrial dysfunction one month after cessation, indicating a more extended recovery period is required after toxicant removal. Furthermore, our observations suggest that NRF2-related miRNAs, particularly mir-196a, and increases in sperm mtDNAcn may serve as viable biomarkers of paternal alcohol use and adverse alterations in the sperm-inherited epigenetic program.

4. ROLE OF ALCOHOL AND ARTIFICAL SWEETENER CONSUMPTION ON MALE MOUSE MICROBIOME AND METABOLOME

4.1 **Introduction**

Lifestyle habits and environmental exposures directly affect an individual's overall health and wellbeing. Alcohol consumption among males is deemed acceptable by society, and its intake continues to grow in the United States. The Alcohol Research Group reported that 72% of men consume some amount of alcohol on a weekly basis (Greenfield et al., 2023). However, research has consistently verified that chronic alcohol consumption can result in gut dysbiosis, oxidative stress, increased permeability of the intestinal barrier, gastrointestinal tract (GIT) inflammation, alcoholic liver disease, and other pathogenic complications (Engen et al., 2015; Bishehsari et al., 2017; Keshavarzian et al., 2009; Banan et al., 2000; Perez et al., 2020). Secondly, nonnutritive artificial sweeteners (NAS) are among the most-used food and drink additives (Gardner et al., 2012). NAS are also often added to human alcoholic beverages and used in animal research to increase palatability and encourage consumption while keeping caloric content low (Roberts et al., 1999; Ruiz-Ojeda et al., 2019). Although NAS are perceived as beneficial and generally safe, supporting scientific evidence of NAS altering gut microbiota, increasing intestinal permeability, oxidative stress, inflammation, glucose intolerance, and obesity remains controversial (Suez et al., 2014; Bian et al., 2017; Pearlman et al., 2017; Ruiz-Ojeda et al., 2019; Shil et al., 2020; Hasan et al., 2023). These previous works have shown that chronic alcohol or NAS intake can cause a myriad of deleterious effects on the symbiotic relationship between the microbiome and the host. Nonetheless, the role of artificially sweetened alcohol on intestinal microbiota and metabolites remains almost completely undescribed.

To date, there is a single study describing the dual interaction of ethanol and the sweetener, saccharin, on the pregnant and nonpregnant female mouse microbiome (Labrecque et al., 2015). Here, they found Clostridium in EtOH and NAS treated pregnant mice was significantly reduced, Helicobacter levels rose in nonpregnant mice in response to EtOH and NAS consumption, and EtOH and NAS produced contrasting levels of Eubacterium with elevated abundance in pregnant mice but reduced its abundance in non-pregnant mice (Labrecque et al., 2015). This examination only focused on the microbial communities and did not measure fecal or blood serum metabolites. Analyzing circulating metabolites is considered a direct reflection of the host-microbiota relationship (Krautkramer et al., 2021). An investigation on NAS, specifically saccharin's, influence on the microbiome and SCFA in mice showed distinct alterations to microbiota composition and function with a significant increase in the abundance of Bacteroides and decrease in Clostridiales and Lactobacillis rerteri abundance, which induced glucose intolerance metabolic syndrome (Suez et al., 2014). Also, they found substantial increased levels of acetate and propionate SCFAs in NAS-treated fecal samples (Suez et al., 2014), but blood serum SCFA concentrations were not measured. In context of only alcohol consumption, there is debate/conflicting evidence that microbial populations can process alcohol into metabolites. Earlier studies claim that intestinal microbes can metabolize alcohol into the highly reactive metabolite acetaldehyde, resulting in higher intestinal permeability and liver damage (Zhong and Zhou, 2014; Chen et al., 2015; Hamarneh et al., 2017; Nieminen and Salaspuro, 2018). A more recent publication by the Zengler lab showed that mouse cecal microbiota do not directly metabolize alcohol *ex vivo* and proposed that EtOH alterations to the microbiome are the consequence of increased acetate concentrations (Martino et al., 2022);

theorized as the “acetate switch” (Wolfe, 2005). Further research is warranted to confirm or refute these findings on microbiota function and SCFA production during chronic ethanol intake.

Due to both alcohol and NAS being consumed regularly and in conjunction by men, the indirect effect of alcohol and NAS consumption after interacting with the microbiome on the reproductive tract and gametes remains completely undefined. It is crucial to discover the role microbiota and their subsequent metabolites, from lifestyle exposures, on epigenetic modifications within spermatozoa that could be transmitted to offspring and result in onset of disease.

This study was designed to identify changes in microbial populations and SCFA profile alterations in the blood serum of males consuming varying doses of EtOH with or without NAS. To accomplish this, we utilized a C57BL/6J strain mouse model that mirrors binge-like drinking behaviors in humans and compared fecal microbiota diversity measures and blood serum SCFA concentrations from Control and treated mice. Based on previous publications, we hypothesized that voluntary male alcohol or artificial sweetener exposure would induce a shift in abundance and family composition of microbiota, and therefore, an alteration in circulating SCFA concentrations. Moreover, we theorize that the alteration in SCFA concentrations can modify epigenetic programming in spermatozoa, downstream. We used deep shotgun sequencing and analysis of alpha and beta diversity of microbial communities and gas chromatography-mass spectrometry (GCMS) of blood serum metabolites between two timepoints. Our studies reveal that EtOH, in combination with the NAS saccharin (Sweet’N Low®, SNL), exhibit a dual interaction/double toxicant effect. To our knowledge, this is the first study to explore the impact of artificially sweetened alcoholic beverages on the male intestinal microbiome and metabolite production in humans or animal models. By studying alterations in the microbiome-gut axis, this

could provide a mechanistic explanation of how epigenetic changes in sperm are induced. This study explores a dose of ethanol effect and double toxicant effect including ethanol and saccharin. This will allow us to deduce if the concentration of alcohol plays a role in the gut of males for future studies.

4.2 Materials and Methods

4.2.1 Animal Studies and Ethanol Exposures

All experiments were completed following IACUC guidelines and regulations, and the study design was approved by the Texas A&M University IACUC, under protocol number AUP: IACUC 2017-0308, Reference Number: 096737. We utilized C57BL/6J strain male mice (RRID:IMSR_JAX:000664), which were generated from a breeder nucleus and housed and maintained in the Texas A&M Institute for Genomic Medicine. We sustained males on an ad libitum standard chow diet (catalog # 2019, Teklad Diets, Madison, WI, USA) with free water access on a reverse 12-hour light/dark cycle (lights off at 8:30 AM). We added shelter tubes (catalog # K3322, Bio-Serv, Flemington, NJ, United States) to reduce animal stress and improve cage enrichment.

Commencing on postnatal day 90, we individually caged males for acclimatization and randomly assigned them to one of 6 treatment groups. We initiated the control, ethanol (**EtOH**) and Sweet'N Low® (**SNL**) treatments using an extended version of the Drinking in the Dark (DID) model on postnatal day 104 (Thiele and Navarro, 2014). Using our published methods, we exposed males (n=8 per treatment) to control (water alone), 3%, 6%, 10% (w/v) EtOH (catalog # E7023, Millipore-Sigma, St. Louis, MO, USA), 0.066% Sweet'N Low® (w/v) (Cumberland

Packing Corp, Brooklyn, NY), or 0.066% Sweet'N Low® plus 10% EtOH treatments. The treatment exposures began one hour after the beginning of the dark (active) cycle and lasted for 4 hours, daily, for 7 weeks. We concurrently exchanged water bottles across the control, EtOH, and SNL treatments to ensure identical handling. During the regular cage change each week, we recorded the weight of each mouse (g) and the total weekly fluid consumption (g), then calculated their weekly fluid consumption as g of fluid consumption/kg body weight.

4.2.2 **Fecal Sample Collection, Extraction, and Sequencing**

After one week of acclimation (PND 97), we sterilized the procedure room workbench with Ready-To-Use Peroxigard (catalog # PRTU242105, Cincinnati Lab Supply Inc., 11385 Sebring Dr. Cincinnati, OH, USA) and placed the males into a tube rodent holder (catalog # 464010000, Bel-Art Products, Pequannock, NJ, USA). Before male mice were given treatment, we collected 250mg of whole fecal boluses into sterile 1.7 mL microcentrifuge tubes (catalog # 87003-294, VWR, Radnor, PA, USA), snap-froze them on dry ice, and stored them in -80 ℃ before DNA extraction. We deemed this time point as "Week 0" of treatment fecal samples. We then repeated this collection step at the end of 6th week of treatment after the 4-hour exposure period and refer to it as "Week 6" of treatment. Both time points of fecal samples remained frozen and shipped to Diversigen (600 County Rd D, West, Suite 8, New Brighton, MN 55112) for DNA extraction, whole-genome shotgun sequencing using Illumina 2x150 paired-end reads with a mean read depth of at least 2 million sequences per sample. At least 90% of samples achieved 800,000 reads (40% of specification), excluding samples failing prior QC and whole-genome shotgun sequencing, using Illumina 2x 150 paired-end reads with a mean read depth of

at least 2 million sequences per sample.

4.2.3 **Fecal Microbiota Informatic Analysis**

We used metagenome shotgun sequencing to characterize the microbial community composition from the fecal sample. The subsequent raw sequencing data was quality filtered (with trim_galore) to remove adapter contamination and subjected to taxonomic classification using MetaPhlAn v3.0 (Truong et al., 2015). MetaPhlAn utilizes a database of unique clade-specific marker genes, facilitating high-resolution taxonomic profiling down to the species level. The output of MetaPhlAn was a table listing the relative abundances of microbial taxa across the samples.

The resulting abundance table was then imported into the R package Phyloseq (McMurdie & Holmes, 2013), a tool designed for the import, storage, analysis, and graphical display of microbiome census data. Alpha diversity indices, which measure the diversity within individual samples, was computed using the estimate_richness function. Comparisons of alpha diversity between treatment groups was performed using non-parametric Kruskal-Wallis tests. Principal component analysis (PCA) was used to assess community dissimilarity based on Bray-Curtis distances visually. PERMANOVA tests, implemented through the adonis function of the vegan package (Oksanen et al., 2019), were used to evaluate the differences in microbial community composition between pairs of treatment groups. All statistical analyses were performed in R v4.0 (R Core Team, 2020), and p-values less than 0.05 were considered significant.

4.2.4 **Blood Sample Collection and Plasma Extraction**

At the end of the 4th and 7th week of treatment, we sterilized the procedure room workbench with peroxigaurd and used the tube rodent holder for the mice at the end of the 4-hour treatment window. We sterilized their tail with 70% EtOH solution (catalog # MDS098017, Medline, Three Lakes Drive Northfield, IL, USA), allowed the tail to dry, made a 1mm incision at the tail tip with a sterile single edge razor blade (catalog # 55411-05, VWR, Radnor, PA, USA), and collected 400 µl of blood into an EDTA (catalog # 6381-92-6, VWR, Radnor, PA, USA), coated 0.5 mL microcentrifuge tubes (catalog # 76004-088, VWR, Radnor, PA, USA) The blood samples remained at room temperature until we centrifuged them at 2000 G-force for 15 minutes. Next, we pipetted the blood serum (~100 ul) into a new 0.5 mL tube and stored them at -80 ℃ until metabolite extraction.

4.2.5 **Blood Plasma Metabolite Extraction**

We followed the Texas A&M University Integrated Metabolomics Analysis Core (TAMU IMAC) SCFA extraction protocol. 50 µl blood serum into extraction tubes. Fecal Extraction Protocol for SCFA Targeted Analysis on TSQ EVO 8000, TAMU IMAC, Protocol (Texas A&M University, College Station, TX, USA).

4.2.6 **Statistical Analysis**

We collected and recorded physiological measures for each male, by hand, and then copied and pooled these data into Microsoft Excel or Google Sheets. After metabolite extraction, TAMU IMAC ran GCMS on the extracted samples and generated result files of the concentrations (uM) circulating metabolites in each male. We used the post-blank subtraction

concentration (uM) results for acetic, butyric, and propionic acids in each male to run statistical analyses. Then we transferred the molecular and physiological data into GraphPad Prism 9 (RRID: SCR_002798; GraphPad Software, Inc., La Jolla, CA, USA) for statistical analysis, and we set the statistical significance at $\alpha = 0.05$, used the ROUT test ($Q = 1\%$) to identify any outlier. We then confirmed the normality of the datasets with a Shapiro–Wilk test. If the data passed normality ($\alpha = 0.05$), we applied a One-way or Two-way ANOVA or an unpaired, parametric (two-tailed) *t*-test. If the data failed the test for normality or if there was unequal variance (Brown Forsythe test), we proceeded with a Kruskal–Wallis test, followed by a Dunn's multiple comparisons test.

4.3 Results

4.3.1 A Physiologically Relevant Mouse Model to Examine the Influence of Chronic Alcohol and Saccharin Consumption on Intestinal Microbiota and Metabolome

To identify the impact of male alcohol use on the gut microbiome and metabolome, we applied a proven mouse model of voluntary alcohol exposure that promotes daily alcohol consumption, with or without saccharin, and imitates binge drinking (Allen et al., 2003; Boehm et al., 2008). We then collected fecal boluses and blood from treated males and extracted and analyzed fecal DNA and blood plasma SCFA from the samples through whole-genome shotgun sequencing and GCMS (Fig. 4.1A). We utilized a limited-access model known as Drinking in the Dark (DID) and subjected postnatal day 104, C57BL/6J male mice to 3%, 6%, and 10% (w/v) ethanol (EtOH), 0.066% Sweet'N Low® (w/v), or 0.066% Sweet'N Low® and 10% EtOH treatments. We treated Control males with plain water and provided identical handling by

simultaneously exchanging between two water bags. We continued the treatment period for 8 weeks, while collecting fecal samples before treatment (Week 0) and after 6 weeks of treatment (Week 6) and blood samples at the end of treatment weeks 4 and 7. We did not observe any significant changes in body weight between the groups during treatment (Fig. 4.1B), which is consistent with our prior works employing EtOH consumption, without or with SNL (Chang et al., 2017; Bedi et al., 2019; Thomas et al., 2022; Roach at el., 2023). Males in the 3% EtOH group consumed an average daily dose of 0.69 g/kg, the 6% EtOH group received an average daily dose of 1.29 g/kg, the mice in the 10% EtOH treatment group consumed an average daily dose of 1.78 g/kg, and the SNL 10% EtOH males received 3.2 g/kg (Fig. 4.1C).

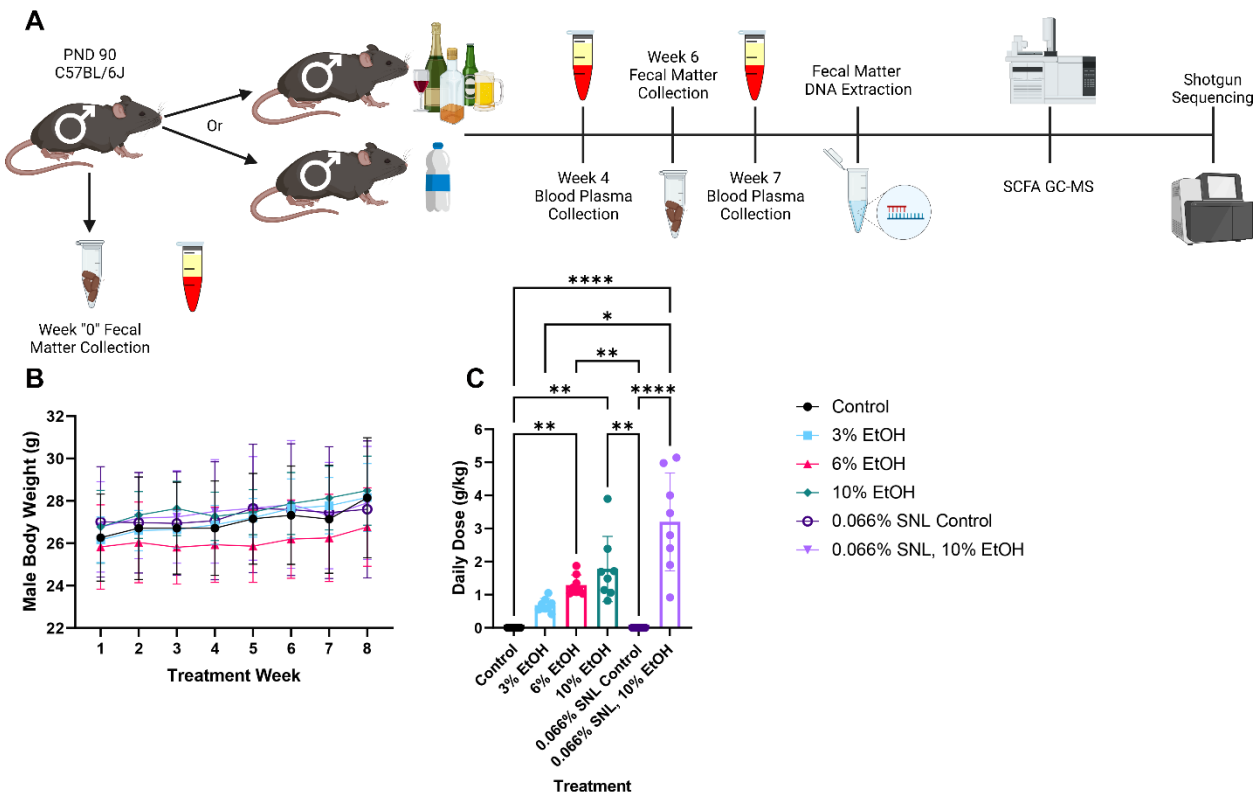

Figure 4.1. A physiologically relevant mouse model to examine the influence of chronic alcohol and saccharin consumption on intestinal microbiota and metabolome. (A) Experimental schematic used to inspect the influence of male chronic EtOH and saccharin exposure on gut microbiota and metabolome. Comparison of (B) average weekly body weights and (C) average daily dose of EtOH between treatment groups (n = 8). We analyzed treatment data by using a one-way or two-way ANOVA. Error bars correspond to the standard deviation of the mean, *P < 0.05, **P < 0.01, ****P < 0.0001.

4.3.2 **Broad Variations in Fecal Microbial Communities at the Family Level Before Treatment**

Before the males started treatment, we collected fecal samples at Week 0 to identify changes in microbiota after 6 weeks of exposure. Overall, the 48 fecal samples yielded 1104 operational taxonomic units (OTUs) (Fig. 4.2). Based on the relative abundance, the top 3 families were Erysipelotrichaceae (18.259%, Phylum Firmicutes), Muribaculaceae (16.246%, Phylum Bacteroidetes), and Bifidobacteriaceae (13.659%, Phylum Actinobacteria). To date,

there have been few metagenomic sequencing of animals prior to treatment (Bull-Otterson et al., 2013). We suggest that this practice should be standardized to give a baseline of conventional rodent models and the ability to visualize change in the microbiome over the course of treatment.

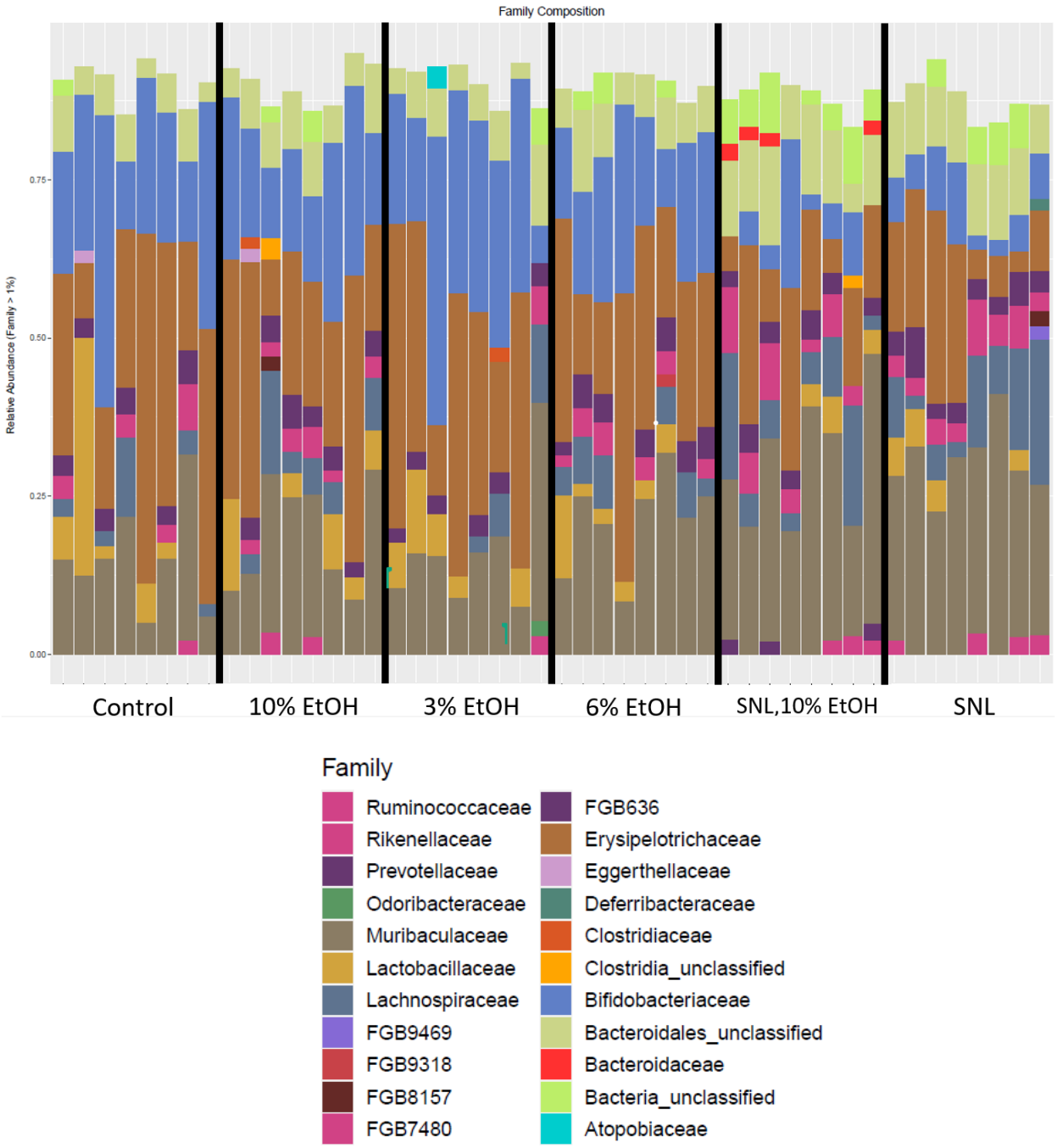

Figure 4.2. Broad variations at Week 0, before treatment, fecal microbiota communities at the family level. Taxonomy chart of relative abundance of OTUs at the family level observed for each fecal sample (n = 8 per treatment) using Phyloseq. Vertical black line divides samples by treatment group.

4.3.3 **Change in Fecal Microbiota Communities at the Family Level After 6 Weeks of Treatment**

After six weeks of treatment, we collected stool samples at timepoint Week 6 to determine changes in microbial communities from Week 0. Again, the 48 fecal samples returned with 1104 OTUs (Fig. 4.3). The top 3 families based on relative abundance remained the same across all treatments at Week 6. The family Erysipelotrichaceae (18.954%, Phylum Firmicutes) saw a minute increase, while Muribaculaceae (10.196%, Phylum Bacteroidetes) levels decreased by 6% total composition, and the Bifidobacteriaceae family (9.699%, Phylum Actinobacteria) was reduced by ~4%.

When sorting microbial families by treatment, we observe Control males had the least amount of change with an 0.18% increase in Erysipelotrichaceae, and 7.284% decrease in Bifidobacteriaceae, and 2.518% decrease in Muribaculaceae. This is likely due to time and fecal-oral transmission of microbes from females placed in the cages for mating to produce offspring for a separate study. Males in the 10% EtOH group presented with a 2.096% elevation in Erysipelotrichaceae and a 5.755% , 6.629% decline in Bifidobacteriaceae and Muribaculaceae, respectively. The 3% EtOH group experienced a reduction in Erysipelotrichaceae by 9.696%, Muribaculaceae by 1.683%, and Bifidobacteriaceae by 12.693%. 6% EtOH males underwent a decline in Muribaculaceae by 5.747%, Bifidobacteriaceae by 7.635%, and Erysipelotrichaceae by 12.738%. In the SNL, 10% EtOH group, we detected a rise in Erysipelotrichaceae by 4.015% increase, loss of Muribaculaceae by 3.906%, while Bifidobacteriaceae populations fell from

8.215% to undetectable representation. Lastly, the SNL water group exhibited a 9.647% and 3.26% uptick in Erysipelotrichaceae and Bifidobacteriaceae, and a diminution in Muribaculaceae by 19.336% (Fig. 4.3). These results indicate that alcohol alone causes a decrease in these specific microbial families, and that the addition of saccharin to alcohol increases Erysipelotrichaceae. This also suggests that SNL alone causes growth in the Bifidobacteriaceae taxa, meaning that alcohol and saccharin rodent models are not indicative of the community alterations caused by alcohol alone.

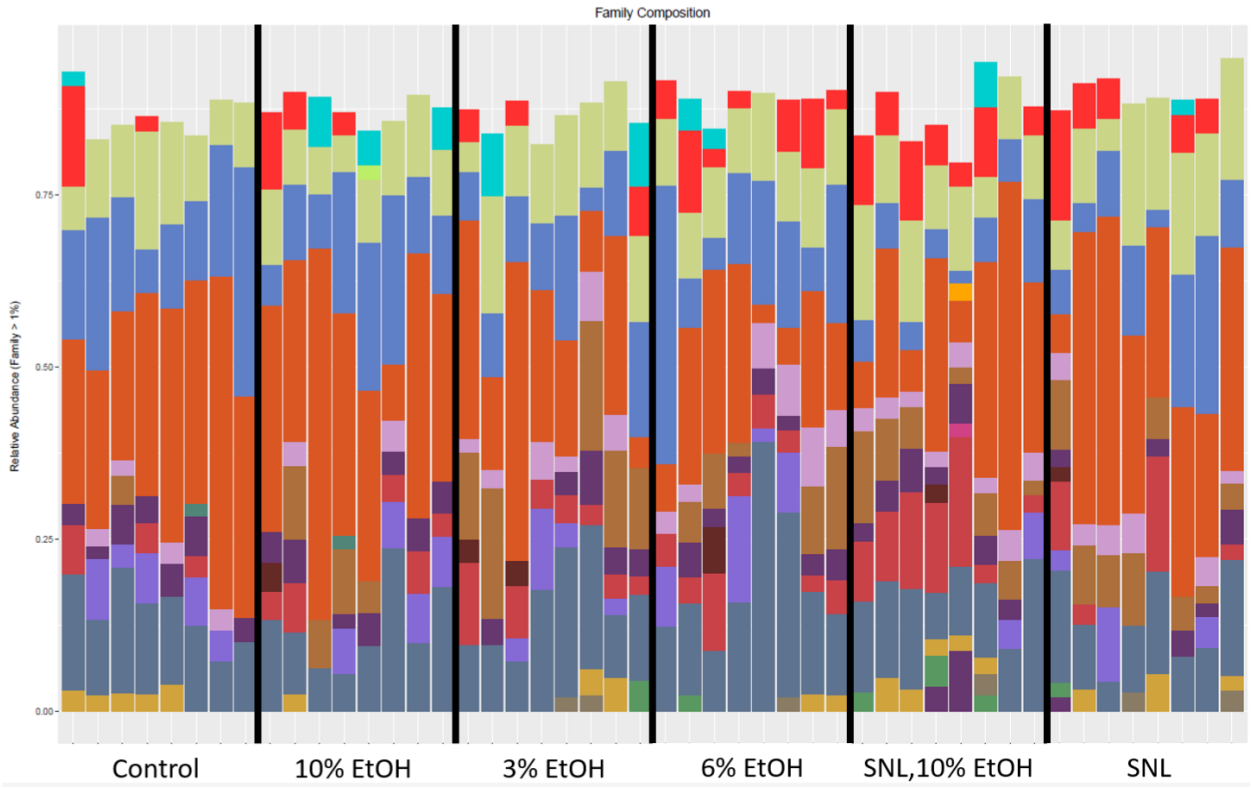

Family

- Ruminococcaceae
- Rikenellaceae
- Prevotellaceae
- Odoribacteraceae
- Muribaculaceae
- Lactobacillaceae
- Lachnospiraceae
- FGB9469
- FGB8157
- FGB7480
- FGB637
- FGB636
- Eubacteriaceae
- Erysipelotrichaceae
- Clostridiaceae
- Bifidobacteriaceae
- Bacteroidales_unclassified
- Bacteria_unclassified
- Atopobiaceae
- Akkermansiaceae

Figure 4.3. Changes in fecal microbiota communities at the family level after 6 weeks of treatment. Taxonomy chart of relative abundance of OTUs of families observed for each fecal sample (n = 8 per treatment) using Phyloseq. Vertical black line divides samples by treatment group.

4.3.4 **Chronic Alcohol and Saccharin Exposure Alters Beta Diversity**

To further understand alcohol and saccharin's impact on intestinal microbiota, we conducted a principal component analysis (PCA) using the Bray-Curtis Dissimilarity Matrix to measure beta diversity between fecal samples (n=8 per treatment). The PCA revealed a tight clustering of the Control samples, whereas the 3% EtOH samples displayed high variability and overlapped with all treatment samples (Figure 4.3). In contrast, samples derived from the SNL only males exhibited distinct clustering from the Controls, while the SNL, 10% EtOH group clustered with the EtOH groups and SNL only treatment. These variabilities were not unexpected, given the total number of families represented across all samples and the shared toxicants between treatments.

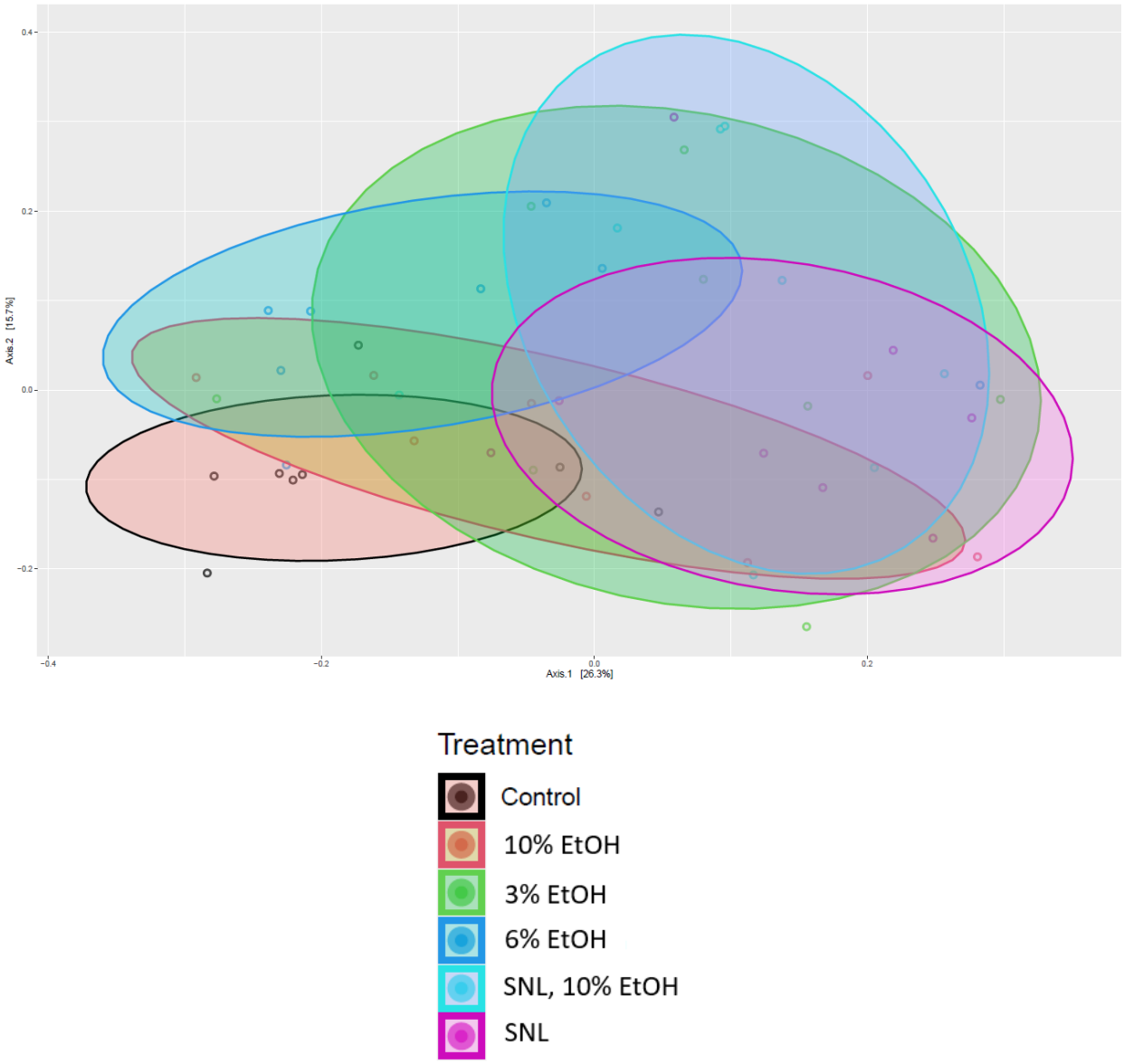

Figure 4.4. Chronic alcohol and saccharin exposure alters beta diversity. Principal Component Analysis (PCA), using Bray-Curtis distances to assess community dissimilarity visually, comparing fecal samples after 6 weeks of exposure.

4.3.5 **General Variances in Alpha Diversity Indices Before Exposure**

Based on the fecal samples we collected at Week 0, we compared the richness and diversity of microbial species using Observed, Choa1, and ACE estimators (Fig. 4.5). The Observed alpha diversity index displays the number of observed OTUs. A higher Chao1 value

suggests a larger number of low abundance taxonomic groups (Chao, 1984; Montgomery-Smith and Schmidt, 2010). The ACE index is an indicator of species richness, or the total number of species in a sample, that is sensitive to rare OTUs. The higher the value, the higher the diversity in that sample.

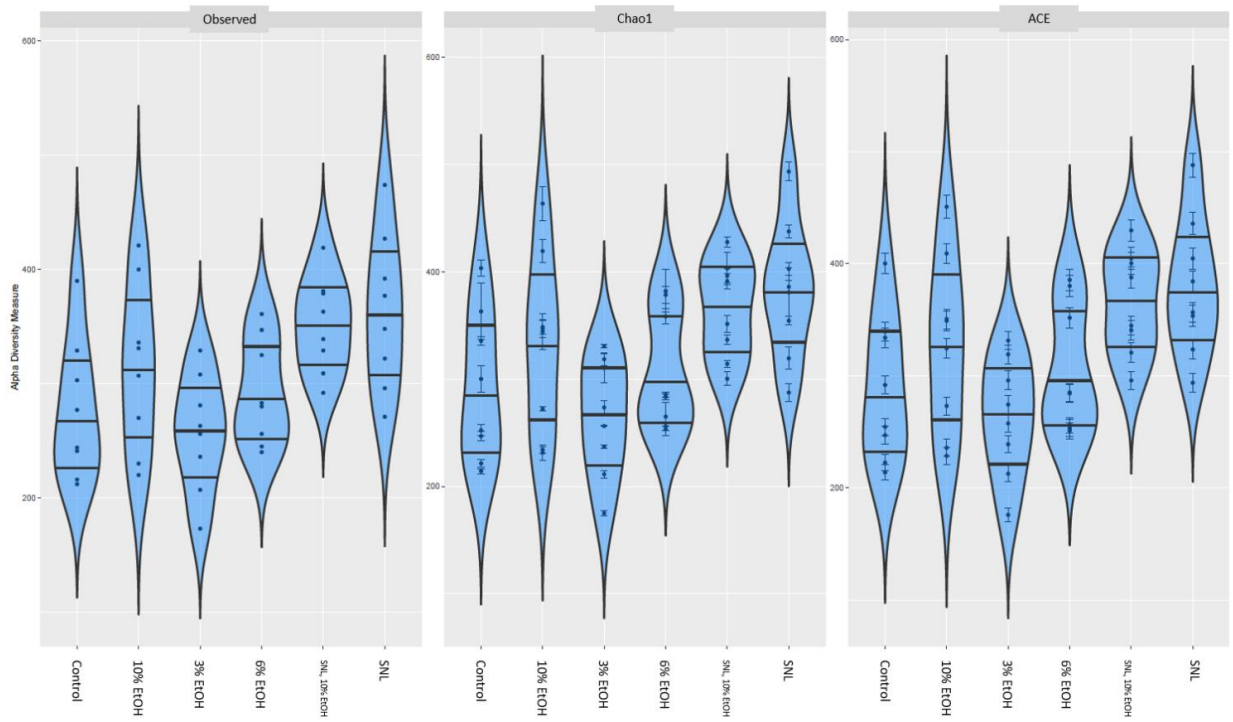

Figure 4.5. General variances in alpha diversity indices before exposure. Left to right: Observed, Choa1, ACE indices. Violin plots depicting range and distribution of samples within each treatment for each index. Alpha diversity indices. Alpha diversity indices, which measure the diversity within individual samples, was computed using the estimate_richness function. Comparisons of alpha diversity between treatment groups was performed using non-parametric Kruskal-Wallis tests.

4.3.6 **Chronic Alcohol and Saccharin Consumption Transforms Gut Microbial Richness**

To visualize the change in microbial richness, we compared the fecal samples metagenome sequencing data at Week 6 using Observed, Choa1, and ACE estimators (Fig. 4.6). When comparing Fig. 4.5 to Fig 4.6, we observe a common pattern between all three indices

showing a decrease in range for all treatments except SNL, 10% EtOH, which indicates an increase in rare and abundant species. Therefore, studies using EtOH and SNL together greatly affect species richness and abundance.

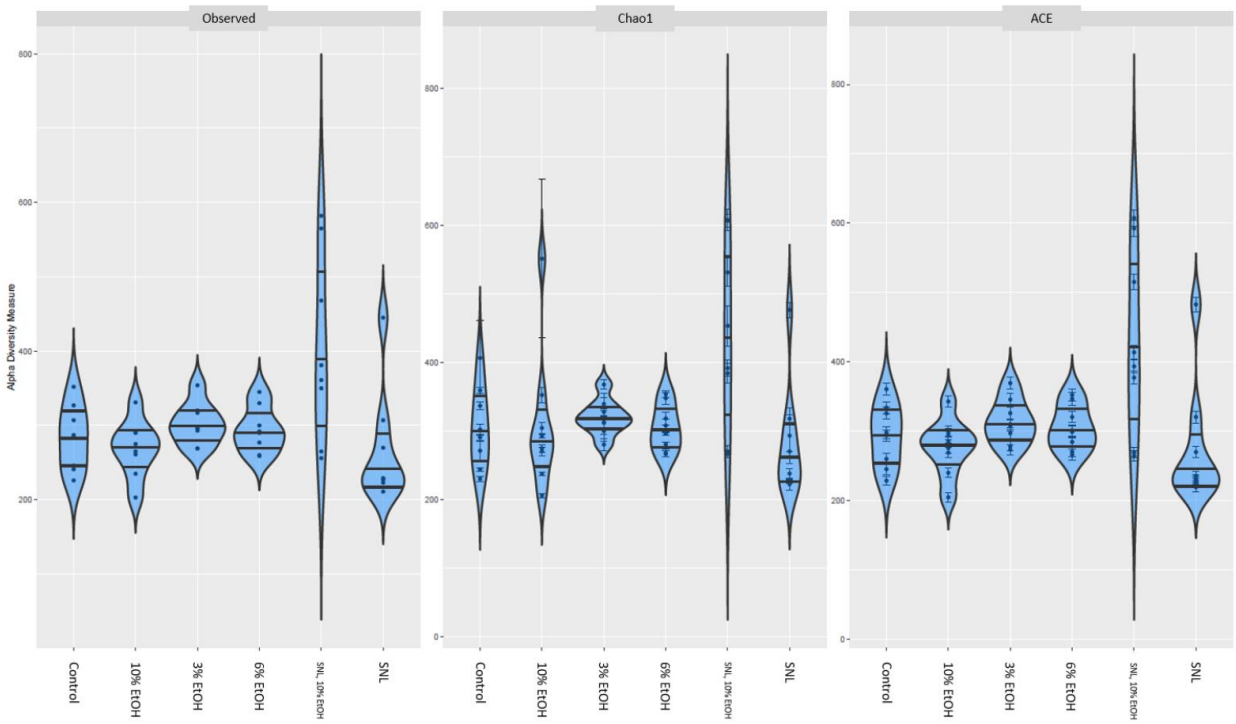

Figure 4.6. Chronic alcohol and saccharin consumption transforms gut microbial richness. Left to right: Observed, Choa1, ACE indices. Violin plots depicting range and distribution of samples within each treatment for each index. Alpha diversity indices. Alpha diversity indices, which measure the diversity within individual samples, was computed using the estimate_richness function. Comparisons of alpha diversity between treatment groups was performed using non-parametric Kruskal-Wallis tests.

4.3.7 **Alcohol and Saccharin Exposure Elevates Acetate Short-Chain Fatty Acid Concentrations**

Using blood plasma collected from treated males at the end of Week 4 and 7, we set out to determine extracted SCFAs to determine circulating metabolite concentrations using GCMS

(Fig. 4.7). We focused our analysis on the top three SCFAs, which include acetate, butyrate, and propionate. We then determined that the higher concentrations of EtOH groups had a tighter clustering using beta diversity measures, therefore we removed 3% EtOH blood plasma from the analysis. After 4 weeks of voluntary consumption, both the SNL, 10% EtOH plasma contained significantly higher levels of acetic acid than all other treatments (Fig. 4.7A). Additionally, the SNL only plasma showed significant increases in acetic acid when compared to the Control and 10% EtOH group (Fig. 4.7A). Butyric acid concentrations were significantly higher in the 10% EtOH group (Fig. 4.7B). Plasma collected at the conclusion of 7 weeks of treatment revealed the SNL, 10% EtOH males had substantial levels of acetic acid (Fig. 4.7D). After 7 weeks, butyric acid levels indicated no differences between treatment groups (Fig. 4.7E). Finally, there was no significant change in propionic acid levels at either plasma collection timepoint (Fig. 4.7C and F). Several studies report increases in acetate in mice and humans when using alcohol or saccharin treatments separately (Suez et al., 2014; Martino et al., 2022; Sarkola et al., 2002). Therefore, acetate is the main metabolite after saccharin or alcohol metabolism. Our data suggests that combined SNL and alcohol increases acetate levels greater than either treatment alone. These increased acetate levels may contribute to other downstream systems, including impacts on the reproductive tract and germline.

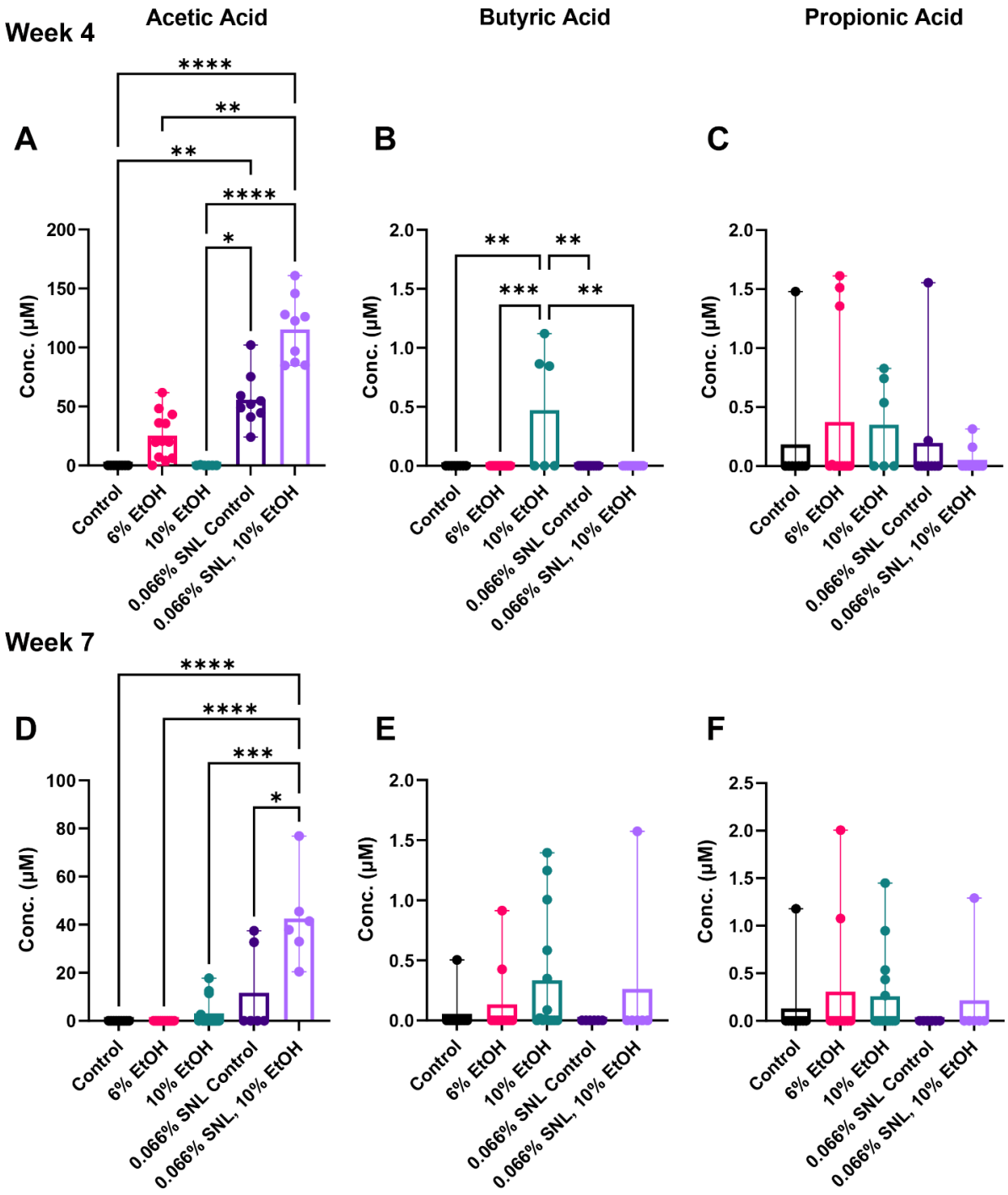

Figure 4.7. Alcohol and saccharin exposure significantly elevates acetate short-chain fatty acid concentrations. After 4 weeks of exposure, (A) Acetic acid, (B) Butyric acid, and (C) Propionic acid concentrations. After 7 weeks of consumption, (D) Acetic acid, (D) Butyric acid, and (E) Propionic acid concentrations (n=6-14 per treatment group). We analyzed treatment data by using a one-way ANOVA. Error bars correspond to the standard deviation of the mean, *P < 0.05, **P < 0.01, ***P < 0.001, ****P < 0.0001.

4.4 Discussion and Conclusions

Over the course of this experiment, we showed that the microbiota identified before treatment (Week 0) were separately altered by EtOH alone, SNL alone, and EtOH and SNL in combination. The greatest modifications to the microbial communities were found in the EtOH and SNL treatment. NAS are often used in animal research to increase palatability and encourage consumption while keeping caloric content low (Roberts et al., 1999; Allan et al., 2003; Ruiz-Ojeda et al., 2019). However, our data reveal that alcohol and saccharin exhibit a cumulative interaction and complicate deciphering the changes in microbiota and acetic acid levels due to alcohol exposure alone. This result was unanticipated, given that many animal model alcohol studies and humans ingest alcohol and artificial sweeteners together (Roberts et al., 1999; Allan et al., 2003; Patten et al., 2014; Chang et al., 2017, Chang et al., 2019a, Chang et al., 2019b; Bedi at al., 2019; Ruiz-Ojeda et al., 2019; Chang et al., 2021). These findings suggest that both alcohol and NAS elicit more alterations than once perceived.

From a clinically translational standpoint, rodent animal models are highly sought after and widely utilized due to their high replacement rates and reproducibility. Here, we used male C57BL/6J mice, which are bred for addictive behaviors and their propensity to consume high levels of EtOH (Rhodes et al., 2005; Thiele and Navarro, 2014). These traits have made C57BL/6Js one of the most commonly used strains for toxicological and pharmacological research. We employed the DID method on the mice to mimic binge-like drinking behaviors that are similar to male human alcohol consumption patterns (Boehm et al., 2008). The average daily dose recorded for the 6% EtOH group (1.29 g EtOH/kg of body weight) can be converted to a 75 kg man drinking roughly seven beers or standard alcoholic beverages in 4 hours. When we apply

the same calculation for the average daily dose for the 10% treatment (1.78 g EtOH/kg of body weight) and SNL 10% EtOH males (2.13 g EtOH/kg of body weight), the number of standard drinks increases to nine and a half and 12, respectively. These translations meet the criteria for male binge drinking characterized by the National Institute on Alcohol Abuse and Alcoholism as five alcoholic drinks in 2-3 hours or less (NIAAA, 2023), which suggests that we attained a physiologically relevant model.

As for Sweet'N Low® consumption, the FDA determined the acceptable daily intake of pure saccharin for humans to be 15 mg/kg of body weight/day (USFDA, 2023), and one packet of SNL contains 36 mg of true saccharin. Therefore, a 75 kg man could safely consume 1,125 mg of pure saccharin per day or thirty-one and a quarter packet of SNL. Using the same acceptable daily intake for the mice in our study, the maximum safe amount of pure saccharin a 27 g mouse can ingest is 0.405 mg daily. Previous works administered high, toxic concentrations of pure saccharin to establish its role in gut permeability and metabolic syndromes, where the rodent model consumed 6.3 g saccharin/kg of body weight (Suez et al., 2014). Such extreme concentrations of saccharin in mice revealed increased acetate levels, altered gut microbiota, and drove the development of glucose intolerance. Our lab initially used SNL to establish drinking patterns in our alcohol-exposed mice with low concentrations of pure saccharin. The SNL only group consumed less than 0.135 mg of true saccharin each day, which is only one third of the FDA recommendation conversion. Even so, this extremely small quantity of pure saccharin was associated with altered intestinal microbiota composition and a notable reduction in the Muribaculaceae family, known to produce butyrate and predicted to metabolize carbohydrates into propionate (Smith et al., 2019; Wang et al., 2020; Smith et al., 2021). The low

concentrations of both butyric and propionic acid could be due to the 20% decrease in Muribaculaceae family abundance.

The relative abundance data depicted the same top 3 families of microbiota inhabiting the gut before and after voluntary alcohol and/or SNL consumption. Erysipelotrichaceae, Muribaculaceae, and Bifidobacteriaceae made up roughly 40% of the GIT microbiota compositions. This suggests microbial members of these families would be the cause for the alterations in SCFAs we see after 4 and 7 weeks of treatment. Erysipelotrichaceae tend to favor breaking down foodstuffs into butyrate (Pozuelo et al., 2015), while Bifidobacteriaceae produce acetate from carbohydrates and is undergoing further investigation by the Zengler lab (Martino et al., 2022). However, the SCFA concentrations we observed do not support this. This could be due to the voluntary drinking model where an animal drank more or less on a given day before blood collection, or it may be a result of a batch effect during GCMS.

On the phylum level, the top 3 phyla represented include Bacteroidetes, Firmicutes, and Actinobacteria. The SNL only males displayed an increase in Actinobacteria while all other treatments decreased in Actinobacteria richness. Firmicutes abundance were always downregulated in the EtOH treatments, whereas Controls, SNL alone, and SNL-10% EtOH groups saw an increase in Firmicutes. All EtOH in water groups decreased in Firmicutes, which was the same result to the Firmicute phyla in a study conducted by Yan and colleagues where they administered alcohol via oral gavage for 3 weeks (Yan et al., 2011). However, toxicant administration through gavage has proven to induce stress on the animal, and increased levels of corticosterone can also modify gut microbial composition (Brown et al., 2000; Walker et al., 2012; Geng et al., 2019). Furthermore, all SNL treated groups saw an increase in Firmicutes, unlike Suez et al. Their study showed decreased Firmicutes, but it was completed ex vivo.

Lastly, there was no pattern detected in Bacteroidetes. These data indicate that time (age) and dietary habits have the propensity to alter microbial communities at the family level.

In this study, I showed that alcohol and NAS have a dual interaction on the microbiome-metabolome axis. This suggests that animal model studies examining EtOH effects on the microbiome-metabolome axis do not faithfully approximate the alpha and beta diversity of fecal samples and SCFA concentrations reliably. Therefore, studies on the effects of EtOH on the gut microbiome and other physiology measures must be EtOH in water treatment only for accurate results. While the effects of alcohol or NAS on mammalian microbiomes have been reported hitherto, our research has provided evidence that EtOH in combination with NAS for rodent models causes its own alterations to the microbiome and circulating SCFAs. One of the consequences of our findings is that EtOH and NAS are not suitable or reliable for the effects of only alcohol on fecal samples or circulating SCFA. Finally, more uniform applications should be ascertained to continue to enhance and advance microbiome-metabolite studies.

A limiting factor in this study is that we held a mating paradigm for studies, and fecal-oral transmission contributed to the change in microbial communities from females being placed into treated male cages.

Our results data supports that the well-established Sweet'N Low® and EtOH drinking model modifies the gut bacterial profile of male mice, and that this interactive-toxicant effect continues to affect downstream metabolite concentrations. Subsequent studies are warranted to confirm our findings and to determine the influence of alcohol, with or without NAS, on the male intestinal microbiota populations and reproductive tract. The reproductive tract is a downstream system that is affected by the compounds metabolized by the digestive system. By studying alterations in the microbiome-metabolome axis, we will be able to correlate and

validate changes in the metabolome of the of the males exposed to alcohol. This could provide a mechanistic explanation of how epigenetic changes in sperm are induced.

5. CONCLUSIONS AND FUTURE DIRECTIONS

The research in this dissertation aimed to evaluate the function of paternal preconception and conception environments for embryo and fetal development. As indicated in Chapter 1, the damaging effects of alcohol consumption on fetal programming have exclusively focused on maternal contributions. As of late, investigations of the second half of the reproductive equation, paternal alcohol exposure, has become more of an imperative for fetal and offspring health predictions (Baber and Koren 2015; Easey et al. 2019; Watkins et al. 2020). Many groups have contributed to the literature in this field through mammalian model research, specifically rodents, and describe multiple biological mechanisms that may assist in understanding how lifestyle choices and environmental exposures create epigenetic retention in gametes and are passed down to progeny. Even though there is no agreement on an exact mechanism, recent evidence suggests the mode(s) of epigenetic inheritance are facilitated by alterations to the components of chromatin, DNA, and sncRNAs in sperm could play a role.

Throughout our research, we utilized a mouse strain with the predisposition for addiction habits. Male C57BL/6Js (Thiele and Navarro, 2014), voluntarily consume a range of EtOH concentrations for 4 hours per day during the beginning of the dark cycle (their active cycle). We employed this model to simulate binge drinking behaviors in humans. This technique is used to shorten the window of exposure to avoid the adverse effects of constant alcohol consumption including dehydration, alcohol poisoning, cirrhosis of the liver, and excess caloric intake. This time of active drinking provides for sire daily dose averages ranging from 1.7-2.2 g EtOH/kg body weight, which imitates the alcohol consumption routines of alcoholics and young adults who binge drink (Greenfield et al., 2023; NIAAA, 2023). To ensure that alcohol-impacted sperm

were produced, we established the male mice on the drinking regimen for 70 days, which encompasses 2 spermatogenic cycles, before collecting mature caudal sperm for IVF procedures or employing alcohol cessation. During gestation, products of conception were terminated to measure the effects of sire EtOH consumption on IVF fetoplacental growth/parameters.

In our IVF experiment, we observed no difference in fetal growth across treatment or sex at GD 16.5 while we saw a significant fetal weight decrease for male offspring naturally sired by males, regardless of treatment, in our previous examination (Thomas et al., 2022; Roach et al., 2023). By using embryonic transcription analyses, we were able to determine paternal alcohol influenced IVF disturbs embryonic gene expression for implantation and modeling, and regulatory network pathways for some imprinted genes, oxidative phosphorylation, and mitochondrial function. We also witnessed immense change in the histological organization of placentae of IVF EtOH sired offspring when we compare them to naturally-mated derived placentae. The inverse relationship between these placental parameters suggests that ARTs are yet another facet driving placental adaptation/compensation during ex vivo development and that paternal EtOH exposures to sperm causes alternate ART outcomes.

Another integral biological process associated with epigenetic inheritance in sperm includes altered sncRNAs and histones after EtOH cessation for one month. In Chapter 3, we present confirmation that sperm sncRNAs and male tissue mtDNAcn remain affected, but the degree of change is less than those of active chronic EtOH consumption. Therefore, more time is necessary to induce full reproductive restoration.

Furthermore, we discussed the effects of EtOH and NAS consumption on male microbiome and SCFA in Chapter 4. When used in conjunction, EtOH and NAS significantly alter intestinal microbiota relative abundance, richness, and diversity, as well as acetate production and

circulation. This discovery will be used in future studies to determine if the increased level of acetate and other metabolites are crossing the blood-testis barrier and causing the epigenetic alterations to developing spermatozoa that we see in mature sperm.

Lastly, we conducted a preliminary study of the female reproductive tract response to alcohol-exposed seminal fluid. Multiple studies have demonstrated that when seminal plasma is deposited into a female's reproductive tract, her immune responses and other signaling pathways are affected to promote preparation for pregnancy (Robertson, 2006; Schjenken and Robertson 2015; Bromfield, 2016; Schjenken and Robertson, 2020; Schjenken et al., 2021). Our hypothesis for this investigation was that the memory of alcohol exposure is only transmitted through sperm, and that seminal plasma from alcohol-exposed males will not have an impact on the female reproductive tract. Here, we investigate how the female reproductive tract responds to alcohol-exposed seminal fluid and identify any signaling pathways that may affect embryo and fetal development.

The fluid that accompanies sperm is known as seminal fluid or seminal plasma. Seminal plasma makes up 95-98% of semen while spermatozoa make up the remainder of semen (Vitku et al., 2017). Seminal fluid contains high levels of fructose, which provides mature sperm with energy to swim up the female reproductive tract (Bromfield, 2014). Recent research has shown that seminal fluid has its own distinct microbiome, different from that found in the gastrointestinal tract, and it can be influenced by diet (Javurek et al., 2016; Javurek et al., 2017). Seminal fluid has been found to have a positive impact on the health of offspring by introducing compounds into the female reproductive tract and regulating the uterine environment before pregnancy by triggering pro-inflammatory reactions that prevent the female tract from rejecting a potential pregnancy (Bromfield, 2014). In rodent models, the absence of seminal fluid during

insemination has led to pregnancy complications and offspring with metabolic issues, obesity, and hypertension later in life (Bromfield et al., 2014) These findings suggest that seminal fluid plays a crucial role in conception, pregnancy, and the health of offspring. So far, studies on epigenetic programming in mice have only looked at non-coding RNA and chromatin structure in sperm, without examining how alcohol exposure may affect seminal fluid.

Following insemination, components in seminal fluid and sperm themselves trigger an immune response in the female reproductive system through inflammatory and cytokine responses to prepare for pregnancy (Schjenken and Robertson, 2020; Sharkey et al., 2007; Johansson et al., 2004; Schuberth et al., 2008; Rametse et al., 2018; Robertson, et al., 2006; Schjenken et al., 2015; Robertson et al., 2002). Additionally, elements in the female tract can impact how semen programs the development of a fetus (Bromfield et al., 2014).

To investigate this, we used male mice that underwent vasectomies and were then exposed to ethanol, at varying concentrations (0% or 6% (w/v)), for 6 weeks. After the 4-hour drinking window, naïve, nulligravida females were placed into male cages to generate pseudopregnancies (Fig. 5.1). Upon observation of the presence of a copulatory plug, we sacrificed the female mice at GD 0.5, using CO_2 asphyxiation followed by cervical dislocation, and collected their reproductive tracts. Next, we separated the oviducts from the tracts and isolated RNA for transcriptomic analysis. We compared the changes in gene expression in the post-coitus oviducts between experimental groups to determine if ethanol-exposed semen has a different impact on female reproductive tract RNA profiles.

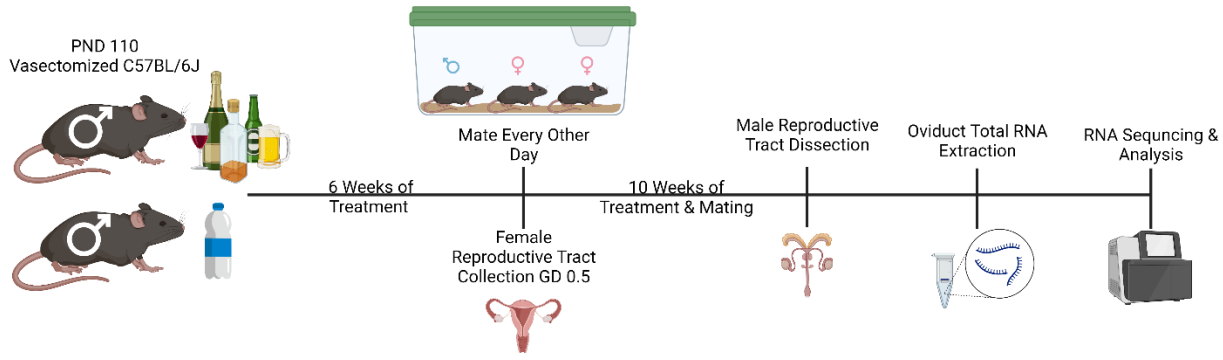

Figure 5.1. Experimental design of EtOH-treated seminal fluid influence on inseminated female reproductive tracts.

Here, I observed that alcohol-exposed seminal fluid does, in fact, alter the gene expression of female tract in preparation for pregnancy (Fig. 5.2). Using DEseq2 and IPA, we identified genes that are involved in decidualization, immune response, oocyte maturation, and sperm guidance are the most affected after alcohol-influenced seminal fluid contact. This indicates that because the female's response has been modified, the fertilization, implantation, and development of the embryo is also altered. This also supports the literature that diet alteration changes seminal fluid and its influence on the female tract (Javurek et al., 2017). Finally, some future directions that will complete this study are to extract, sequence, and analyze the uteri of the females that were inseminated for differentially expressed genes, and conduct proteomic analysis of the seminal vesicles of alcohol-exposed males.

Figure 5.2. EtOH-influenced seminal plasma affects the transcriptional profiles of the oviduct. Principal component analysis of inseminated oviduct RNA sequencing using DESeq2.

Overall, these works suggest that paternal environmental factors and lifestyle choices are retained in the sperm epigenome and play a significant role in the epigenetic inheritance of offspring health and development. Here, we are aiding in filling the knowledge gap how the epigenetic memory of alcohol exposure of the male reproductive tract and germline are transmitted to descendants, contrary to the common assumption that only maternal drinking leads to alcohol induced etiologies. Using NGS on the complex sperm internal components and embryos, we provide proof that connects the effects of paternal EtOH intake to internal alterations that persist in male reproductive tract, germline, and resulting embryos and placentae. These discoveries also highlight the necessity for more holistic approaches for comprehending

the impact of paternal alcohol exposure on offspring. Furthermore, these examinations and analyses will assist the physiology and toxicology fields understand the influence of toxicants and teratogens on fetal growth and offspring health and development from the paternal standpoint of contribution and change the way people perceive drinking alcohol during their reproductive years.

REFERENCES

Adler ID. Comparison of the duration of spermatogenesis between male rodents and humans. Mutat Res 1996; 352:169–172.

Afgan E, Baker D, Batut B, van den Beek M, Bouvier D, Cech M, Chilton J, Clements D, Coraor N, Grüning BA, Guerler A, Hillman-Jackson J, et al. The Galaxy platform for accessible, reproducible and collaborative biomedical analyses: 2018 update. Nucleic Acids Res 2018; 46:W537–W544.

Akingbemi BT, Rao PV, Aire TA. Chronic ethanol intake may delay the onset of gossypol-induced infertility in the male rat. Andrologia 1997; 29:201–207.

Allan AM, Chynoweth J, Tyler LA, Caldwell KK. A mouse model of prenatal ethanol exposure using a voluntary drinking paradigm. Alcohol Clin Exp Res 2003; 27:2009–2016.

Alves MBR, Arruda RP de, Batissaco L, Garcia-Oliveros LN, Gonzaga VHG, Nogueira VJM, Almeida FDS, Pinto SCC, Andrade GM, Perecin F, da Silveira JC, Celeghini ECC. Changes in miRNA levels of sperm and small extracellular vesicles of seminal plasma are associated with transient scrotal heat stress in bulls. Theriogenology 2020; 161:26–40.

Anderson RA, Willis BR, Oswald C, Reddy JM, Beyler SA, Zaneveld LJ. Hormonal imbalance and alterations in testicular morphology induced by chronic ingestion of ethanol. Biochem Pharmacol 1980; 29:1409–1419.

Bai D, Sun J, Chen C, Jia Y, Li Y, Liu K, Zhang Y, Yin J, Liu Y, Han X, Ruan J, Kou X, et al. Aberrant H3K4me3 modification of epiblast genes of extraembryonic tissue causes placental defects and implantation failure in mouse IVF embryos. Cell Rep 2022; 39:110784.

Banan A, Fields JZ, Decker H, Zhang Y, Keshavarzian A. Nitric oxide and its metabolites mediate ethanol-induced microtubule disruption and intestinal barrier dysfunction. J Pharmacol Exp Ther 2000; 294:997–1008.

Barratt CLR, De Jonge CJ, Sharpe RM. "Man Up": the importance and strategy for placing male reproductive health centre stage in the political and research agenda. Hum Reprod 2018; 33:541–545.

Bavister BD. Early history of in vitro fertilization. Reproduction 2002; 124:181–196.

Bedi Y, Chang RC, Gibbs R, Clement TM, Golding MC. Alterations in sperm-inherited noncoding RNAs associate with late-term fetal growth restriction induced by preconception paternal alcohol use. Reprod Toxicol 2019; 87:11–20.

Bedi YS, Wang H, Thomas KN, Basel A, Prunier J, Robert C, Golding MC. Alcohol induced increases in sperm Histone H3 lysine 4 trimethylation correlate with increased placental CTCF occupancy and altered developmental programming. Sci Rep 2022; 12:8839.

Bhadsavle SS, Golding MC. Paternal epigenetic influences on placental health and their impacts on offspring development and disease. Front Genet 2022; 13:1068408.

Bian X, Chi L, Gao B, Tu P, Ru H, Lu K. Gut microbiome response to sucralose and its potential role in inducing liver inflammation in mice. Front Physiol 2017; 8:487.

Bishehsari F, Magno E, Swanson G, Desai V, Voigt RM, Forsyth CB, Keshavarzian A. Alcohol and Gut-Derived Inflammation. Alcohol Res 2017; 38:163–171.

Bloise E, Lin W, Liu X, Simbulan R, Kolahi KS, Petraglia F, Maltepe E, Donjacour A, Rinaudo P. Impaired placental nutrient transport in mice generated by in vitro fertilization. Endocrinology 2012; 153:3457–3467.

Boehm SL, Moore EM, Walsh CD, Gross CD, Cavelli AM, Gigante E, Linsenbardt DN. Using drinking in the dark to model prenatal binge-like exposure to ethanol in C57BL/6J mice. Dev Psychobiol 2008; 50:566–578.

Bokulich NA, Blaser MJ. A bitter aftertaste: unintended effects of artificial sweeteners on the gut microbiome. Cell Metab 2014; 20:701–703.

Bolger AM, Lohse M, Usadel B. Trimmomatic: a flexible trimmer for Illumina sequence data. Bioinformatics 2014; 30:2114–2120.

Braun JM, Messerlian C, Hauser R. Fathers matter: why it's time to consider the impact of paternal environmental exposures on children's health. Curr Epidemiol Rep 2017; 4:46–55.

Bromfield JJ. A role for seminal plasma in modulating pregnancy outcomes in domestic species. Reproduction 2016; 152:R223–R232.

Bromfield JJ. Seminal fluid and reproduction: much more than previously thought. J Assist Reprod Genet 2014; 31:627–636.

Bromfield JJ, Schjenken JE, Chin PY, Care AS, Jasper MJ, Robertson SA. Maternal tract factors contribute to paternal seminal fluid impact on metabolic phenotype in offspring. Proc Natl Acad Sci USA 2014; 111:2200–2205.

Brown AP, Dinger N, Levine BS. Stress produced by gavage administration in the rat. Contemp Top Lab Anim Sci 2000; 39:17–21.

Burton GJ, Fowden AL, Thornburg KL. Placental origins of chronic disease. Physiol Rev 2016; 96:1509–1565.

Carson SA, Kallen AN. Diagnosis and management of infertility: A review. JAMA 2021; 326:65–76.

Castaldelli-Maia JM, Segura LE, Martins SS. The concerning increasing trend of alcohol beverage sales in the U.S. during the COVID-19 pandemic. Alcohol 2021; 96:37–42.

Chan JC, Nugent BM, Bale TL. Parental advisory: maternal and paternal stress can impact offspring neurodevelopment. Biol Psychiatry 2018;83:886–894.

Chang H-Y, Hwu W-L, Chen C-H, Hou C-Y, Cheng W. Children conceived by assisted reproductive technology prone to low birth weight, preterm birth, and birth defects: a cohort review of more than 50,000 live births during 2011-2017 in Taiwan. Front Pediatr 2020;8:87.

Chang RC, Thomas KN, Mehta NA, Veazey KJ, Parnell SE, Golding MC. Programmed suppression of oxidative phosphorylation and mitochondrial function by gestational alcohol exposure correlate with widespread increases in H3K9me2 that do not suppress transcription. Epigenetics Chromatin 2021; 14:27.

Chang RC, Wang H, Bedi Y, Golding MC. Preconception paternal alcohol exposure exerts sex-specific effects on offspring growth and long-term metabolic programming. Epigenetics Chromatin 2019a; 12:9.

Chang RC, Thomas KN, Bedi YS, Golding MC. Programmed increases in LXRα induced by paternal alcohol use enhance offspring metabolic adaptation to high-fat diet induced obesity. Mol Metab 2019b; 30:161–172.

Chang RC, Skiles WM, Chronister SS, Wang H, Sutton GI, Bedi YS, Snyder M, Long CR, Golding MC. DNA methylation-independent growth restriction and altered developmental programming in a mouse model of preconception male alcohol exposure. Epigenetics 2017;12:841–853.

Chao, A. Nonparametric estimation of the number of classes in a population. Scand. J. Stat. 1984, 265–270.

Chastain LG, Sarkar DK. Alcohol effects on the epigenome in the germline: Role in the inheritance of alcohol-related pathology. Alcohol 2017; 60:53–66.

Chen J, Zeng F, Forrester SJ, Eguchi S, Zhang M-Z, Harris RC. Expression and function of the epidermal growth factor receptor in physiology and disease. Physiol Rev 2016; 96:1025–1069.

Chen P, Miyamoto Y, Mazagova M, Lee K-C, Eckmann L, Schnabl B. Microbiota Protects Mice Against Acute Alcohol-Induced Liver Injury. Alcohol Clin Exp Res 2015; 39:2313–2323.

Chen Y, Zhang H, Han F, Yue L, Qiao C, Zhang Y, Dou P, Liu W, Li Y. The depletion of MARVELD1 leads to murine placenta accreta via integrin β4-dependent trophoblast cell invasion. J Cell Physiol 2018; 233:2257–2269.

Clavijo V, Flórez MJV. The gastrointestinal microbiome and its association with the control of pathogens in broiler chicken production: A review. Poult Sci 2018; 97:1006–1021.

Coan PM, Vaughan OR, Sekita Y, Finn SL, Burton GJ, Constancia M, Fowden AL. Adaptations in placental phenotype support fetal growth during undernutrition of pregnant mice. J Physiol (Lond) 2010; 588:527–538.

Collier AC, Miyagi SJ, Yamauchi Y, Ward MA. Assisted reproduction technologies impair placental steroid metabolism. J Steroid Biochem Mol Biol 2009; 116:21–28.

Condorelli RA, Calogero AE, Vicari E, La Vignera S. Chronic consumption of alcohol and sperm parameters: our experience and the main evidences. Andrologia 2015; 47:368–379.

Conine CC, Rando OJ. Soma-to-germline RNA communication. Nat Rev Genet 2022; 23:73–88.

Conine CC, Sun F, Song L, Rivera-Pérez JA, Rando OJ. Small RNAs Gained during Epididymal Transit of Sperm Are Essential for Embryonic Development in Mice. Dev Cell 2018; 46:470-480.e3.

Cook JL, Green CR, Lilley CM, Anderson SM, Baldwin ME, Chudley AE, Conry JL, LeBlanc N, Loock CA, Lutke J, Mallon BF, McFarlane AA, et al. Fetal alcohol spectrum disorder: a guideline for diagnosis across the lifespan. CMAJ 2016; 188:191–197.

de Waal E, Vrooman LA, Fischer E, Ord T, Mainigi MA, Coutifaris C, Schultz RM, Bartolomei MS. The cumulative effect of assisted reproduction procedures on placental development and epigenetic perturbations in a mouse model. Hum Mol Genet 2015; 24:6975–6985.

Delle Piane L, Lin W, Liu X, Donjacour A, Minasi P, Revelli A, Maltepe E, Rinaudo PF. Effect of the method of conception and embryo transfer procedure on mid-gestation placenta and fetal development in an IVF mouse model. Hum Reprod 2010; 25:2039–2046.

Deichmann U. Epigenetics: The origins and evolution of a fashionable topic. Dev Biol 2016; 416:249–254.

Dobin A, Davis CA, Schlesinger F, Drenkow J, Zaleski C, Jha S, Batut P, Chaisson M, Gingeras TR. STAR: ultrafast universal RNA-seq aligner. Bioinformatics 2013; 29:15–21.

Dodge LE, Missmer SA, Thornton KL, Hacker MR. Women's alcohol consumption and cumulative incidence of live birth following in vitro fertilization. J Assist Reprod Genet 2017; 34:877–883.

Dong J, Guo X, Qian C, Wang J, Lei H, Chen S, Wang X. In vitro fertilization causes excessive glycogen accumulation in mouse placenta. Placenta 2021; 114:29–38.

Donkin I, Barrès R. Sperm epigenetics and influence of environmental factors. Mol Metab 2018; 14:1–11.

El Osta R, Almont T, Diligent C, Hubert N, Eschwège P, Hubert J. Anabolic steroids abuse and male infertility. Basic Clin Androl 2016; 26:2.

Emanuele MA, Emanuele N. Alcohol and the male reproductive system. Alcohol Res Health 2001; 25:282–287.

Engen PA, Green SJ, Voigt RM, Forsyth CB, Keshavarzian A. The gastrointestinal microbiome: alcohol effects on the composition of intestinal microbiota. Alcohol Res 2015; 37:223–236.

Esser MB, Hedden SL, Kanny D, Brewer RD, Gfroerer JC, Naimi TS. Prevalence of alcohol dependence among US adult drinkers, 2009-2011. Prev Chronic Dis 2014; 11:E206.

Esquiliano DR, Guo W, Liang L, Dikkes P, Lopez MF. Placental glycogen stores are increased in mice with H19 null mutations but not in those with insulin or IGF type 1 receptor mutations. Placenta 2009; 30:693–699.

Ewels P, Magnusson M, Lundin S, Käller M. MultiQC: summarize analysis results for multiple tools and samples in a single report. Bioinformatics 2016; 32:3047–3048.

Finelli R, Mottola F, Agarwal A. Impact of alcohol consumption on male fertility potential: A narrative review. Int J Environ Res Public Health 2021; 19.

Fleming TP, Watkins AJ, Velazquez MA, Mathers JC, Prentice AM, Stephenson J, Barker M, Saffery R, Yajnik CS, Eckert JJ, Hanson MA, Forrester T, et al. Origins of lifetime health around the time of conception: causes and consequences. Lancet 2018; 391:1842–1852.

Gardner C, Wylie-Rosett J, Gidding SS, Steffen LM, Johnson RK, Reader D, Lichtenstein AH, American Heart Association Nutrition Committee of the Council on Nutrition, Physical Activity and Metabolism, Council on Arteriosclerosis, Thrombosis and Vascular Biology, Council on Cardiovascular Disease in the Young, American Diabetes Association. Nonnutritive sweeteners: current use and health perspectives: a scientific statement from the American Heart Association and the American Diabetes Association. Diabetes Care 2012; 35:1798–1808.

Geng S, Yang L, Cheng F, Zhang Z, Li J, Liu W, Li Y, Chen Y, Bao Y, Chen L, Fei Z, Li X, et al. Gut Microbiota Are Associated With Psychological Stress-Induced Defections in Intestinal and Blood-Brain Barriers. Front Microbiol 2019; 10:3067.

Giorgi G, Marcantonio P, Del Re B. LINE-1 retrotransposition in human neuroblastoma cells is affected by oxidative stress. Cell Tissue Res 2011; 346:383–391.

Go H, La P, Namba F, Ito M, Yang G, Brydun A, Igarashi K, Dennery PA. MiR-196a regulates heme oxygenase-1 by silencing Bach1 in the neonatal mouse lung. Am J Physiol Lung Cell Mol Physiol 2016; 311:ajplung.00428.2015.

Greenfield TK, Karriker-Jaffe K, Ye Y. US DRINKING NORMS UPDATED. Alcohol Research Group 2023.

Griswold MD. Spermatogenesis: the commitment to meiosis. Physiol Rev 2016; 96:1–17.

Gümüş B, Yiğitoğlu MR, Lekili M, Uyanik BS, Müezzinoğlu T, Büyüksu C. Effect of long-term alcohol abuse on male sexual function and serum gonadal hormone levels. Int Urol Nephrol 1998; 30:755–759.

Hamarneh SR, Kim BM, Kaliannan K, Morrison SA, Tantillo TJ, Tao Q, Mohamed MMR, Ramirez JM, Karas A, Liu W, Hu D, Teshager A, et al. Intestinal Alkaline Phosphatase Attenuates Alcohol-Induced Hepatosteatosis in Mice. Dig Dis Sci 2017; 62:2021–2034.

Hamilton TRDS, Mendes CM, de Castro LS, de Assis PM, Siqueira AFP, Delgado J de C, Goissis MD, Muiño-Blanco T, Cebrián-Pérez JÁ, Nichi M, Visintin JA, Assumpção MEOD. Evaluation of lasting effects of heat stress on sperm profile and oxidative status of ram semen and epididymal sperm. Oxid Med Cell Longev 2016; 2016:1687657.

Hart K, Tadros NN. The role of environmental factors and lifestyle on male reproductive health, the epigenome, and resulting offspring. Panminerva Med 2019; 61:187–195.

Hayward CE, Lean S, Sibley CP, Jones RL, Wareing M, Greenwood SL, Dilworth MR. Placental Adaptation: What Can We Learn from Birthweight:Placental Weight Ratio? Front Physiol 2016; 7:28.

Henshaw SK. Unintended pregnancy in the United States. Fam Plann Perspect 1998; 30:24–9, 46.

Higgins JS, Vaughan OR, Fernandez de Liger E, Fowden AL, Sferruzzi-Perri AN. Placental phenotype and resource allocation to fetal growth are modified by the timing and degree of hypoxia during mouse pregnancy. J Physiol (Lond) 2016; 594:1341–1356.

Hornstein MD. Lifestyle and IVF outcomes. Reprod Sci 2016; 23:1626–1629.

Institute of Medicine (US) Committee on Unintended Pregnancy. The Best Intentions: Unintended Pregnancy and the Well-Being of Children and Families. Washington (DC): National Academies Press (US); 1995.

Ishikawa H, Seki R, Yokonishi S, Yamauchi T, Yokoyama K. Relationship between fetal weight, placental growth and litter size in mice from mid- to late-gestation. Reprod Toxicol 2006; 21:267–270.

Javurek AB, Spollen WG, Ali AMM, Johnson SA, Lubahn DB, Bivens NJ, Bromert KH, Ellersieck MR, Givan SA, Rosenfeld CS. Discovery of a novel seminal fluid microbiome and influence of estrogen receptor alpha genetic status. Sci Rep 2016; 6:23027.

Javurek AB, Spollen WG, Johnson SA, Bivens NJ, Bromert KH, Givan SA, Rosenfeld CS. Consumption of a high-fat diet alters the seminal fluid and gut microbiomes in male mice. Reprod Fertil Dev 2017; 29:1602–1612.

Jawaid A, Jehle K-L, Mansuy IM. Impact of parental exposure on offspring health in humans. Trends Genet 2021; 37:373–388.

Jeanblanc J, Rolland B, Gierski F, Martinetti MP, Naassila M. Animal models of binge drinking, current challenges to improve face validity. Neurosci Biobehav Rev 2019; 106:112–121.

Jensen TK, Swan S, Jørgensen N, Toppari J, Redmon B, Punab M, Drobnis EZ, Haugen TB, Zilaitiene B, Sparks AE, Irvine DS, Wang C, et al. Alcohol and male reproductive health: a cross-sectional study of 8344 healthy men from Europe and the USA. Hum Reprod 2014; 29:1801–1809.

Jiménez-Marín A, Collado-Romero M, Ramirez-Boo M, Arce C, Garrido JJ. Biological pathway analysis by ArrayUnlock and Ingenuity Pathway Analysis. BMC Proc 2009; 3 Suppl 4:S6.

Johansson M, Bromfield JJ, Jasper MJ, Robertson SA. Semen activates the female immune response during early pregnancy in mice. Immunology 2004; 112:290–300.

Johnson MH. A short history of in vitro fertilization (IVF). Int J Dev Biol 2019; 63:83–92.

Kanny D, Naimi TS, Liu Y, Lu H, Brewer RD. Annual total binge drinks consumed by U.S. adults, 2015. Am J Prev Med 2018; 54:486–496.

Klonoff-Cohen H, Lam-Kruglick P, Gonzalez C. Effects of maternal and paternal alcohol consumption on the success rates of in vitro fertilization and gamete intrafallopian transfer. Fertil Steril 2003; 79:330–339.

Kolde R. Pheatmap: Pretty Heatmaps. R Package; 2012.

Kost K, Landry DJ, Darroch JE. The effects of pregnancy planning status on birth outcomes and infant care. Fam Plann Perspect 1998; 30:223–230.

Krämer A, Green J, Pollard J, Tugendreich S. Causal analysis approaches in Ingenuity Pathway Analysis. Bioinformatics 2014; 30:523–530.

Kulaksiz D, Toprak T, Tokat E, Yilmaz M, Ramazanoglu MA, Garayev A, Sulukaya M, Degirmentepe RB, Allahverdiyev E, Gul M, Verit A. Sperm concentration and semen volume increase after smoking cessation in infertile men. Int J Impot Res 2022.

Kuo Y-W, Li S-H, Maeda K-I, Gadella BM, Tsai PSJ. Roles of the reproductive tract in modifications of the sperm membrane surface. J Reprod Dev 2016; 62:337–343.

Lane M, Robker RL, Robertson SA. Parenting from before conception. Science 2014; 345:756–760.

Le Blévec E, Muroňová J, Ray PF, Arnoult C. Paternal epigenetics: Mammalian sperm provide much more than DNA at fertilization. Mol Cell Endocrinol 2020; 518:110964.

Lee GS, Conine CC. The Transmission of Intergenerational Epigenetic Information by Sperm microRNAs. Epigenomes 2022; 6.

Lee HY, Naseer MI, Lee SY, Kim MO. Time-dependent effect of ethanol on GnRH and GnRH receptor mRNA expression in hypothalamus and testis of adult and pubertal rats. Neurosci Lett 2010; 471:25–29.

Lee KM, Coehlo M, McGregor HA, Waltermire RS, Szumlinski KK. Binge alcohol drinking elicits persistent negative affect in mice. Behav Brain Res 2015; 291:385–398.

Lempiäinen JK, Garcia BA. Characterizing crosstalk in epigenetic signaling to understand disease physiology. Biochem J 2023; 480:57–85.

Lesciotto KM, Motch Perrine SM, Kawasaki M, Stecko T, Ryan TM, Kawasaki K, Richtsmeier JT. Phosphotungstic acid-enhanced microCT: Optimized protocols for embryonic and early postnatal mice. Dev Dyn 2020; 249:573–585.

Li Y, Behringer RR. Esx1 is an X-chromosome-imprinted regulator of placental development and fetal growth. Nat Genet 1998; 20:309–311.

Liao Y, Smyth GK, Shi W. featureCounts: an efficient general purpose program for assigning sequence reads to genomic features. Bioinformatics 2014; 30:923–930.

Lismer A, Kimmins S. Emerging evidence that the mammalian sperm epigenome serves as a template for embryo development. Nat Commun 2023; 14:2142.

Little RE, Sing CF. Father's drinking and infant birth weight: report of an association. Teratology 1987; 36:59–65.

Liu B-J, Li F-F, Xie Y-X, Fan C-Y, Liu W-J, Qiu J-G, Jiang B-H. miR-196a Upregulation Contributes to Gefitinib Resistance through Inhibiting GLTP Expression. Int J Mol Sci 2022; 23.

Love MI, Huber W, Anders S. Moderated estimation of fold change and dispersion for RNA-seq data with DESeq2. Genome Biol 2014; 15:550.

Luense LJ, Wang X, Schon SB, Weller AH, Lin Shiao E, Bryant JM, Bartolomei MS, Coutifaris C, Garcia BA, Berger SL. Comprehensive analysis of histone post-translational modifications in mouse and human male germ cells. Epigenetics Chromatin 2016; 9:24.

Lv X, Huang J, Wang H. MiR-30a-3p ameliorates oxidative stress in rheumatoid arthritis synovial fibroblasts via activation of Nrf2-ARE signaling pathway. Immunol Lett 2021.

Lyngsø J, Ramlau-Hansen CH, Bay B, Ingerslev HJ, Strandberg-Larsen K, Kesmodel US. Low-to-moderate alcohol consumption and success in fertility treatment: a Danish cohort study. Hum Reprod 2019; 34:1334–1344.

Mahnke AH, Adams AM, Wang AZ, Miranda RC. Toxicant and teratogenic effects of prenatal alcohol. Curr Opin Toxicol 2019; 14:29–34.

Mann MRW, Lee SS, Doherty AS, Verona RI, Nolen LD, Schultz RM, Bartolomei MS. Selective loss of imprinting in the placenta following preimplantation development in culture. Development 2004; 131:3727–3735.

McMurdie PJ, Holmes S. phyloseq: an R package for reproducible interactive analysis and graphics of microbiome census data. PLoS ONE 2013; 8:e61217.

Meistrich ML. Effects of chemotherapy and radiotherapy on spermatogenesis in humans. Fertil Steril 2013; 100:1180–1186.

Mohllajee AP, Curtis KM, Morrow B, Marchbanks PA. Pregnancy intention and its relationship to birth and maternal outcomes. Obstet Gynecol 2007; 109:678–686.

Montagnoli C, Ruggeri S, Cinelli G, Tozzi AE, Bovo C, Bortolus R, Zanconato G. Anything New about Paternal Contribution to Reproductive Outcomes? A Review of the Evidence. World J Mens Health 2021; 39:626–644.

Montgomery-Smith SJ, Schmidt FJ. Statistical methods for estimating complexity from competition experiments between two populations. J Theor Biol 2010; 264:1043–1046.

Muthusami KR, Chinnaswamy P. Effect of chronic alcoholism on male fertility hormones and semen quality. Fertil Steril 2005; 84:919–924.

Naimi TS, Brewer RD, Mokdad A, Denny C, Serdula MK, Marks JS. Binge drinking among US adults. JAMA 2003; 289:70–75.

Nakagata N. Cryopreservation of mouse spermatozoa and in vitro fertilization. Methods Mol Biol 2011; 693:57–73.

National Institute on Alcohol Abuse and Alcoholism. Drinking Levels Defined; 2023. https://www.niaaa.nih.gov/alcohol-health/overview-alcohol-consumption/moderate-binge-drinking. Accessed May 12, 2023.

Nassir F, Ibdah JA. Role of mitochondria in alcoholic liver disease. World J Gastroenterol 2014; 20:2136–2142.

Nicolau P, Miralpeix E, Solà I, Carreras R, Checa MA. Alcohol consumption and in vitro fertilization: a review of the literature. Gynecol Endocrinol 2014; 30:759–763.

Nieminen MT, Salaspuro M. Local Acetaldehyde-An Essential Role in Alcohol-Related Upper Gastrointestinal Tract Carcinogenesis. Cancers (Basel) 2018; 10.

Okada K, Fujisawa M. Recovery of Spermatogenesis Following Cancer Treatment with Cytotoxic Chemotherapy and Radiotherapy. World J Mens Health 2019; 37:166–174.

Oksanen J, Blanchet FG, Friendly M, Kindt R, Legendre P, McGlinn D, Minchin PR, O'Hara RB, Simpson GL, Solymos P, Stevens MHH, Szoecs E, et al. vegan:Community Ecology Package. R Package; 2019.

Oliveros JC. Venny, An Interactive Tool for Comparing Lists withVenn's Diagrams. Venn's Diagrams; 2015.

O'Neill K, Liao W-W, Patel A, Hammell MG. Tesmall identifies small rnas associated with targeted inhibitor resistance in melanoma. Front Genet 2018; 9:461.

Patten AR, Fontaine CJ, Christie BR. A comparison of the different animal models of fetal alcohol spectrum disorders and their use in studying complex behaviors. Front Pediatr 2014; 2:93.

Paul N, Talluri TR, Nag P, Kumaresan A. Epididymosomes: A potential male fertility influencer. Andrologia 2021; 53:e14155.

Pajarinen J, Savolainen V, Perola M, Penttilä A, Karhunen PJ. Glutathione S-transferase-M1 “null” genotype and alcohol-induced disorders of human spermatogenesis. Int J Androl 1996; 19:155–163.

Pearlman M, Obert J, Casey L. The association between artificial sweeteners and obesity. Curr Gastroenterol Rep 2017; 19:64.

Peng J, Meng Z, Zhou S, Zhou Y, Wu Y, Wang Q, Wang J, Sun K. The non-genetic paternal factors for congenital heart defects: A systematic review and meta-analysis. Clin Cardiol 2019; 42:684–691.

Perez NB, Dorsen C, Squires A. Dysbiosis of the gut microbiome: A concept analysis. J Holist Nurs 2020; 38:223–232.

Petrelli B, Weinberg J, Hicks GG. Effects of prenatal alcohol exposure (PAE): insights into FASD using mouse models of PAE. Biochem Cell Biol 2018; 96:131–147.

Pokusaeva K, Fitzgerald GF, van Sinderen D. Carbohydrate metabolism in Bifidobacteria. Genes Nutr 2011; 6:285–306.

Pozuelo M, Panda S, Santiago A, Mendez S, Accarino A, Santos J, Guarner F, Azpiroz F, Manichanh C. Reduction of butyrate- and methane-producing microorganisms in patients with Irritable Bowel Syndrome. Sci Rep 2015; 5:12693.

US Department of Health and Human Services. Prevention and Health. US Department of Health and Human Services:Healthy People 2010.; 2000. https://health.gov/healthypeople. Accessed January 22, 2020.

R Core Team. R: A Language and Environment for Statistical Computing. 2022. Vienna,Austria: R Foundation for Statistical Computing.

Rametse CL, Adefuye AO, Olivier AJ, Curry L, Gamieldien H, Burgers WA, Lewis DA, Williamson A-L, Katz AA, Passmore J-AS. Inflammatory cytokine profiles of semen influence cytokine responses of cervicovaginal epithelial cells. Front Immunol 2018; 9:2721.

Rampon C, Bouillot S, Climescu-Haulica A, Prandini M-H, Cand F, Vandenbrouck Y, Huber P. Protocadherin 12 deficiency alters morphogenesis and transcriptional profile of the placenta. Physiol Genomics 2008; 34:193–204.

Ren L, Xin Y, Sun X, Zhang Y, Chen Y, Liu S, He B. Small Noncoding RNAs Contribute to Sperm Oxidative Stress-Induced Programming of Behavioral and Metabolic Phenotypes in Offspring. Oxid Med Cell Longev 2022; 2022:6877283.

Ren X, Chen X, Wang Z, Wang D. Is transcription in sperm stationary or dynamic? J Reprod Dev 2017; 63:439–443.

Rennie MY, Detmar J, Whiteley KJ, Jurisicova A, Adamson SL, Sled JG. Expansion of the fetoplacental vasculature in late gestation is strain dependent in mice. Am J Physiol Heart Circ Physiol 2012; 302:H1261-73.

Rhodes JS, Best K, Belknap JK, Finn DA, Crabbe JC. Evaluation of a simple model of ethanol drinking to intoxication in C57BL/6J mice. Physiol Behav 2005; 84:53–63.

Roach AN, Zimmel KN, Thomas KN, Basel A, Bhadsavle SS, Golding MC. Preconception paternal alcohol exposure decreases IVF embryo survival and pregnancy success rates in a mouse model. Mol Hum Reprod 2023; 29.

Robertson SA, O'Leary S, Armstrong DT. Influence of semen on inflammatory modulators of embryo implantation. Soc Reprod Fertil Suppl 2006; 62:231–245.

Robertson SA, Ingman WV, O'Leary S, Sharkey DJ, Tremellen KP. Transforming growth factor beta--a mediator of immune deviation in seminal plasma. J Reprod Immunol 2002; 57:109–128.

Rompala GR, Homanics GE. Intergenerational effects of alcohol: A review of paternal preconception ethanol exposure studies and epigenetic mechanisms in the male germline. Alcohol Clin Exp Res 2019; 43:1032–1045.

Rompala GR, Mounier A, Wolfe CM, Lin Q, Lefterov I, Homanics GE. Heavy chronic intermittent ethanol exposure alters small noncoding rnas in mouse sperm and epididymosomes. Front Genet 2018; 9:32.

Rossi BV, Berry KF, Hornstein MD, Cramer DW, Ehrlich S, Missmer SA. Effect of alcohol consumption on in vitro fertilization. Obstet Gynecol 2011; 117:136–142.

Rossi BV, Chang G, Berry KF, Hornstein MD, Missmer SA. In vitro fertilization outcomes and alcohol consumption in at-risk drinkers: the effects of a randomized intervention. Am J Addict 2013; 22:481–485.

Roszkowski M, Mansuy IM. High Efficiency RNA Extraction From Sperm Cells Using Guanidinium Thiocyanate Supplemented With Tris(2-Carboxyethyl)Phosphine. Front Cell Dev Biol 2021; 9:648274.

Ruiz-Ojeda FJ, Plaza-Díaz J, Sáez-Lara MJ, Gil A. Effects of sweeteners on the gut microbiota: A review of experimental studies and clinical trials. Adv Nutr 2019; 10:S31–S48.

Salonen I, Pakarinen P, Huhtaniemi I. Effect of chronic ethanol diet on expression of gonadotropin genes in the male rat. J Pharmacol Exp Ther. 1992;260:463–467.

Sánchez MC, Fontana VA, Galotto C, Cambiasso MY, Sobarzo CMA, Calvo L, Calvo JC, Cebral E. Murine sperm capacitation, oocyte penetration and decondensation following moderate alcohol intake. Reproduction 2018; 155:529–541.

Sansone A, Di Dato C, de Angelis C, Menafra D, Pozza C, Pivonello R, Isidori A, Gianfrilli D. Smoke, alcohol and drug addiction and male fertility. Reprod Biol Endocrinol 2018; 16:3.

Sarkola T, Iles MR, Kohlenberg-Mueller K, Eriksson CJP. Ethanol, acetaldehyde, acetate, and lactate levels after alcohol intake in white men and women: effect of 4-methylpyrazole. Alcohol Clin Exp Res 2002; 26:239–245.

Schmittgen TD, Livak KJ. Analyzing real-time PCR data by the comparative C(T) method. Nat Protoc 2008; 3:1101–1108.

Schjenken JE, Moldenhauer LM, Sharkey DJ, Chan HY, Chin PY, Fullston T, McPherson NO, Robertson SA. High-fat Diet Alters Male Seminal Plasma Composition to Impair Female Immune Adaptation for Pregnancy in Mice. Endocrinology 2021; 162.

Schjenken JE, Robertson SA. The female response to seminal fluid. Physiol Rev 2020; 100:1077–1117.

Schjenken JE, Robertson SA. Seminal Fluid Signalling in the Female Reproductive Tract: Implications for Reproductive Success and Offspring Health. Adv Exp Med Biol 2015; 868:127–158.

Schjenken JE, Glynn DJ, Sharkey DJ, Robertson SA. TLR4 signaling is a major mediator of the female tract response to seminal fluid in mice. Biol Reprod 2015; 93:68.

Schuberth HJ, Taylor U, Zerbe H, Waberski D, Hunter R, Rath D. Immunological responses to semen in the female genital tract. Theriogenology 2008; 70:1174–1181.

Schwenzer H, Jühling F, Chu A, Pallett LJ, Baumert TF, Maini M, Fassati A. Oxidative Stress Triggers Selective tRNA Retrograde Transport in Human Cells during the Integrated Stress Response. Cell Rep 2019; 26:3416-3428.e5.

Senaldi L, Smith-Raska M. Evidence for germline non-genetic inheritance of human phenotypes and diseases. Clin Epigenetics 2020; 12:136.

Sender R, Fuchs S, Milo R. Revised estimates for the number of human and bacteria cells in the body. PLoS Biol 2016; 14:e1002533.

Serafini P. Outcome and follow-up of children born after IVF-surrogacy. Hum Reprod Update 2001; 7:23–27.

Sermondade N, Elloumi H, Berthaut I, Mathieu E, Delarouzière V, Ravel C, Mandelbaum J. Progressive alcohol-induced sperm alterations leading to spermatogenic arrest, which was reversed after alcohol withdrawal. Reprod Biomed Online 2010; 20:324–327.

Sferruzzi-Perri AN, Vaughan OR, Coan PM, Suciu MC, Darbyshire R, Constancia M, Burton GJ, Fowden AL. Placental-specific Igf2 deficiency alters developmental adaptations to undernutrition in mice. Endocrinology 2011; 152:3202–3212.

Sharkey DJ, Macpherson AM, Tremellen KP, Robertson SA. Seminal plasma differentially regulates inflammatory cytokine gene expression in human cervical and vaginal epithelial cells. Mol Hum Reprod 2007; 13:491–501.

Sharma U. Paternal contributions to offspring health: role of sperm small rnas in intergenerational transmission of epigenetic information. Front Cell Dev Biol 2019; 7:215.

Sharma U, Sun F, Conine CC, Reichholf B, Kukreja S, Herzog VA, Ameres SL, Rando OJ. Small RNAs Are Trafficked from the Epididymis to Developing Mammalian Sperm. Dev Cell 2018; 46:481-494.e6.

Shcherbitskaia AD, Komarova EM, Milyutina YP, Ishchuk MA, Sagurova YM, Safaryan GK, Lesik EA, Gzgzyan AM, Bespalova ON, Kogan IY. Oxidative Stress Markers and Sperm DNA Fragmentation in Men Recovered from COVID-19. Int J Mol Sci 2022; 23.

Shi J, Fok KL, Dai P, Qiao F, Zhang M, Liu H, Sang M, Ye M, Liu Y, Zhou Y, Wang C, Sun F, et al. Spatio-temporal landscape of mouse epididymal cells and specific mitochondria-rich segments defined by large-scale single-cell RNA-seq. Cell Discov 2021; 7:34.

Shil A, Olusanya O, Ghufoor Z, Forson B, Marks J, Chichger H. Artificial Sweeteners Disrupt Tight Junctions and Barrier Function in the Intestinal Epithelium through Activation of the Sweet Taste Receptor, T1R3. Nutrients 2020; 12.

Smith BJ, Miller RA, Schmidt TM. Muribaculaceae Genomes Assembled from Metagenomes Suggest Genetic Drivers of Differential Response to Acarbose Treatment in Mice. MSphere 2021; 6:e0085121.

Smith BJ, Miller RA, Ericsson AC, Harrison DC, Strong R, Schmidt TM. Changes in the gut microbiome and fermentation products concurrent with enhanced longevity in acarbose-treated mice. BMC Microbiol 2019; 19:130.

Soubry A. Epigenetics as a driver of developmental origins of health and disease: did we forget the fathers? Bioessays 2018; 40.

Soubry A. POHaD: why we should study future fathers. Environ Epigenet 2018; 4:dvy007.

Suez J, Korem T, Zeevi D, Zilberman-Schapira G, Thaiss CA, Maza O, Israeli D, Zmora N, Gilad S, Weinberger A, Kuperman Y, Harmelin A, et al. Artificial sweeteners induce glucose intolerance by altering the gut microbiota. Nature 2014; 514:181–186.

Sullivan R. Epididymosomes: a heterogeneous population of microvesicles with multiple functions in sperm maturation and storage. Asian J Androl 2015; 17:726–729.

Tan K, Zhang Z, Miao K, Yu Y, Sui L, Tian J, An L. Dynamic integrated analysis of DNA methylation and gene expression profiles in in vivo and in vitro fertilized mouse post-implantation extraembryonic and placental tissues. Mol Hum Reprod 2016; 22:485–498.

Tanaka S, Kunath T, Hadjantonakis AK, Nagy A, Rossant J. Promotion of trophoblast stem cell proliferation by FGF4. Science 1998; 282:2072–2075.

Tang Q, Pan F, Wu X, Nichols CE, Wang X, Xia Y, London SJ, Wu W. Semen quality and cigarette smoking in a cohort of healthy fertile men. Environ Epidemiol 2019; 3:e055.

Thanh NX, Jonsson E. Life Expectancy of People with Fetal Alcohol Syndrome. J Popul Ther Clin Pharmacol 2016; 23:e53-9.

Thiele TE, Navarro M. “Drinking in the dark” (DID) procedures: a model of binge-like ethanol drinking in non-dependent mice. Alcohol 2014; 48:235–241.

Thomas KN, Srikanth N, Bhadsavle SS, Thomas KR, Zimmel KN, Basel A, Roach AN, Mehta NA, Bedi YS, Golding MC. Preconception paternal ethanol exposures induce alcohol-related craniofacial growth deficiencies in fetal offspring. J Clin Invest 2023.

Thomas KN, Zimmel KN, Basel A, Roach AN, Mehta NA, Thomas KR, Dotson LJ, Bedi YS, Golding MC. Paternal alcohol exposures program intergenerational hormetic effects on offspring fetoplacental growth. Front Cell Dev Biol 2022; 10:930375.

Thomas KN, Zimmel KN, Roach AN, Basel A, Mehta NA, Bedi YS, Golding MC. Maternal background alters the penetrance of growth phenotypes and sex-specific placental adaptation of offspring sired by alcohol-exposed males. FASEB J 2021; 35:e22035.

Tonetto S, Weikop P, Brudek T, Thomsen M. Behavioral and biochemical effects of alcohol withdrawal in female C3H/HeNRj and C57BL/6JRj mice. Front Behav Neurosci 2023; 17:1143720.

Truett GE, Heeger P, Mynatt RL, Truett AA, Walker JA, Warman ML. Preparation of PCR-quality mouse genomic DNA with hot sodium hydroxide and tris (HotSHOT). BioTechniques 2000; 29:52–54.

Truong DT, Franzosa EA, Tickle TL, Scholz M, Weingart G, Pasolli E, Tett A, Huttenhower C, Segata N. MetaPhlAn2 for enhanced metagenomic taxonomic profiling. Nat Methods 2015; 12:902–903.

Tunster SJ, Creeth HDJ, John RM. The imprinted Phlda2 gene modulates a major endocrine compartment of the placenta to regulate placental demands for maternal resources. Dev Biol 2016a; 409:251–260.

Tunster SJ, McNamara GI, Creeth HDJ, John RM. Increased dosage of the imprinted Ascl2 gene restrains two key endocrine lineages of the mouse Placenta. Dev Biol 2016b; 418:55–65.

United States Food and Drug Administration. Aspartame and Other Sweeteners in Food; 2023. https://www.fda.gov/food/food-additives-petitions/aspartame-and-other-sweeteners-food. Accessed June 16, 2023.

Van Heertum K, Rossi B. Alcohol and fertility: how much is too much? Fertil Res Pract 2017; 3:10.

Vicari E, Arancio A, Giuffrida V, D'Agata R, Calogero AE. A case of reversible azoospermia following withdrawal from alcohol consumption. J Endocrinol Invest 2002:473–6.

Vitku J, Kolatorova L, Hampl R. Occurrence and reproductive roles of hormones in seminal plasma. Basic Clin Androl 2017; 27:19.

Vrooman LA, Rhon-Calderon EA, Chao OY, Nguyen DK, Narapareddy L, Dahiya AK, Putt ME, Schultz RM, Bartolomei MS. Assisted reproductive technologies induce temporally specific

placental defects and the preeclampsia risk marker sFLT1 in mouse. Development 2020;147:dev186551.

Vrooman LA, Rhon-Calderon EA, Suri KV, Dahiya AK, Lan Y, Schultz RM, Bartolomei MS. Placental abnormalities are associated with specific windows of embryo culture in a mouse model. Front Cell Dev Biol 2022;10:884088.

Walker MK, Boberg JR, Walsh MT, Wolf V, Trujillo A, Duke MS, Palme R, Felton LA. A less stressful alternative to oral gavage for pharmacological and toxicological studies in mice. Toxicol Appl Pharmacol 2012; 260:65–69.

Wallace DC. Mitochondrial genetic medicine. Nat Genet 2018; 50:1642–1649.

Wang B, Kong Q, Li X, Zhao J, Zhang H, Chen W, Wang G. A High-Fat Diet Increases Gut Microbiota Biodiversity and Energy Expenditure Due to Nutrient Difference. Nutrients 2020; 12.

Wang N, Zhang L, Lu Y, Zhang M, Zhang Z, Wang K, Lv J. Down-regulation of microRNA-142-5p attenuates oxygen-glucose deprivation and reoxygenation-induced neuron injury through up-regulating Nrf2/ARE signaling pathway. Biomed Pharmacother 2017; 89:1187–1195.

Watanabe K, Miyagawa R, Tomikawa C, Mizuno R, Takahashi A, Hori H, Ijiri K. Degradation of initiator tRNAMet by Xrn1/2 via its accumulation in the nucleus of heat-treated HeLa cells. Nucleic Acids Res 2013; 41:4671–4685.

Wdowiak A, Sulima M, Sadowska M, Grzegorz B, Bojar I. Alcohol consumption and quality of embryos obtained in programmes of in vitro fertilization. Ann Agric Environ Med 2014; 21:450–453.

West AP, Khoury-Hanold W, Staron M, Tal MC, Pineda CM, Lang SM, Bestwick M, Duguay BA, Raimundo N, MacDuff DA, Kaech SM, Smiley JR, et al. Mitochondrial DNA stress primes the antiviral innate immune response. Nature 2015; 520:553–557.

White AM, Kraus CL, Swartzwelder H. Many college freshmen drink at levels far beyond the binge threshold. Alcohol Clin Exp Res 2006; 30:1006–1010.

Whitten WK, Bronson FH, Greenstein JA. Estrus-inducing pheromone of male mice: transport by movement of air. Science 1968; 161:584–585.

Wilsnack RW, Wilsnack SC, Gmel G, Kantor LW. Gender differences in binge drinking. Alcohol Res 2018; 39:57–76.

Wolfe AJ. The acetate switch. Microbiol Mol Biol Rev 2005; 69:12–50.

Woods L, Perez-Garcia V, Hemberger M. Regulation of Placental Development and Its Impact on Fetal Growth-New Insights From Mouse Models. Front Endocrinol (Lausanne) 2018; 9:570.

Xia R, Jin L, Li D, Liang H, Yang F, Chen J, Yuan W, Miao M. Association between paternal alcohol consumption before conception and anogenital distance of offspring. Alcohol Clin Exp Res 2018; 42:735–742.

Yan AW, Fouts DE, Brandl J, Stärkel P, Torralba M, Schott E, Tsukamoto H, Nelson KE, Brenner DA, Schnabl B. Enteric dysbiosis associated with a mouse model of alcoholic liver disease. Hepatology 2011; 53:96–105.

Zhang S, Wang L, Yang T, Chen L, Zhao L, Wang T, Chen L, Ye Z, Zheng Z, Qin J. Parental alcohol consumption and the risk of congenital heart diseases in offspring: An updated systematic review and meta-analysis. Eur J Prev Cardiol 2020; 27:410–421.

Zhong W, Zhou Z. Alterations of the gut microbiome and metabolome in alcoholic liver disease. World J Gastrointest Pathophysiol 2014; 5:514–522.

Zhou H, Zhu P, Wang J, Toan S, Ren J. DNA-PKcs promotes alcohol-related liver disease by activating Drp1-related mitochondrial fission and repressing FUNDC1-required mitophagy. Signal Transduct Target Ther 2019; 4:56.

Zhou Q, Song L, Chen J. Association of Preconception Paternal Alcohol Consumption With Increased Fetal Birth Defect Risk. JAMA Pediatr 2021:742–743.

Zuccolo L, DeRoo LA, Wills AK, Davey Smith G, Suren P, Roth C, Stoltenberg C, Magnus P. Pre-conception and prenatal alcohol exposure from mothers and fathers drinking and head circumference: results from the Norwegian Mother-Child Study (MoBa). Sci Rep 2016; 7:39535.

APPENDIX

Supplemental Table 1. Detailed descriptions of the statistical testing underlying each figure.

Graph	Statistical Test	Sample Size	Outliers
Figure 1: Experimental design for paternal alcohol exposure and embryo generation			
B. Sire fluid consumption by treatment week * **C.** Sire body weight change by treatment week **	Two-way ANOVA contrasting treatment and time, multiple comparisons using uncorrected Fisher's LSD.	n = 8 Control, 8 6% EtOH, 8 10% EtOH	None
D. Sire daily dose consumption	One-way ANOVA, multiple comparisons using Tukey's test	n = 8 Control, 8 6% EtOH, 8 10% EtOH	1 Control 2 6% EtOH (bottle leak)
Figure 2, Table 1A-C: Embryo survival			
Table 1	Chi-square analysis followed by Fisher's Exact test for individual comparisons.	Numbers provided in tables.	None
A. Percent embryo survival to GD 16.5 **B.** Litter size	Arc sign transformation of percentages, Kruskal-Wallis followed by Dunn's test. One-way ANOVA, multiple comparisons using Tukey's test	n=18 Control, n=27 6% EtOH, n=38 10% EtOH	None
C. Pregnancy Success Rate (recipients at GD 16.5)	Chi-square analysis followed by Fisher's Exact test for individual comparisons.	n= 18 Control, n=27 6% EtOH, n=38 10% EtOH	None
Figure 4. Fetal measures			

Supplemental Table 1. Continued

Graph	Statistical Test	Sample Size	Outliers
A-G. Gestational sac weight, fetal weight, crown-rump length, normalized brain weight, normalized heart weight, and normalized thymus weight	Two-way ANOVA to contrast differences between sex and the preconception treatment groups, multiple comparisons using Uncorrected Fisher's LSD or Kruskal-Wallis followed by Dunn's test.	**A-C** n=45 Control, 31 6% EtOH, 26 10% EtOH male offspring; n=44 Control 23 6% EtOH 16 10% EtOH female offspring). **D-F** n=23 Control, 17 6% EtOH, and 13 10% EtOH male offspring; 20 Control, 13 6% EtOH, and 7-11 10% EtOH female offspring	None
Figure 5. Placental physiological measures			
Placental weight, placental diameter, placental efficiency, volume of the chorion, decidua, junctional zone and labyrinth, Junctional zone: decidua ratio, labyrinth: junctional zone ratio, and glycogen content	Two-way ANOVA to contrast differences between sex and the preconception treatment groups, multiple comparisons using Uncorrected Fisher's LSD. For analysis of placental glycogen, we used a One-way ANOVA with multiple comparisons using Uncorrected Fisher's LSD.	**A-C** n=45 Control, 31 6% EtOH 26 10% EtOH male offspring; n=44 Control 23 6% EtOH 16 10% EtOH female offspring **D-I** n=32 Control, 23 6% EtOH, and 23 10% EtOH male offspring; 23 Control, 16 6% EtOH, and 13 10% EtOH female offspring **J** n=11 Control, 8 6% EtOH, and 8 10% EtOH; male offspring only	None

Supplemental Table 1. Continued

Figure 6. Placental RT-qPCR analysis of gene expression				
MALES				
Gene	**Analysis**		**Control**	**10% Ethanol**
Mt-Nd5	# Y values analyzed	8	7	
	Outliers	2	0	
Mt-Cytb	# Y values analyzed	8	7	
	Outliers	1	0	
Mt-Co1	# Y values analyzed	8	7	
	Outliers	1	0	
Mt-Nd1	# Y values analyzed	8	7	
	Outliers	2	0	
Atp5e	# Y values analyzed	8	7	
	Outliers	1	0	
Atp5mf	# Y values analyzed	8	7	
	Outliers	1	0	
Atp5l	# Y values analyzed	8	7	
	Outliers	0	0	
FEMALES				
Gene	**Analysis**		**Control**	**10% Ethanol**
Mt-Nd5	# Y values analyzed	8	8	
	Outliers	0	0	
Mt-Cytb	# Y values analyzed	8	8	
	Outliers	1	0	
Mt-Co1	# Y values analyzed	8	8	
	Outliers	0	0	
Mt-Nd1	# Y values analyzed	8	8	
	Outliers	1	0	
Atp5e	# Y values analyzed	8	8	
	Outliers	0	0	
Atp5l	# Y values analyzed	8	8	
	Outliers	1	1	

*During week eight, we noted that males in the 6% EtOH treatment group drank more than those in the 10% EtOH treatment group, neither however, were different from the Controls.
**During week seven, males in the 6% EtOH treatment group gained more weight than those in the 10% EtOH treatment. However, the weight gain observed in both EtOH groups was not significantly different from the Control treatment.

Supplementary Table 2. Sire age at collection and number of IVF natural litters.

Sire Information				
Treatment	**Sire ID**	**Age at Collection (Week)**	**# IVF Litters**	**# Natural Litters**
Control	C9	20.86	3	1
	C11	20.86	2	1
	C26	22.00	3	0
	C27	22.00	2	0
	CM1	22.57	0	1
	CM2	22.57	0	2
	CM12	23.71	1	1
	CM14	23.71	1	1
6% EtOH	M4	21.71	1	1
	M7	21.00	3	2
	M8	20.86	1	2
	M215	22.57	1	1
	M216	22.14	1	0
	M217	22.14	1	0
	M2110	22.71	1	0
	M2111	22.71	0	0
10% EtOH	EM1	22.71	1	1
	EM2	22.71	1	1
	EM11	22.57	1	0
	EM12	22.57	1	0
	EM14	22.14	0	0
	EM15	22.14	1	0
	EM26	22.71	1	0
	EM29	22.71	2	0
		Total	**29**	**15**

Supplementary Table 3. Comprehensive embryo transfer log of sire matched 2-cell embryo survival rate to GD 16.5 per recipient.

Sire Treatment	Recipient	# 2-cells Transferred	GD 16.5 Litter Size	% Success
C11	1	10	0	0%
C11	2	10	0	0%
CM14	3	8	0	0%
CM12	4	12	0	0%
CM12	5	13	0	0%
C26	6	11	1	9%
C27	7	10	4	40%
C26	8	11	5	45%
C11	9	10	6	60%
C26	10	11	6	55%
C9	11	12	6	50%
C11	12	10	7	70%
C27	13	10	7	70%
C9	14	12	8	67%
C9	15	12	9	75%
CM12	16	12	9	75%
C26	17	12	11	92%
CM14	18	11	11	100%
M4	1	10	0	0%
M4	2	9	0	0%
M215	3	11	0	0%
M216	4	13	0	0%
M216	5	14	0	0%
M2110	6	13	0	0%
M2110	7	12	0	0%
M2111	8	11	0	0%
M2111	9	11	0	0%
M2111	10	11	0	0%
M217	11	12	0	0%
M217	12	12	0	0%
M8	13	9	0	0%
M8	14	11	1	9%

Supplementary Table 3. Continued

M2111	15	10	2	20%
M8	16	11	2	18%
M8	17	11	3	27%
M4	18	10	3	30%
M217	19	12	4	33%
M2110	20	13	4	31%
M8	21	9	5	56%
M7	22	10	5	50%
M215	23	11	6	55%
M7	24	11	7	64%
M4	25	11	7	64%
M7	26	10	7	70%
M216	27	13	10	77%
EM1	1	12	0	0%
EM2	2	10	0	0%
EM11	3	13	0	0%
EM11	4	12	0	0%
EM12	5	10	0	0%
EM14	6	12	0	0%
EM14	7	12	0	0%
EM14	8	12	0	0%
EM14	9	8	0	0%
EM14	10	8	0	0%
EM15	11	10	0	0%
EM15	12	10	0	0%
EM26	13	10	0	0%
EM26	14	10	0	0%
EM26	15	10	0	0%
EM26	16	10	0	0%
EM26	17	13	0	0%
EM29	18	11	0	0%
EM29	19	11	0	0%
EM26	20	12	0	0%
EM26	21	12	0	0%
EM26	22	12	0	0%
EM26	23	12	0	0%
EM14	24	11	0	0%

Supplementary Table 3. Continued

EM12	33	11	4	36%
EM2	34	10	5	50%
EM26	35	13	5	38%
EM1	36	12	6	50%
EM11	37	13	7	54%
EM29	38	10	7	70%
EM15	25	10	1	10%
EM15	26	10	2	20%
EM15	27	10	3	30%
EM12	28	10	3	30%
EM2	29	10	3	30%
EM1	30	12	3	25%
EM29	31	11	4	36%
EM15	32	9	4	44%

Supplementary Table 4. Differentially Expressed Genes identified in pairwise comparisons between treatment groups.

Morulae differentially expressed genes log2-fold change, q-value < 0.05		
Treatment Comparison	**Number of DEGs**	**Gene Names**
Control vs. 6% EtOH	16	5033406O09Rik, ARL5C, C16orf96, CELSR1, Gm43005, Gm43913, GPA33, HERPUD1, INKA1, JDP2, KCNH7, MARVELD1, MTHFSD, PRAF2, SLC28A1, Uba1y
Control vs. 10% EtOH	35	5033406O09Rik, AC154176.2, ADSS1, ARHGAP28, BRDT, C1orf21, CD1D, Ces2g, D7Bwg0826e, DLL1, EGFR, FAM221A, FGF4, FXYD5, GLRX, GLRX2, Gm19554, GPA33, GSDMA, Gsta4, KLHL14, LCORL, Magea3 family, MLKL, MORC1, PIERCE1, PRKCE, RAC3, RPGRIP1L, SEPTIN6, SERPINB6, SHROOM2, SLC9A3R1, SNN, Uba1y
6% EtOH vs. 10% EtOH	30	BPNT1, BTD, C16orf96, CACNB1, CCDC61, CELSR1, D7Bwg0826e, DDX25, FAM227A, FLT1, Gm16536, Gm20712, Gm3325/Zfp808, Gm37219, Gm43913, Gm4557/Gm6882, Gm9742, GSDMA, KCNH7, KCNK4, KMT2A, Lipo2 family, MAP3K11, MBD2, MIDEAS, MYBL1, NUP210L, PLAG1, RTN2, TRIM2